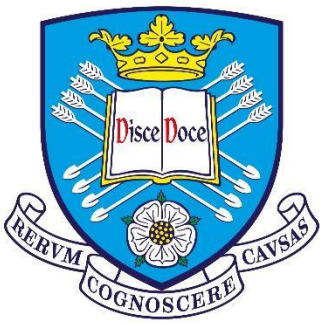

The University Of Sheffield.

The University of Sheffield

Faculty of Engineering

Department of Materials Science and Engineering

Craniofacial bone defect repair with polymer scaffold and cell-derived matrix

Witchayut Sasimonthon

October 2023

A thesis submitted in fulfilment of the requirements for the degree of Doctor of Philosophy

Acknowledgements

First of all, I would like to express all my gratitude to my supervisors Professor Gwendolen Reilly, Dr Helen Colley, and Professor Frederik Claeyssens who have dedicatedly provided such great support and guided my way throughout my journey to PhD. You all have my best sincerely thank you.

Thanks faculty of dentistry, Naresuan University for giving me this opportunity. Thanks to Dr Phairoj Sriarun, Dr Ruedee Sakulrachata, Dr Sasima Puwanun, Dr Supanya Naivikul, and department of pediatric dentistry for supporting me.

Thanks to Julie Marshall for always being there to help me as a great lab manager. You are one of the parts that made this thesis possible. Thanks to Dr Rob Owen, who taught me so much about the first step of cell culture which. Thanks to Dr Dhanak Gupta, that clarified a lot of things in cell culture and made me think more logically. Thanks to Dr Sam Pashneh-Tala who trained me in the fabrication of PGS, and now it has become everything of my thesis. Thanks to Dr Oday Hussein for training on using a pycnometer. Thanks to Dr Amy Harding for always being there to help and guide me a lot in this project. Not only the scientific part but also giving mentally support and encouraging me every time we met. Thanks to Dr Marzieh Tehrani for always being a nice fellow in working out of hour. Thanks to Dr Fer Velazquez de la Paz for being a great buddy as always. I really look up to you for always being energetic in everything. I've also learnt a lot from you. Thanks to Tugba for being a nice support, we're always have a chat while we're working in the lab. Thanks to the coffee break gang, Denata, Jose, and Alice, for always being mentally supported. I really love and enjoy the time having a chat with you guys. A little special to Alice, thanks to you for doing the proofread the first two chapters of this thesis. I really appreciate it.

I have to admit that This journey was not easy for me who had so little background in this field, yet my first language is not English. But thanks to Gwen, Helen, Fred, Amy, and all fellows in Lab C+09 (Julie, Rob, Dhanak, Liam, Hossein, Dirar, Zena, Marzieh, Rasmus, Tugba, Denata, Jose, Alice, Hafsah, Areli, and Caitlin) that always made me warmed, enjoyed, and encouraged in every step of this journey. Also, thanks to everyone I've ever met in Kroto, the IMSB group, and Dental school that was always nice to me.

Thanks to Nicholas, Pomme, Sine, JJ, Yongyee, Jo, Jewlew, Ming, Krit, and Deem, Thai friends in the UK along my journey for making my life in the UK become greater than I thought. Also those fellows in Thailand, thanks for being a safe zone for me when I was lost. Even a text or a call was enough to make me feel I'm home.

Thanks to Sheffield for being a nice city and being very closed to peak district. Nature always brings us the calm. I already feel like here's my second home.

Lastly, Thanks to mom and dad for always supporting me in every way. I made this so far because of you.

To this point, I don't know how many "Thanks" words I've used, it may be very brief and repeated. But this is my sincerity feeling that I would like to express to everyone who was along my journey. Every one of you has contributed this thesis to become possible.

Thanks to the moon and back!

Your Ballad

Summary

Craniofacial defects can affect the area functions, strength, and aesthetics. While autograft has been used as gold standard to regenerate the tissue, the graft still has its drawbacks such as long operational time, limited tissue to harvest, donor site morbidity. Scientists have tried to overcome these by using tissue engineering and biomaterials. Poly(Glycerol sebacate) (PGS) is biocompatible and biodegradable. It's not frequently used in bone tissue regeneration. Decellularised extracellular matrix (ECM) is rich in growth factors essential for various cell behaviours. However, repairing craniofacial defect only bony part can lead to scar formation or graft failure from soft tissue invasion [1-5]. PGS was used as an implantable scaffold aiming to support co-culture of tissue regeneration of both bone and soft tissue with an option of decellularised ECM.

PGS scaffolds were fabricated by mixing various ratios of NaCl to polymer (2.5:1, 3.0:1, 3.5:1, 4.0:1, 4.5:1 w/w). After cross-linking at 120°C under vacuumed atmosphere for 24 hours, the salt was dissolved by submerging with deionised water. Human Telomerase Reverse Transcriptase mesenchymal stem cells (Y201) were cultured on these scaffolds for 14 days. All scaffolds could support Y201 attachment and growth similarly. A3.5 PGS was selected to seed with Y201 and culture for 21 days, cell matrix was then decellularised by incubating with 20 mM NH_4OH + 0.5% Triton x-100 for 24 hours and DNAse-I for another 24 hours. After recellularisaiton with the new set of Y201, decellularised matrix on PGS didn't enhance cell growth, differentiation or mineralisation when compared with PGS alone. Therefore PGS only was selected to move on to the next step; PGS scaffolds were seeded with Y201 and grown for 7 days before being flipped over and seeded with collagen and Human oral fibroblasts followed by (NOF343) and Human oral keratinocytes (FNB6) on top. The co-culture was grown for 10 days before being fixed, cryosectioned, and stained with H&E. A layer of Y201 matrix and a layer of NOF343 + FNB6 were observed on each side of PGS without any invasion noted.

Therefore, PGS has a possible potential as an implantable scaffold in craniofacial tissue defect repair both bony and soft tissue part.

Table of contents

List of Abbreviations

µg	Microgram
µm	Microlitre
µm	Micrometre
2D	Two dimensional
3D	Three dimensional
ALP	Alkaline phosphatase
ANOVA	Analysis of variance
ASCs	Adipose stem cells
BAG	Bioactive glass
BCA	Bicinchoninic acid
BGS	Bone graft substitutes
BMPs	Bone Morphogenic Proteins
C	Celsius
cm	Centimetre
CNC	Computer numerical control
DBM	Demineralised bone matrix
DMEM	Dulbecco's Modified Eagle Medium
DMSO	Dimethyl sulfoxide
DNA	Deoxyribonucleic acid
dsDNA	Double stranded deoxyribonucleic acid
ECL	Enhanced chemiluminescence
ECM	Extracellular matrix
EDTA	Ethylenediaminetetraacetic acid disodium salt dihydrate
ESCs	Embryonic stem cells
FBS	Foetal bovine serum
FDA	The Food and Drug Administration
FGF	Fibroblast growth factor
g	Gram

GAGs	Glycosaminoglycans
H&E	Hematoxylin and eosin
HIPE	High-internal-phase-emulsions
hPL	Human Periodontal Ligament
HRP	Horseradish peroxidase
hTERT	Human telomerase reverse transcriptase
IBSP	Integrin binding Sialoprotein or Bone sialoprotein II
IgG	Immunoglobulin G
kPa	Kilo pascal
mg	Milligram
min	Minute
ml	Millilitre
mm	Millimetre
MPa	Mega pascal
MSCs	Human bone marrow-derived stromal cells
MSCs	Mesenchymal stem cells, stromal cells
ng	Nanogram
nm	Nanometre
nmol	Nanomolar
OCT	Optimal cutting temperature
PCL	Poly-Caprolactone
PDMS	Polydimethylsiloxane
PGA	Poly(glycolic-acid)
PGS	Poly(glycerol sebacate)
PLA	Poly(lactic-acid)
PLGA	Poly(lactic-co-glycolic acid)
Pmma	Polymethyl meth-acrylate
pNP	p-nitrophenol
pNPP	p-nitrophenyl phosphate

PolyHIPE	Polymerised high-internal-phase-emulsions
PU	Poly(ester urethane)
rpm	Revolution per minute
RUNX2	Runt-related transcription factor 2
SD	Standard deviation
SDS	Sodium dodecyl sulphate
SEM	Scanning Electron Microscopy
SHG	Second harmonic generation
TBP	Tri(n-butyl)phosphate
TCP	Tissue culture plastic
TEM	Transmission electron microscopy
TGF-β	Transforming growth factor beta
v/v	Volume per volume
w/w	Weight per weight

.

List of Figures

List of Tables

Chapter 1

Introduction

Craniofacial tissue consists of a bony layer with oral mucosa or epithelium on the top. Whilst the bony layer of craniofacial tissue acts as a core, giving a support to all the vital organs on a head, face, and oral cavity, the soft tissue layer acts as a protective sheet to the bone, blood vessels and nervous system, which lead to normal function of this whole region.

Craniofacial tissue defects can be a health problem in general regardless of age or sex since the defects affect various functions, such as swallowing, breathing or chewing. About 1% of newborns worldwide were reported to have birth defect anomalies [6]. Although there is no collective data for the number of congenital craniofacial anomalies in UK overall, the incidence of facial cleft alone was reported to be 0.127% in the UK [7]. While on the other side of the world, there was a report in Thailand showing an incidence of newborns with facial cleft to be 0.22% [8, 9]. In adults, craniofacial tissue defects are most commonly caused by traffic accidents. The incidence can be up to 50% in developing countries. Other reasons may be non-traffic accident trauma, inflammation, infection, tumor, or cancer. As the area is highly related to aesthetics, as well as the aforementioned vital functions craniofacial defects will storngly affect a person's quality of life in terms of mental health, which in some cases can be a serious issue [10-12].

Treatment choices nowadays to regenerate the area are typically surgical technique using bone autografts, allografts, xenografts, or bioactive glass to fill the defect. Whilst bone autografts have been used as a gold standard for bone repair, these creates donor site morbidity and there is limited tissue available for harvest. The other graft types were introduced to overcome these drawbacks of autografts, but they are still inferior in terms of enhancing bone regeneration and create issues of immunocompatibility.

Tissue engineering using bone graft substitutes to repair the defect has gained attraction from researchers recently. Bone graft substitutes can be made up of various biomaterials. Polymers

have been regularly used as biomaterials because they are easy to fabricate in porous forms, can be degradable, and have tuneable mechanical properties. Poly(glycerol sebacate) (PGS) is a polymer with good biocompatibility and biodegradability, recently proposed for medical uses, having already been tested in soft tissue engineering. PGS has not been examined as a bone graft substitute in clinical applications, but the polymer was shown to be biocompatible to bone cells, supporting them to lay down their matrices [13, 14].

In parallel, laboratory cultivation and harvesting of extra cellular matrix (ECM) is gaining attraction as a method to fabricate or supplement scaffolds for bone tissue regeneration. Initially decellularisation has been used as a technique to wash out cells from xenografts, when tissues of other species are used clinically, to reduce immunological response [15, 16]. However, the richness of ECM in valuable proteins has been well demonstrated and ECM matrix can support reseeded cells to attach, proliferate, and differentiate.

Therefore, decellularised bone matrix on porous PGS scaffold is a promising approach to produce an implantable bone graft substitute. Also, as mentioned before, both a bony and oral mucosa layer are important for the craniofacial area. Therefore in order to treat a craniofacial defect fully, both layers need to be repaired. Thus, it is very interesting to identify whether a scaffold could support a multilayer co-culture of the bony layer and soft tissue layer, aiming to fully repair craniofacial tissue defects.

The project aims to produce an implantable biomaterial, capable of also supporting a soft tissue layer, to repair craniofacial bone defects using PGS with the option of decellularised cell-derived matrix. Chapter 2 will consist of a literature review on craniofacial bone structure, craniofacial defects, materials used in craniofacial repair, cells used in tissue engineering for craniofacial tissue repair, potential supplementation of scaffold with cell-derived ECM, and co-culture growth of cells on scaffolds.

Chapter 2

Literature review

2.1 Craniofacial bone defects

Craniofacial area defects are reported to affect various ranges of age. About 1% of newborns worldwide were reported to have birth defect anomalies [6]. In the UK, the incidence of facial cleft defects alone was reported as 0.127% [7]. While in the developing countries such as Thailand, the facial cleft defect incidence of newborns was reported to be 0.22% or around 1,000 people per year [8, 9]. Road traffic accidents are the largest cause of defects in adults (the incidence can be up to 50% in developing countries) [17]. Non-traffic accident trauma, inflammation, infection, tumour, or cancer can also cause defects to develop in the area as well as alveolar bone loss due to periodontitis or tooth removal.

Current available treatment choices are bone grafting, other tissue grafting, and bioceramics with or without metal plate and screw. Even though, autogenic bone grafting is the gold standard, but it can also cause donor site morbidity as well as the others which has its own limitations (*Table 2.1*). Trying to overcome these drawbacks, tissue engineering using other synthetic biomaterials are introduced to the field. Researchers has tried to improve this to-be-alternative choice of treatment to be as good as autografts with infinite reproducibility. As mentioned before, repairing the area is challenging by its structure, functions, and aesthetics, so addressing the best materials for tissue repair is warranted. Therefore, bringing innovations to improve methods to repair defects in a cost-efficient manner is an important objective, needed to better help patients.

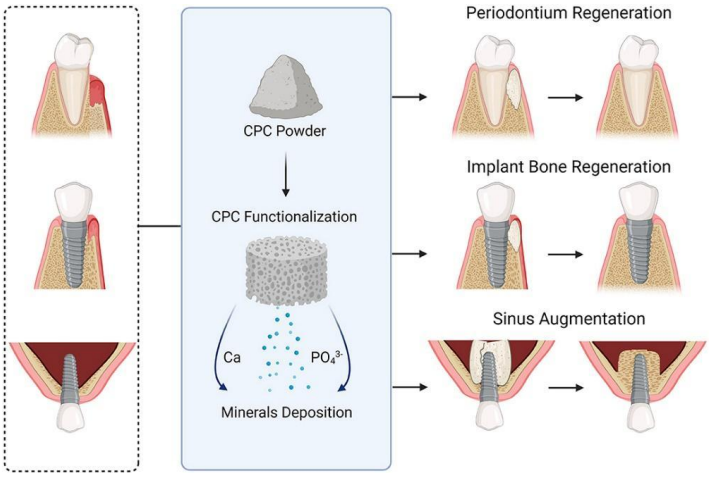

Figure 2.1 *Alveolar bone lost from periodontitis (Left) can strongly affect therapeutic efficacy of a dental implant. Bone graft substitutes (see section 2.3.3.), which in this case is calcium phosphate cement (Bioceramic) can be used to support and enhance bone regeneration of the defect. The diagram was reproduced from R. A. Alsahafi, H. A. Mitwalli, A. A. Balhaddad, M. D. Weir, H. H. K. Xu, and M. A. S. Melo, "Regenerating Craniofacial Dental Defects With Calcium Phosphate Cement Scaffolds: Current Status and Innovative Scope Review," (in English), Frontiers in Dental Medicine, Systematic Review vol. 2, 2021-August-30 2021 under Creative commons license [18].*

Figure 2.2 *A patient with a history of car accident who lost some part of skull bone (arrow (A)). An implant made of polymethyl meth-acrylate (PMMA) covered with Bioactive glass (BAG) was prepared in a model before the operation in order to repair the defect (B). The pre-made implant was placed onto the defect area (C). The diagram was reproduced from M. J. Peltola, P. K. Vallittu, V. Vuorinen, A. A. J. Aho, A. Puntala, and K. M. J. Aitasalo, "Novel composite implant in craniofacial bone reconstruction," European Archives of Oto-Rhino-Laryngology, vol. 269, no. 2, pp. 623-628, 2012-02-01 2012 under Creative commons license [19].*

Table 2.1 Current treatments of craniofacial bone defect

Treatment choices	Examples of materials used		Drawbacks
Bone grafting	Autologous bone	Iliac crest	Donor site morbidity.
		Fibula free flap	Peripheral vascular compromise should be concerned [20].
		Ribs	Extremely painful experience.
	Allogenic bone		Complicated procedure of processing with hardly predictable outcome.
	Xenogenic bone		Different species increasing risk of disease transmission. A lot of patients do not trust.
Reconstruction using other tissue	Soft tissue (tongue, skin and its underneath muscle, oral cavity tissue)		Often requires conjunction with bone graft to increase its strength [20].
Bioactive glass	Bioglass® 45S5, BonAlive® and 19-93B3 bioactive glasses		Sometimes requires other materials to give a structural support. Having problems with blood vessels penetration

2.2 Bone

Connective tissue acts as a supportive layer, protective layer, and a structural support to tissues and organs. Connective tissue is usually made up of cells and fibres. It can be categorised by its characteristics, cell components, and function into 4 types: blood, fat, cartilage, and bone.

2.2.1. Bone tissue

Bone is a hard tissue which protects all other important organs and gives structural support to the body. It is a mineralised tissue which is made of 25% organic matter (90% of which consist of collagen type I), 70% inorganic matter (calcium phosphate holds the largest proportion) and 5% water, with the collagen acting as a guide for the mineral component. It is composed of 2 categories which are cortical (compact) bone and trabecular (cancellous or spongy) bone. Bone tissue, contains specialised bone cells as follows:

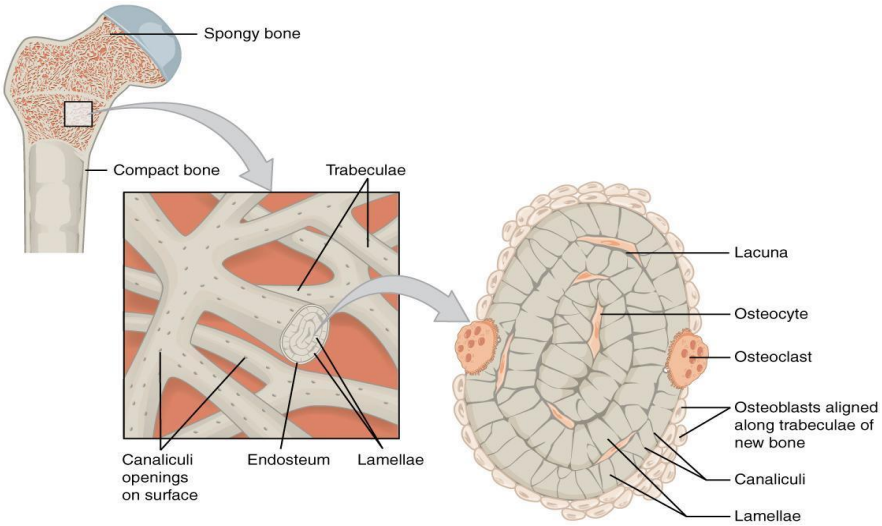

Figure 2.3 *Bone consists of 2 parts which are compact bone and spongy bone (Left). Spongy bone, is the area rich with blood vessels surrounding the structural units which are called trabeculae. The structure is a cylinder of bone tissue with several canaliculi (channels) opened to the surface (Left). The cross section shows each layer inside a trabecula which comprises of osteoblasts aligned to the surface of the bone. Osteoclasts located not too far from osteoblasts are responsible for bone resorption. While osteocytes are trapped inside spaces called "lacuna" surrounded by mineralised bone matrix and connected to the outside blood vessels by canaliculi (Right) The diagram was reproduced from L. M. Biga, S. Dawson, A. Harwell, R. Hopkins, J. Kaufmann, M. Lemaster, P. Matern, K. Morrison-Graham, D. Quick, and J. Runyeon, Anatomy & Physiology. Corvallis, Oregon, United states: Open stax/Oregon state university, 2019 under Creative commons license [21].*

Mesenchymal stem cells, stromal cells (MSCs) are the stem cells found in connective tissue that can renew themselves and differentiate into specialised cells. Their differentiation ability is multipotent (later to be discussed in detail), which briefly means they can differentiate into multiple types of cells (multilineage differentiation). It is for this reason mesenchymal stem cells are also popular to be used in tissue engineering (see section 2.3.3.). MSCs in which can

be induced to differentiate into osteoblasts are known as osteoprogenitors, and are generally found in periosteum, bone marrow, or sutures of the craniofacial area [22].

Osteoblasts are derived from osteoprogenitors and are responsible for producing an amorphous matrix which eventually becomes a dense fibrous tissue mostly containing collagen fibres, called an osteoid. Moreover, the cells are also accountable for calcium ion secretion which then forms hydroxyapatite which creates the calcified bone tissue.

Osteocytes are trapped inside newly formed osteoid. These cells take control of the mineral concentration of the matrix in a vital bone phenomenon called bone remodelling, a dynamic process of the removal of old or damaged bone and replacement with new bone.

Osteoclasts are multinucleated cells derived from the haematopoietic lineage. They have a ruffled edge to secrete bone-resorbing enzymes for the bone-break down process known as resorption.

2.2.2. Bone formation

The process of bone formation is termed ossification and can be classified into 2 types: Endochondral ossification and Intramembranous ossification.

Endochondral ossification

This type of bone-formation takes place in long bones such as legs or arms, the base of the skull, and during the healing process after bone fracture. Endochondral ossification begins when the mesoderm derived mesenchymal cells differentiate to chondrocytes. Chondrocytes gather and become hypertrophic to form hyaline cartilage by secreting a lot of collagen X and fibronectin, which in turn then becomes dense tissue, blocking any blood vessel penetration. The cells obtain a nutrient supply from blood vessels in the surrounding tissue, known as the perichondrium. However, blood supply also brings osteoblasts to gather at the outside of the cartilage tissue, and later form a calcified tissue which prevents the nutrient supply into the centre of cartilage tissue, and consequently results in the death of chondrocytes at the centre of the cartilage tissue. The central area then becomes a hollow space which later allows blood vessels to occupy the area. The blood vessels bring mesenchymal cells to the site, the cells

then differentiate into osteoblasts and this region is now termed the “primary ossification centre”.

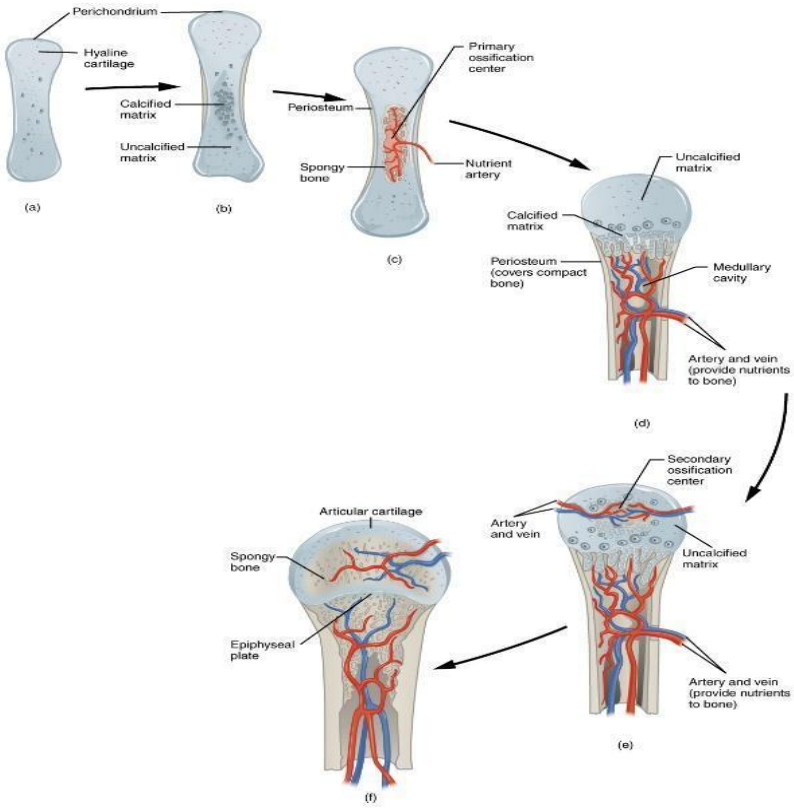

Figure 2.4 *A process of endochondral ossification (a) Chondrocytes build up the hyaline cartilage by secreting their extracellular matrix. (b) The nutrient for chondrocytes at the centre is blocked by a bony collar at the edge of the cartilage tissue. The cells become dead leaving a hollow space. (c) Primary ossification centre is formed. (d) Epiphyseal plate continues to grow, increasing the bone length. (e) Secondary ossification centre developed. (f) The bone becomes mature at the end, that is when bone stops growing along its length. The diagram was reproduced from L. M. Biga, S. Dawson, A. Harwell, R. Hopkins, J. Kaufmann, M. Lemaster, P. Matern, K. Morrison-Graham, D. Quick, and J. Runyeon, Anatomy & Physiology. Corvallis, Oregon, United states: Open stax/Oregon state university, 2019 under Creative commons license [21].*

The primary ossification centre then expands towards the distal aspect of the bone by nutrient support of blood vessels in the spongy bone. This is called the “diaphysis”. The chondrocytes on the distal end continue to proliferate, creating the matrix and increasing the bone length. This area is called the “epiphyseal plate”. Then after birth and up to adulthood, there is “secondary ossification centre” developed at the centre of the bone distal end (at the very distal end of epiphyses). The centre that develops resembles the first centre of formation. *[21].*

Intramembranous ossification

Intramembranous ossification normally takes place in flat bones, such as the craniofacial bones. Unlike endochondral ossification, the cartilaginous template is not needed for intramembranous ossification, the bone is formed directly from the connective tissue of MSCs. Some MSCs differentiate into osteoblasts and start secreting osteoid bone matrix, making the area become an "ossification centre". Some MSCs then differentiate into endothelial cells, bringing blood supply into the area. The osteoid matrix becomes mineralised consequently, and encompasses the osteoblast, causing it to terminally differentiates into an osteocyte. This event induces the mesenchymal cells surrounding the tissue to differentiate into osteoblasts, which results in an expansion of the region of bone formation, forming a trabeculae network with abundant blood vessels.

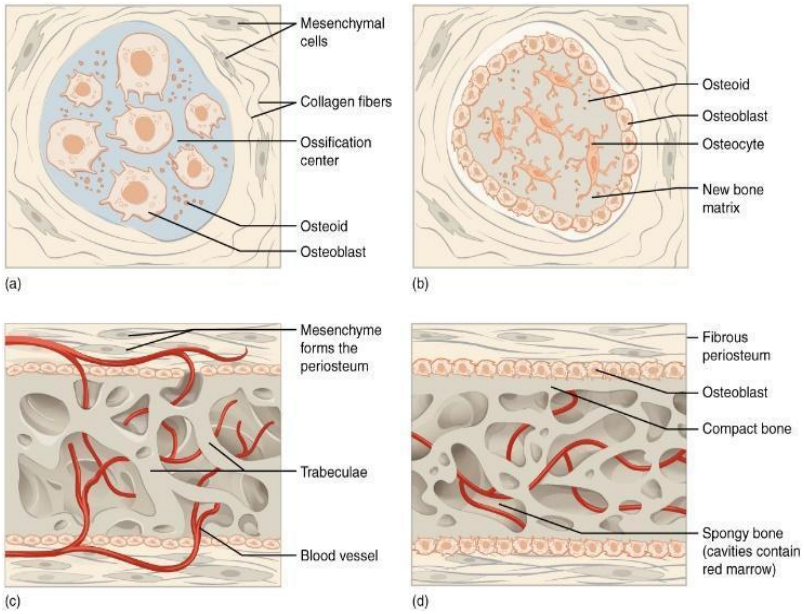

Figure 2.5 *Intramembranous ossification: (a,b) the ossification centre has started from osteoblasts entrapped in the osteoid matrix which leads those osteoblasts to become osteocytes. (c) Some MSCs differentiate into endothelial cells bringing blood supply to the area (d) While, the outer zone of the ossification centre consists of mesenchymal cells which later developed to be fibrous periosteum. The diagram was reproduced from L. M. Biga, S. Dawson, A. Harwell, R. Hopkins, J. Kaufmann, M. Lemaster, P. Matern, K. Morrison-Graham, D. Quick, and J. Runyeon, Anatomy & Physiology. Corvallis, Oregon, United states: Open stax/Oregon state university, 2019 under Creative commons license [21].*

2.3. Craniofacial defect repair

2.3.1. Natural bone regeneration

Bone fracture can be healed spontaneously over 3 stages:

- Inflammation

After bone fracture, blood vessels in that fractured area also become damaged. Inflammatory signals in blood vessels start to work together until a blood clot is formed. This can be called “blood hematoma”.

- Bone production

Blood vessels bring mesenchymal cells to the fracture site, which then differentiate into chondrocytes. Fibrocartilaginous tissue, known as a “soft callus” is formed, which later is replaced by “hard callus” via endochondral ossification.

- Bone remodelling

Once the hard callus is formed at the fracture site, the osteoclasts and osteoblasts work together in the remodelling stage to regenerate the area. This stage takes a several months before the fracture site returns to a healthy bone.

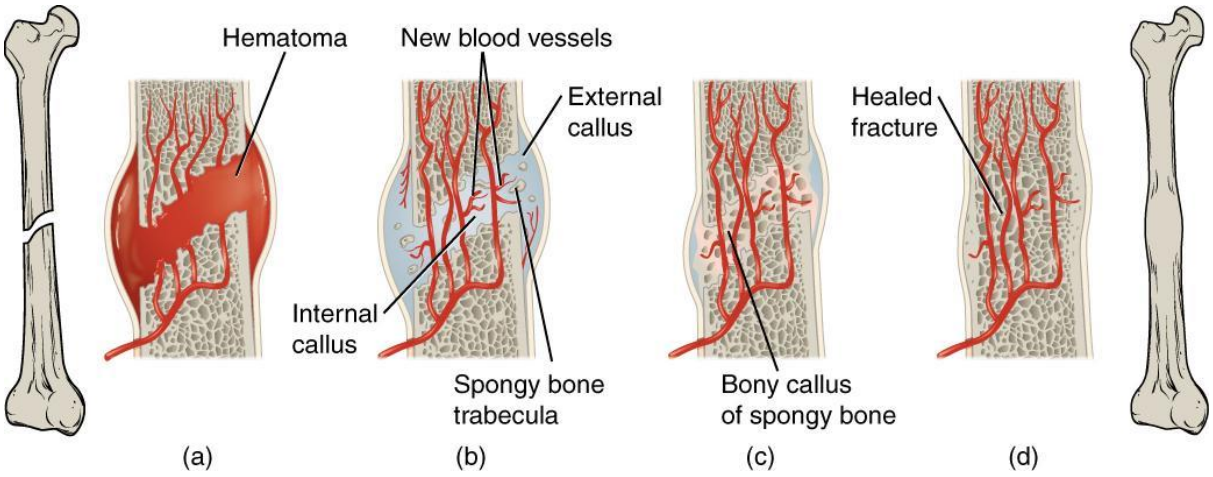

Figure 2.6 *Bone fracture healing model (a) hematoma from blood clot is formed. (b) Soft callus which is secreted from chondrocytes act as a scaffold for hard callus to be formed later. (c) The hard callus is remodelled by osteoblasts and osteoclasts slowly regenerating the fracture site. (d) It takes up to 6 months for bone to be fully healed. The diagram was reproduced from L. M. Biga, S. Dawson, A. Harwell, R. Hopkins, J. Kaufmann, M. Lemaster, P. Matern, K. Morrison-Graham, D. Quick, and J. Runyeon, Anatomy & Physiology. Corvallis, Oregon, United states: Open stax/Oregon state university, 2019 under Creative commons license [21].*

2.3.2. Conventional Bone regeneration

During the bone fracture healing process, spontaneous bone remodelling occurs. However, in larger size bone defects, it is not possible for the bone to grow over the defect and naturally heal itself. In those cases, bone supports, or regenerative treatments are needed. Bone regeneration aims to restore structure, mechanical strength, and function. In order to restore the defect, typically healthy bone tissue from another source is used. The process of surgery is called “tissue grafting” which places the graft into the defect site, with the aim to induce tissue regeneration. Grafting has been introduced for bone tissue regeneration widely especially in craniofacial regions such as the midface area (the area between eyes and mouth), maxilla, mandible, or skull due to accident, inflammation, cancer, of cleft anomalies [23-27]. These various studies used a graft from various sources which can be easily classified as 3 groups: autografts, allografts, and xenografts.

Autograft

Grafts can be classified based on the sources which are autograft, allograft, and xenograft. An autograft is the graft taken from another part of the patient’s body. It has been used as a gold standard for a long time for due to beneficial characteristics such as good mechanical properties, histocompatibility, immunocompatibility, osteoconductivity and osteoinductivity [27-29]. However, a significant drawback is the limited amount of tissue available to be harvested. If a lot of tissue is taken, the donor site function might be affected. Especially for a large defect, this can be difficult to harvest sufficient tissue without any interference in the source tissue function. Also, the morbidity of the donor site and the additional invasive surgical site should be considered as one of the drawbacks of autologous bone grafts [28, 30, 31].

Allograft

An allograft is a graft that is collected from another body, but same species seems to be a preferable choice to overcome the disadvantages of autografts. Nonetheless, their risk of immune rejection and disease transmission is still their undeniable weaknesses as well as their significantly high cost [28, 32-35]. To avoid risk of those drawbacks and to enable access to the growth factors that are trapped in mineralised tissue, allograft bone which usually is

collected from a cadaveric is demineralised and sterilised before use. Demineralised bone matrix (DBM) is bone where the mineral content has been dissolved and then washed out, resulting in an osteoconductive bone organic matrix with necessary growth factors for osteoinductivity without a report of severe immunological rejection [26, 36, 37]. There are a number of commercially available DBM allografts, which are used in craniofacial repair mostly to fill bone voids in the area [38]. However, using DBM alone was found to have various success rates in bone regeneration from even using the same batch of commercially available DBM. None of them could compete with autograft [38, 39].

Xenograft

Xenografts are another alternative to autografts. The graft is derived from the other species, which then causes limitations such as strong immune reaction, cross-species disease transmission, and its animal derivation able to affect the agreement of patients using the graft for the treatment. Most clinicians nowadays refuse to use xenografts for bone grafting [40-42]. There are a number of commercially available of bone xenografts which have generally gone through various processes such as decellularisation, cross-linking, and sterilisation. Also the donor animal to be harvested must meet a list of certain requirements of The United States Food and Drug Administration (FDA) in animal breeding and tissue harvesting [43, 44].

2.3.3. Alternative bone regenerative medicine techniques

Bone regenerative medicine is one branch of medicine aiming to develop a method that can restore the bone defect area, in order to become fully functional and overcome the drawbacks of those conventional bone regeneration techniques. The field branches into 3 broad terms: bone graft substitutes, tissue engineering, and biomaterials, by where each term is not a subset but overlapped with another.

Bone graft substitutes (BGS)

Recently, tissue engineering using bone graft substitutes has been introduced to overcome the complications of using conventional bone graft. Researchers working with BGSs have tried to accomplish development of unlimited availability of BGS which can mimic bone autograft's regenerative feature without causing donor site morbidity or any other complications to the

host body. There 4 common sources of BGS materials: calcium sulphate, calcium phosphate, tricalcium phosphate, and coralline hydroxyapatite. However, as it is a brittle powder and has no shape it therefore limits BGS to be used in a large defect. It also lacks the ability to recruit vasculature to penetrate to the centre of the graft [42, 45, 46].

Tissue engineering approach

Tissue Engineering is the multidisciplinary research area comprised of experts from clinical medicine, mechanical engineering, materials science, genetics, and related fields working together. This cooperative field focuses on delivering live cells and tissue to the defect area. It contains 3 parts:

1. Scaffold: acts as a carrier and gives a structural support which can be varying from bone graft, bone graft substitutes, or biomaterials.
2. Growth factors: such as Bone Morphogenic Proteins (BMPs) which are added to enhance the cells differentiation, therefore enhancing the bone regeneration.
3. Live cells: Lastly but the most important key of this approach, ideally live cells are autologous mesenchymal stem cells. It is the best cell choice because of their non-adverse immune response, but drawbacks such as being time-consuming, limited cell survival after biopsy, and low expansion rates should be considered.

However, there are commercially available tissue engineering products such as Osteocel Plus®, Trinity Evolution®, Cellentra VCBM®, and Allostem® which comprise of bone tissue and MSCs which are both harvested from cadaveric tissue, making them allogenic. There is only one company claiming their product, Ovation®, comes with cells harvested from a living donor [47].

Stem cells

Stem cells are undifferentiated cells, capable of renewing themselves and differentiation to other cell types. As discussed in previously discussed in section 2.2.1. mesenchymal stem cells are the origin of osteoblasts. Due to these attractive properties, they have been used in tissue engineering, in vitro cell culture and medical regenerative medicine for a decade. They can be classified into two types.

- **Based on their capability of differentiation**
    - Totipotent stem cells: zygote and early blastocyst from day 1-3 after fertilization can differentiate to all cell types.
    - Pluripotent stem cells: inner cell mass of blastocyst during day 4-14 after fertilisation can differentiate to all cell types except extra-embryonic cells. Best known for this cell type are Embryonic stem cells.
    - Multipotent stem cells: can differentiate into cells within one specific cell lineage.

- **Based on their source of origin**
    - Embryonic stem cells: derive from inner cell mass of the blastocyst and have the promising ability to differentiate to all germ layers (Ectoderm, Mesoderm, and Endoderm). Their use is still controversial.
    - Adult stem cells: are distributed in various areas of the body, and also can differentiate into any cells in any germ layers. In last few decades, this cell type has been used generally in scientific laboratories, especially in tissue engineering [48-50].

A popular stem cell type for clinical use is the human bone marrow-derived stromal cell (MSC), an adult multipotent stem cell. Due to its ability to differentiating into adipose, cartilage, or bone progenitor cells, it has been frequently used in the tissue regeneration field. However, the cells do have the drawback that a population of MSCs will contain cells that are heterogenous in terms of their differentiation ability, and are donor-dependent [51]. This is very challenging for those who aim to create a repeatable homogenous matrix for tissue repair..

Human telomerase reverse transcriptase (hTERT) MSCs, are immortalised clonal cells, which have been previously developed by our collaborators, originally developed to understand differentiation of primary MSCs. Y201 sub-clonal cells have been demonstrated to have multipotent properties, including the potential to differentiate into osteoblasts, as expression of specific bone markers were shown such as Runt-related transcription factor 2 (RUNX2), osteopontin and alkaline phosphatase (ALP) genes expression, and deposition of mineralised matrix [52, 53]. Immortalised cells are attractive for use in the current project because the

aims require a consistent batch of cells which can be frequently passaged and tested under a range of conditions. Avoiding the drawback of limited cell life span and variance between donors that occurs with primary cells.

Using stem cells in tissue engineering has created high expectations in providing a recreation of the tissue in the defect area. However, there were some reports demonstrated that even using tissue engineering products with live cells successfully support bone regeneration, but the major drawback is that a product with live cells needs to be frozen and thawed at the right time to avoid losing cell viability, so it is unpopular before routine clinical use. Furthermore, the needs to pre-harvest the cells and expand their number to the required amount is very challenging [47, 54, 55].

Biomaterials

The field of biomaterials focuses on developing materials, either acellular or used in combination with tissue engineering methods, for use as a model for diagnostic use, or as an architectural framework for bone tissue engineering. It is usually considered as a temporary scaffold for tissue regeneration.

Cell-free scaffolds were developed to avoid the issue of dealing with live cells in terms of the need to pre-obtain the cells, expand their numbers, store and thaw them correctly. The key to a cell-free scaffold is that it should be biocompatible, biodegradable, and able to allow or even attract cells to migrate into the scaffold, attach to the scaffold, proliferate, and differentiate, to eventually result in tissue formation [56, 57].

Microstructure such as porosity, average pore size, and interconnection size should be considered when designing a scaffold. High porosity promotes cell attachment, proliferation, and nutrient or signalling molecule distribution. An appropriate pore size for bone tissue regeneration has been suggested to be in a range from 100-500 μm [57, 58]. But the challenge of a cell-free scaffold is whether it can really support tissue regeneration without the complex biomolecules involved in natural bone healing..

- **Metal**

  Iron, Magnesium and Titanium based scaffolds are frequently used in bone tissue engineering as they have suitable mechanical strength and stiffness to give support to the

regenerated area. However, metal biomaterials also have disadvantages that need to be considered such as inflammatory stimulation and systemic toxicity of Iron, corrosion and toxicity Magnesium, and lack of biodegradability and bioactivity of Titanium [59-64]. Metals are stiffer and stronger than bone itself which can lead to a phenomenon called 'stress shielding' as the bone does receive sufficient load transfer from the implant, resulting in poor osteointegration around the metal [63, 65].

- **Bioactive ceramic**

Hydroxy-apatite, bio glass and β-Tricalcium phosphate have been frequently used in bone regeneration. Bioactive ceramics have a higher mechanical strength than polymers, but a much lower fracture toughness compared to human bone, as ceramics are not able to resist cracks, whereas bone is a composite that can absorb microdamage prior to failure [66].

- **Polymers**

Many polymers have a range of fabrication routes that make it easy to create the desired shape, size, biological properties, microstructures (porosity, pore size and interconnectivity) and to finely tune these properties. Many polymer types have good biocompatibility and biodegradability. The mechanical strength is lower than for metals and ceramics, but it can be very different depending on the polymer composition. Furthermore, polymers have the advantage of being quite flexible and tough relative to other materials.

Natural polymer Silk, alginate, and chitosan have the potential of being a good scaffold for tissue regeneration. However, they are complicated in their structure, hard to be purified and easily transmit pathogens [67].

Poly-Caprolactone (PCL) is one of the best-known promising materials in bone tissue engineering. However, PCL is highly hydrophobic which affects cell attachment, as the cells are less able to attach on hydrophobic surfaces compared to hydrophilic. PCL is also very slowly degradable. A lot of research have tried to overcome these limitations by blending PCL with other materials [68-72] and surface treatment [72, 73] which make the scaffold is more complicated to produce.

Poly (α-hydroxyacids) is the group of polymers frequently used in medical-related fields even FDA such as Poly(lactic-acid) (PLA), Poly(glycolic-acid) (PGA), and their derivatives. However, their most concerning drawbacks are the difficulty of tuning their bioactivity due to an absence of a functional group on the chain, a bulk degradation and byproducts from degradation which are acidic [74-76].

Table 2.2 Summarising of bone tissue repair

Bone repair materials	Components			Advantage	Limitation
	Scaffold	Growth factors	Live cells		
Autograft	Bone tissue	Yes	Yes	- Immunocompatible - Osteoconductive - Osteoinductive	- Donor site morbidity - Long operational time - Limited tissue
Allograft	Processed bone tissue	Varying depended on bone processing	No in general but a new set of cells can be added	- More tissue to be harvested	- Risk of immune reaction - Disease transmission - Various success rates
Xenograft	Processed bone tissue	Varying depended on bone processing	No but a new set of cells can be added	- Abundant tissue to be harvested	- Strong immune reaction - Disease transmission - Lots of clinicians refuse to use - High standard to meet
Bone graft substitutes (BGS)	Bioceramics	No but can be added	No but can be added	- Unlimited amount - Immunocompatible - Osteoconductive	- Not suitable for large defects - Vascularisation able to penetrate to the centre is still challenged

Tissue engineering	Any	Depends on scaffolds material	Yes (usually is added)	- Using several components to mimic autografts	- Complicated in terms of storage and thawing before uses - High money and time consuming
Biomaterials (cell-free scaffold)	Biomaterials	No but can be added	No	- It is synthetic which means it is tunable - Unlimited amount	- The best materials that can overcome autograft is still warrant

2.4. Poly (glycerol Sebacate) (PGS)

PGS is a tough elastomeric polymer derived from lipid molecules. It has been used on its own or combined with other materials in various laboratory trials of medical regenerative applications, such as Temporomandibular disc, cartilage tissue, cardiovascular vessels, cardiac muscles, nerve tissue and retinal tissue [77-81]. PGS also plays a role in controlled drug delivery and other medical application such as surgical sealant preventing postoperative abdominal adhesions [82-84].

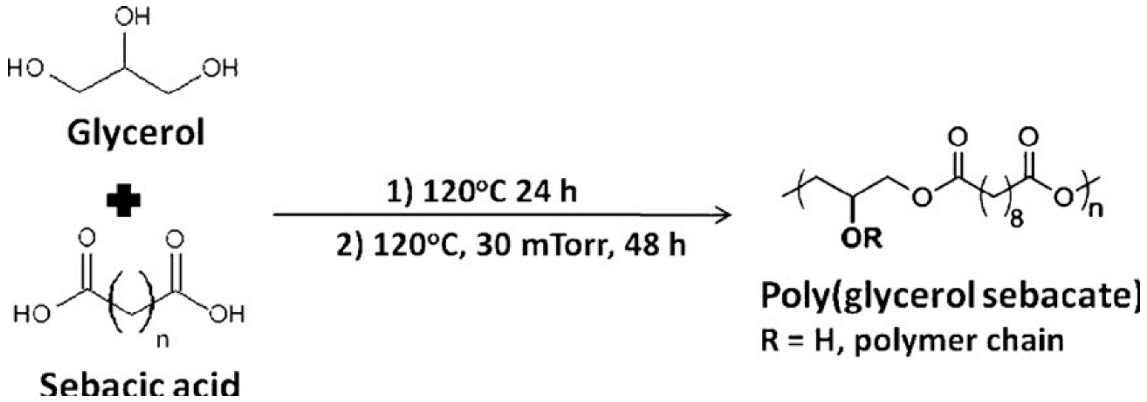

Figure 2.7 *Chemical structure of glycerol and sebacic acid (on the left side of the arrow). They can be mixed and undergo high temperature (120 C for 24 hour) which induces a cross-linking reaction. The cross-linked prepolymer becomes poly(glycerol sebacate) as shown on the right of the arrow.*

PGS is said to be a biocompatible, biodegradable soft elastomeric polymer. It is a product made of Glycerol and Sebacic acid through polycondensation. Glycerol is the metabolite generally found in the human body and Sebacic acid is a saturated, naturally occurring

dicarboxylic chain generally found in human urine [85]. So, both components of the material can be excreted from the body through natural routes without harm to the body. The prepolymer needs to be cured via cross-linking; either thermal curing [86-88] or chemically curing [89, 90]. It was reported that with increasing curing temperature, then the density of crosslinking of the material is increased [87]. Since it is degraded by surface erosion, the scaffold structure can be slowly replaced with bone matrix, which is good for bone regeneration in terms of retaining the structure. Wang *et. al.* showed that the polymer can be absorbed, in vivo, within 60 days and decreases in mechanical strength by about 8% per week [91, 92].

PGS was reported to be soft with a range of Young's moduli from 0.004-0.280 MPa. One said salt leached PGS (of unknown porosity) was reported to have 270% elongation and tensile Young's modulus of 0.282±0.0250 MPa. It was discussed that the Modulus was about that of ligaments [93]. Alternatively, Gao *et al.* found 80% porosity of salt leached PGS had a Young's modulus at 0.004±0.001MPa [94], while Zaky et.al. discovered their 90% porosity of salt leached PGS had Young's modulus similar to osteoid tissue at 0.038±0.03 MPa [95]. This may be caused by different salt volume incorporated or porosity which the first study didn't state. Since PGS is known to have elastomeric properties, some used it to increase elasticity of tricalcium phosphate. Adding only 15% v/v PGS to tricalcium phosphate increased 3.7-fold of tensile strength and 200-fold compared to the tricalcium phosphate alone. [96]. Being more hydrophilic than other polymers, it was combined with PCL and electrospun. Whilst the electrospun PCL had its contact angle as high as 130±3°, the PGS/PCL was wetted completely within a few seconds, and subsequently giving better attachment [97]. The other advantage of PGS is its inexpensiveness compared to other commonly used biomaterial polymers [98, 99].

As stated above, PGS has been studied for use in various tissues, especially in soft tissues in animal models. Unlike soft tissue, PGS studies in bone tissue engineering has not been carried out frequently. Despite low mechanical strength compared to bone tissue, PGS has been found to be able to support cell mineralisation which could imply that the cells are able to differentiate on soft PGS scaffold. One group using salt leached PGS alone (3x3x2 mm^3) discovered MC3T3-E1 cells can proliferate on the scaffold and differentiate into osteoblasts [13]. Another group found that salt leached PLA based scaffolds coated with PGS seeded with MSCs produce mineralised tissue not different from PLA alone [100]. Adding only 15% v/v PGS

to tricalcium phosphate allowed rat MSCs to proliferate and differentiate better than tricalcium phosphate alone [96]. Zaky *et al.* transplanted a hollow tube of salt leached PGS (90% porosity) into an induced ulna defect of a rabbit. There were 3 groups transplanted: (1) PGS alone (2) PGS + 20% Hydroxyapatite (3) PGS + rabbit MSCs. 8 weeks after implantation, bone volume was assessed using a microCT. This showed that PGS with MSCs had the highest bone volume as expected, but surprisingly that PGS alone had a higher bone volume than PGS with hydroxyapatite, suggesting future research into osteoconductive properties of PGS may show promising results [101].

Although PGS has shown biodegradability, biocompatibility, and osteoconductivity, it does not show osteoinductivity. As bone graft substitutes should mimic bone autograft as close as possible, a study aimed at tuning the PGS to have osteoinductivity will be carried out in this project.

Table 2.3 Comparing advantages and disadvantages of materials

Materials	Advantage	Disadvantage
PCL	- Widely used in medical research especially in bone regeneration. - It can be manufactured with various techniques.	- Highly hydrophobic which cells are less likely to attach. - poor mechanical properties, slow degradation rate, and low cell adhesion.
PLGA	- Frequently used in medical related fields. - It is soluble in various common solvents.	- Its byproducts are acidic. - Difficulty in tuning its bioactivity.
PGS	- Easy in tailoring mechanical properties and degradation kinetic. - Cost-effective production with the possibility of up scaling to industrial production.	- Not much details of using in bone tissue engineering. - Its soft consistency might not be a good choice for those require strengthening.

2.5. Processing Porous polymer scaffolds

2.5.1. 3D printing

3D printing is an increasingly popular process to create a porous polymer scaffold because of its ability to create a precisely designed structure. The process is also known as additive manufacturing or the layer-by-layer method. 3D printing has a great potential to enable the user to tailor most details of scaffolds at a micro-scale range. It can create a scaffold in precisely shape or specific pattern depends on design. It was widely used in medical related field where recreating a specific shape of organ or a complicated structure is needed especially in craniofacial region. It was introduced in tissue engineering to construct a scaffold as designated [102, 103], construct a tissue model with cells prompted [104-106]. However, this method is expensive and complicated to optimise [107]

2.5.2. PolyHIPE

Polymer high-internal-phase-emulsions (HIPEs) are used to make porous scaffolds by using droplets (internal phase) to create pores inside the polymer (external phase). Various techniques have shown that so far only small structures can be made with PolyHIPEs, it is difficult to control the size of the pores which in general are too small for blood vessel invasion, so to include larger pores it would need to be combined with another technique such as stereolithography, making fabrication time consuming and expensive [108, 109]

2.5.3. Porogen leaching

Porogen leaching is frequently used for making porous polymer scaffolds because it is an easy, cost effective and rapid process. The porogen consists of particles that can be embedded into a polymer solution and then dissolved or melted after the polymer has set, leaving behind voids which create the pores. Various particles can be used as the porogen such as sugar, salt, paraffin beads or ammonium carbonate. Some residual porogen might affect the biocompatibility of the scaffold and affect the cells seeded in the scaffold. Therefore, full removal of the porogen is important in the fabrication of porogen leached porous scaffold casting.

Table 2.4 Manufacturing methods of porous polymeric scaffolds

Manufacturing methods	Advantage	Disadvantage
3D printing	- Great potential of tailoring details of scaffold in a micro scale.	- Expensive and complicated to optimise or reproduce. - Highly require expertise in using and maintenance.
PolyHIPE	- Does not need a technology as expensive as 3D printing. - Less time consuming	- Difficult to control the size of the pores. - Only small structures can be made.
Porogen leaching	- The method is simple - Reasonable cost suitable for limited resource project.	- The leftover porogen can affect biocompatibility depends on the porogen material. - Challenging in controlling pore size and pore distribution.

2.6. Microstructure of scaffold

The microstructure is known to play an important role in scaffold properties, whether biological or mechanical properties, and would also play an important role in guiding the deposition of extracellular matrix (ECM) (to be discussed later in section 2.7). Pore size, in terms of surface area has been demonstrated to affect the adhesion of cells, for example smaller pore sizes in the range of 50-100 μm seem to benefit cell attachment according to previous studies. Larger pore sizes of 300-800 μm are needed for the growth of vascular systems [58, 110-113]. In addition, the average pore size is known to affect the mechanical properties by affecting overall porosity and polymer distribution. Smaller average pore size results in a higher Young's modulus [113]. Thus, distribution of pore sizes and average pore size needs to be considered in the optimisation of scaffolds both biologically and mechanically.

The porosity of salt leached porous PGS scaffolds can be controlled directly by the amount of salt that is being used. As shown in some previous studies, 70-90% by weight of salt demonstrated the best interconnection between pores [114].

2.7. Extracellular matrix as a scaffold

Extracellular matrix is where abundant proteins act as a protective and supportive layer to the cells they encapsulate. It contains extracellular proteins such as collagen, fibronectin, and other cell adhesive proteins and proteoglycans which play the role of supporting cells and regulating cellular function. Also, ECM contains a lot of signaling molecules and transcription factors essential for cell metabolism and tissue maturation.

As well as other tissues, bone ECM consists of abundant proteins and gives a support to osteocytes. Key proteins of bone tissue are collagen type I, fibronectin, Osteopontin (bone sialoprotein 1), and integrin-binding sialoprotein (IBSP; bone sialoprotein 2). ECM directly influences many essential signaling molecules such as Bone Morphogenic proteins (BMPs), Wingless and int-1 (WNT), Parathyroid Hormone-related Protein (PTHrP) and or transcription factors such as SRY-related HMG-box 9 (SOX9) and Runt-related transcription factor 2 (Runx2).

Table 2.5 Key proteins in bone extracellular matrix using in this thesis

Proteins	Roles in bone tissue
Collagen type I	Provides a structural support to cells and tissue.
Fibronectin	A glycoprotein that involves in several steps of fracture healing including acting as a guiding scaffold for ECM to form.
Osteopontin	Relates to bone homeostasis and bone metabolism via cellular activities.
IBSP	Involves in regulating hydroxyapatite crystals forming in bone tissue.

In the past, researchers tried to approach medical problems such as severe injury by using an organ or tissue transplantation, but its limitation caused serious problems such as organ or tissue rejection. Due to the recipient's immune response acting against donor antigens which come with the transplanted tissue, any transplant patient must take immunosuppressive drugs for a long time to prevent rejection of the transplanted tissue. To overcome the problems of rejection, grafts have been developed for substitution of damaged or diseased tissue such as using a porcine heart valve as an artificial heart valve. Because these are allografts or xenografts which would raise a host immune response, they need to be decellularised.

The concept of decellularisation is to modify the organ or tissue by removal of cell components by physical, chemical, detergent, or enzymatic processes to remove the factors that can stimulate a host immune response. The process gives us a tissue or organ without cell components but retaining its protein rich matrix. The ECM was used as a directly implanted graft, a scaffold in tissue engineering, or a modifying part on biomaterials in tissue regeneration [115-117].

2.7.1. Decellularisation techniques

Decellularisation techniques have been developed for decades for clinical practice and in tissue engineering. There are various methods of decellularisation, these can be classified as physical, chemical, detergent and enzymatic. There is no gold standard for the process of decellularization. The optimal method depends on tissue or organ differences of cell density, matrix density, thicknesses, shapes of tissue and composition of tissue [118, 119]. It is currently not possible to obtain a perfect decellularisation as cell remnants are not always totally eliminated, nor is every ECM structure conserved in the form it was prior to the decellurisation process [118].

Physical method

The physical methods are the simplest and most general method of destroying cellular material. This uses freeze-thaw cycles, agitation, or ultrasonic stimuli to destroy cells. Multiple freeze-thaw cycles are the most popular methods, in which the cells are disrupted by swelling from ice crystals until break and collapsing when thawed. Whilst other methods might disrupt

ECM structure, freeze-thaw is popular since it's simple, yet only little change occurs to matrix structure which then results in the mechanical properties of ECM not being altered [29, 102, 120-122].

Chemical method

The chemical method is normally referred to as an acidic and basic solution. There have been several recent trials attempting using acidic solutions. These usually completely removed cells. Whilst peracetic acid had little effect on ECM, acetic acid wiped all collagen out [123-127]. Any kind of base is very strong and is able to wipe out all growth factors in ECM and subsequently reduce ECM strength, so it must be very carefully used.

Ammonium hydroxide (NH_4OH) is frequently used in decellularisation, especially in dense tissue due to the alkaline base's strong ability to denature DNA and cell membrane lipids [127-130]. There are a few reports that use ammonium hydroxide to decellularise a whole organ. Studies reported a use of 50-100 mM sodium hydroxide with 0.5-1% triton x-100 perfused to successfully decellularise a whole liver and also preserve ECM content [131, 132]. It was interestingly used in cell-derived matrices quite frequently, especially in bone-like matrices. All studies used the concentration at around 20 mM which was enough to wash native cells out and preserve the ECM proteins [127-130, 133]. It was usually used conjugately with a detergent such as SDS or triton x-100, but the latter was more common to the bone cell-derived matrix [127-129, 133]

Detergent method

Sodium dodecyl sulphate (SDS) and Triton X-100 have been suggested in this category. SDS is a strong ionic detergent which can completely burst cells, but also affects matrix proteins. Another limitation is that the SDS decellularised matrix can be biologically incompatible, since it is hard to remove SDS from the tissue and SDS itself is cytotoxic [134]. Triton X-100 is an organic detergent which works by dissociating the interaction between lipid molecules which has various results from no cells removed at all to effective cell removal, depending on tissue density and was reported to have less damage to ECM structure [127-129, 133, 135, 136]. Tri(n-butyl)phosphate (TBP) is another organic solvent that is used in some previously published studies. It was comparable to SDS in its ability for cell removal in patellar tendon. The results showed that both had successfully removed cells without altering mechanical

properties. However, after 14 days of recellularisation into the tissue, SDS was shown to have cytotoxicity drawback. Whilst TBP treated samples supported a good rate of growth of human dermal fibroblast [137], it is clear that organic detergent is better for decellularisation than ionic detergent in terms of ECM preservation and cytotoxicity to the cells.

Enzymatic method

DNase is an enzyme frequently added into the detergent mixture to help to cleave DNA strands. It was normally used in a combination with other methods to make sure the DNA structure got cleaved out. There was no evidence that showed its destructive effect to ECM. [102, 119, 138]. Another well-known enzyme is trypsin which can dissociate cells from their matrix. However, collagen structure was reported to be destroyed when it was exposed to trypsin for too long [139, 140]. As with other enzymes there are natural inhibition molecules which can decrease the enzyme working efficacy.

2.7.2. Decellularised tissue source

The tissue to be used as a decellularised tissue graft can be classified based on collection source; which can either be from intact tissues or organs harvested from the donor (Tissue-derived decellularised ECM) or *in-vitro* cultured cell-layers and engineered tissues (Cell-derived decellularised ECM) [136].

Tissue-derived decellularised ECM

Previous studies demonstrated *in vitro* that bone tissue decellularised ECM could reinforce osteogenic differentiation of human embryonic stem cells (ESCs) and human adipose stem cells (ASCs) when reseeded on a decellularised porcine bone [141]. Even without dexamethasone (an essential supplement for bone cell differentiation; see section 2.8.2.), decellularised bone was demonstrated to be able to drive rat MSCs to undergo osteogenic differentiation [142]. Bone tissue engineering has used tissue-derived decellularised ECM as a grafting material due to its biological and mechanical properties which resemble nature bone matrix. However, tissue-derived decellularised ECM has its limitation of shape and size of tissue to be collected and a risk of disease transmission.

Cell-derived decellularised ECM

Cell-derived decellularised ECM can be obtained from in vitro cell culture. At first, it was generally used as a model for studying cell behaviour such as how ECM components influence differentiation behaviour of cells and as an *in vitro* model for regulating stem cell differentiation [136]. However, to use ECM in the tissue engineering field, it needs to be possible to fabricate it in specific sizes and shapes. Thus, procedures have been developed to grow various cells on scaffolds made with a range of biomaterials, to create decellularised ECM and biomaterial combined structures with adjustable size and shape with more promising cellular responses and mechanical properties compared to ECM alone. Replacing tissue-derived decellularised ECM with autogenic cell culture-derived matrix can also reduce the use of allografts or xenografts, which could then be safer in terms of immune response and disease transmission. However, this depends on how healthy the patient and patient's cells are.

Integra™ is one of the best examples of the most recent commercially available cell-derived decellularised matrix. It is made of a bilaminate sheet of cross-linked bovine tendon collagen and shark glycosaminoglycans, which is designated to act as a template for skin regeneration in a patient with severe skin burn [143].

There were several studies attempting to bring cell culture-derived ECM under the spotlight of regenerative medicine. In 2014, Shtrichman *et al*. used mesenchymal progenitor cells to grow ECM on PCL and PLGA electrospun nanofiber layers before the secreted matrix was decellularised by hypertonic solution and agitation. The scaffolds were then placed subcutaneously under animal skin for 8 weeks before being analysed. PCL nanofibers were shown to induce more host response than PLGA, since PCL has a slower rate of degradation. Both PCL and PLGA nanofibers with ECM showed better integration with host tissue and less host immune response compared with the nanofibers without ECM [115]. In another experiment, decellularised ECM from grown mesenchymal stem cells on silk fibroin patch scaffolds was implanted onto a wound on the skin of diabetic mice. The wound healing time was about 7 days faster with the decellularised scaffold compared to only silk fibroin [144].

Some studiesused ECM differently, for example human dermal fibroblasts were seeded and grown on an electrospun fibrous mat of Polycaprolactone (PCL) thendecellularised with ammonium hydroxide and milled into a powder which then was mixed with PCL prepolymer to create a scaffold. The study showed that PCL with decellularised ECM had a superior tensile modulus, and ability to support cell attachment and growth compared to other scaffolds tested [145].

In the bone tissue regeneration field it was found Bbone osteoprogenitor decellularised ECM enhanced the osteoinductive properties of biomaterials. A PCL fibrous mat with secreted ECM from mouse pre-osteoblast cells was subjected to a decellularisation process by multiple freeze thaw cycles. The scaffolds were plasma treated with LF Plasma. Re-seeded preosteoblasts were shown to attach, differentiate and mineralise on PCL with ECM more than they did on pure PCL [16]. Thibault *et al* found that decellularised bone cell-secreted ECM can induce reseeded MSCs to differentiate into osteoblasts without adding dexamethasone, an essential supplement for bone cell differentiation (see section 2.8.2.) [121]. These examples of the osteoinductive properties of MSC derived ECM may indicate that it can be beneficial for craniofacial bone repair.

Generally, bone cell cultivated tissue has been decellularised by NH_4OH with Triton X-100 or Freeze-thaw cycles [127-130, 133]. Recent work demonstrated that 3 cycles of freeze-thaw was enough to satisfactorily decellularise cell-derived matrix on various biomaterials [120, 121]. Although, it has been reported that 3 minutes treated with 0.5% Triton X-100 buffer containing 20 mM NH_4OH in PBS maintained the fibre pattern better than 3 cycles freeze-thaw [122]. However, the property of Triton X-100 and ammonium hydroxide to disrupt lipid molecules may not be suitable for the decellularisaiton of ECM on a PGS base since PGS contains lipid molecules [135].

Table 2.6 Samples of decellularisation techniques in tissue engineering

Tissue or products	Decellularisation technique used				Details in decellularisation
	Physical	Chemical	Detergent	Enzymatic	
mesenchymal progenitor cell ECM on PCL and PLGA electrospun nanofiber layers	•				- Hypertonic solution and agitation - The nanofibers with ECM showed better integration with host tissue and less host immune response compared with the nanofibers without ECM [115].
mesenchymal stem cell ECM on silk fibroin patch scaffolds	•				- Distilled water. - Improved wound healing (within 10 days) and enhanced VEGF cell migration compared to silk fibroin alone [144].
Human dermal fibroblast ECM on an electrospun fibrous mat of Polycaprolactone (PCL)		•			- Ammonium hydroxide and milled into a powder - A scaffold from a mixture of PCL and decellularised ECM powder demonstrated a superior tensile modulus, and ability to support cell attachment and growth compared to PCL alone [146]
Mouse osteoblast on a PCL fibrous mat	•				- Three freeze thaw cycles in deionised water - Re-seeded preosteoblasts were shown to attach, differentiate and mineralise on PCL with ECM more than they did on pure PCL [16]
Murine MSCs ECM on PCL electrospun fibers	•				- Three freeze thaw cycles in deionised water plus 10 minutes of ultrasonication - Decellularised bone cell-secreted ECM can induce reseeded MSCs to differentiate into osteoblasts without adding dexamethasone [121].

Bone cell ECM on various scaffolds	•	•	•		- NH_4OH with Triton X-100 or Freeze-thaw cycles [102, 127, 129, 130, 133].

2.7.3. Evaluation of decellularised ECM

Success of cell removal

To evaluate the success of decellularisation, residual cell components should be evaluated. The evaluation can be done by observation with Scanning Electron Microscopy (SEM) [145, 147], transmission electron microscopy (TEM) [147] or phase contrast microscopy. Microscopy stains or fluorescent labelling can be used to visualise residual cell components, for example by actin staining with Phalloidin [148], Glycosaminoglycans (GAGs) staining with Alcian Blue [127], nuclei staining with DAPI [29, 127].

However, those staining under microscopy techniques may not be appropriate for this project, especially those requiring fluorescence as PGS is auto-fluorescent. Deoxyribonucleic acid (DNA) quantification measuring with PicoGreen is an alternative assay. This can tell us the total amount of DNA precisely as it can be compared to a standard curve to give the exact amount of DNA. This assay is also a cost-effective and simple method to perform [129, 130].

ECM preservation

In addition, the quality of extracellular matrix should be observed by comparing the matrix pre-decellularisation with post- decellularisation. Previous studies used many techniques to identify the ability of the method to maintain the matrix after treatment. The matrix can be observed with SEM analysis [122], TEM [122], or second harmonic generation (SHG). The alternative and cost-effective assay is to stain collagen fibres directly by Sirius red staining and measuring light absorbance of the stained colour using a microplate reader.

Biological effects

Biological effects of decellularised matrices can be tested by reseeding cells into the decellularised scaffold to examine cell attachment, growth, differentiation, and mineralisation to establish whether cells are able to re-create bone tissue.

In an aspect of Bone tissue engineering, studies have shown that decellularised osteogenic matrices contain various proteins (e.g., cell adhesion proteins, enzymes, growth factors, cytokines, etc.) in which osteoconductive and osteoinductive properties still remain in the materials [149, 150]. These properties should be able to enhance PGS scaffold in supporting bone regeneration to be close to the gold standard as much as possible.

Although other researchers have demonstrated good results of biocompatibility of salt leached porous PGS in the soft tissue engineering field [90], there is still no report of salt leached porous PGS combined with bone cell matrix for bone tissue engineering. Finding an appropriate amount of salt to yield a good amount of bone cellular matrix is needed.

2.8. Cell culture

Apart from the scaffold fabrication method that plays an important role in tissue engineering, it is also very important to know about *in vitro* cell culture. Cell culture or cell cultivation is the laboratory process in which cells are grown in a specifically controlled condition, mimicking *in vivo* condition. *In vitro* cell culture can be done to meet various objectives in regenerative medicine. It can be carried out for a therapeutic purpose such as tissue engineering, a drug test model, or a diagnostic model. Also, any certain cells can be cultured on a scaffold made with a certain material in order to test the scaffold's cytotoxic property, growth support, differentiation support, or a support to any specialised function of a certain cell. Lastly, it can be done to provide an ECM on the scaffold to be used as decellularised cell-derived matrix at the end. However, all purposes above can be easily classified depending on the purpose of using the cells, whether they are needed to be differentiated to become specialised cells or only expanded in numbers.

2.8.1. Laboratory Cell expansion

Cells are expanded to the number of cells required, usually without any specified condition in a sterile culture flask. Most expansion techniques are designed to maintain the cells in their original cell lineage, for this a media that supplies the nutrients for cell proliferation is required. Different components of medium can result in different cell growth rates. Culture medium can be briefly classified into 3 main categories.

Serum containing medium

Typical cell culture medium contains serum from blood to provide a full complement of nutrients. Most commonly 'foetal bovine serum (FBS)' is used, which is obtained from the unborn foetus of a cow. FBS provides various essential carriers for nutrients, hormones, growth factors, and enzyme inhibitors. A limitation of FBS is the inconstancy between batches and suppliers [151]. Disease transmission from animal serum is another potential concern if using FBS-containing medium for a clinical application [152].

Xeno-free medium (Human serum)

In xeno-free medium, animal serum is replaced with human serum, or other human blood derived products such as platelet lysate. Human serum was found to support cell growth significantly better than animal serum, especially that of human cells [153-157]. Within our own group we demonstrated that a commercially available serum free medium containing 2% human serum supported proliferation of primary human mesenchymal stem cells in 2D culture significantly better than 10% FBS [158].

Chemically defined serum-free medium

One downside to serum-based medium is that it can have some undefined natural proteins which might risk contamination or a variability in each batch. In order to overcome this issue, chemically defined serum-free medium was developed. In chemically defined media all components known, due to it being entirely synthesised in-lab [159-162].

Cell culture medium can consist of various constituents. However, there are some basic components which they generally all contain, for example a pH indicator (usually Phenol red), inorganic salts, an essential amino acid such as L-Glutamine, sugar, mostly in the form of glucose, vitamins, and serum, which contains nutrient carrier proteins, growth factor, growth inhibitor, and essential nutrients for cells. In the case of a long-term experiment, antibiotics are suggested to be added to the culture medium to avoid bacterial or fungal contamination. Penicillin-Streptomycin and Amphotericin B are widely used to prevent contamination. Some growth factors are needed for certain types of cells such as fibroblast growth factor (FGF) is normally added to help in enhancing osteoblastic lineage cell proliferation and differentiation.

2.8.2. Cell differentiation

Cultivation of cells can be undertaken with the purpose to drive undifferentiated cells to change into a desired cell lineage. For example, in bone tissue engineering, MSCs are grown with the purpose to produce mineralised tissue eventually by differentiating them first into osteoblasts. The standard media used for expansion the cells has to be modified with supplements adding such as ascorbic acid, β-glycerol phosphate, and dexamethasone [163].

2.8. Co-culture

2.8.1. Uses of co-culture

As previously mentioned, to fully treat a craniofacial bone defect, it is not only about the bony layer, but also the surrounding soft tissue covering. Scar formation is one complication that can occur to the surrounding soft tissue after bone repair with implantation. Not only can it cause serious aesthetical changes in noticeable areas such as facial skin or scalp, but it can also affect the tissue's mechanical properties and functions as well. A scar was reported to gain back only 80% of the mechanical strength of normal skin due to the disorganization of the collagen fibres [164]. This commonly happens when the tension of a surgical flap is too high, meaning there is not enough soft tissue to cover the surgical site [165]. Contrary to the skin, the oral mucosa wound healing tends to be more flawless, with the scar being nearly non-observable, which is good in the aesthetic aspect [166, 167]. However, there were still some cases in that excessive fibrosis occurred after an operation, which can severely affect oral organ function and quality of life, with some cases needing subsequent surgical intervention [168-172].

There are a few solutions that have been made previously to attempt to prevent this from occurring. These are flap surgery, soft tissue grafting, and soft tissue graft substitute. Flap surgery is a very popular reconstruction method for skin or oral cavity, by moving one end of a piece of skin or oral mucosa with its original blood supply from an adjacent area of the operational site (one end of a flap still attaches to the original area) to cover a surgical site, which can decrease the tension of the surgical wound. Similarly, soft tissue grafting can be done by taking soft tissue from another area but with no blood supply from the original site required, so it can be taken from anywhere else on the body. However, these 2 techniques

required a secondary surgical site with longer operational time and the tissue to be harvested is limited in some conditions, causing issues when there is a large defect to be covered, or for diabetic patients [173, 174]. A surgical site can be covered by a soft tissue graft substitute which is made from a biocompatible synthetic material that can enhance soft tissue regeneration. However, there haven't been any skin graft substitutes that can perfectly mimic the real soft tissue [175].

Another issue is that soft tissue is known to grow and heal more quickly than bone. Bone was reported to start healing after 2 weeks to months or years, while the first 2-3 weeks was reported to be soft tissue peaks and 12 weeks was reported to be the end of normal wound healing [1-5]. This may sometimes result in soft tissue ingrowth at the implant site, which can interfere with bone regeneration. This is generally found in the oral cavity. The ingrowth of soft tissue can be prevented by using Guided Bone Regeneration (GBR) which is the method of using a barrier to split the bony layer from the gingival layer. One report showed that covering an implanted site with a membrane resulted in more bone volume regenerated compared to those without a membrane [176]. A membrane made of non-resorbable material gives good support but needs a second operation to remove it after the bone is fully regenerated [177]. Resorbable membranes made of collagen or synthetic polymer were reported to be weaker than the first group in supporting the gingival layer and sometimes collapsed [178]. There is currently no GBR membrane that is resorbable, yet strong enough to support tissue structure and requires only one surgery at the present knowledge.

Bone regeneration is not the only key factor for craniofacial tissue repair success. Finding a proper implantable material to support cell growth of both bony and soft tissue layers, and support craniofacial tissue regeneration is an essential key to repairing a craniofacial defect. However, this means that there are at least 2 cell types on one implantable scaffold. Co-culture is the term that has been used to define a model that cultures at least 2 cell types at the same time or the same place. Co-culture has been suggested to be used in various ways within regenerative medicine. This thesis will classify co-culture depending on the purpose of its application:

Co-culture as a study model

In-vitro cell culture can demonstrate an effect that a certain chemical compound in a certain amount will have on a certain type of cell. However, it cannot fully mimic the true nature of the body, which is composed of more than a single population of cells within one small area. Co-culture is hoped to be used as a model to fill this gap of heterotypic cellular interaction. Some co-culture helps enhance the culture of one type of cell, especially seen in bacteria cultures in which it has lately emerged as a model to support drug development [179-181]. A study was conducted to develop drugs by using a co-culture between drug-resistant cancer cells and drug-sensitive cancer cells, in which both cells were differently fluorescently tagged. This can help in understanding the interaction that the new drug has on both the individual cell type and between cell-to-cell [182].

Alais et.al. found culturing found a triculture of cardiomyocytes, smooth muscle cells, and endothelial cells helped improving cell numbers of cardiomyocytes and endothelial cells, especially endothelial cells which was improved more than 5-fold compared to monolayer co-culture [183]. There were a number of studies that focus on direct cell-cell interactions. There was a formation of blood vessel-like tissue within 3 days of co-culture of bone marrow endothelial cells and MSCs. This has shown the synergy between the two cells in creating one specific tissue [184]

Culturing human MSCs with rat cardiomyocytes revealed that MSCs could have human-specific myosin, the marker of differentiation into cardiomyocytes. This supported the idea that MSCs can differentiate through signalling sent from cell-to-cell interactions [185]. This behaviour of MSCs was also supported by a study by Richardson *et al*. that showed MSCs have a marker of differentiating into the Nucleus Pulposus (NP) from intervertebral disc only when they were cultured in direct contact with the NP. This marker was not seen in those that were not in direct contact [186]. This also applied to MSCs to osteoblasts when co-cultured on a 3D scaffold [187].

The use of co-culture was also adapted to focus on paracrine signalling and response to soluble signalling factors. Co-culture of fibroblasts and osteoblasts on a tri-phasic scaffold (a scaffold with a barrier layer in the middle that prevents two populations of cells from making contact with each other) was noted of promoting the production of fibrocartilage by raising

several markers. This model could indicate that both cells might interact in creating fibrocartilage tissue *via* paracrine signals [188]. Some could be conducted through a trans-well insert. Seeding anterior cruciate ligament (ACL) cells in an insert with a permeable membrane can induce the MSCs cultured in a lower chamber to differentiate into ACL-like cells [189, 190]. Using a hydrogel matrix allowed for the complete separation of osteoblasts from osteocytes in their co-culture. This can be used to study their interaction via gene expression without cross-contamination of their RNAs [186]. Some groups have developed co-culture as a model to understand specific events within the body, such as the bone-implant interface, wound healing, or bone remodeling (osteoblast-osteoclast) for better understanding the mechanism, cells interaction, or signaling molecules pathway within a certain event [191-194].

One study carried out a co-culture technique as a biological test for a scaffold made from biomaterial whether the scaffold is suitable to be implanted for tissue regeneration. Osteoblasts and osteoclasts may be co-cultured for various reasons, but one of those could be to test the scaffold if it was able to support bone tissue regeneration in both bone formation and bone resorption [194]. In 2014, Puwanun *et al.* co-cultured human dermal fibroblasts (HDFs), human embryonic stem cell-derived mesenchymal progenitor cells (hESMPs), and MSCs on a trilayer electrospun PCL scaffold, in order to test whether PCL could support full craniofacial tissue regeneration. Seeding each cell type on the different sides of a scaffold, with a middle layer of the scaffold acting as a barrier layer found that there was a mineralised matrix from both cells, hESMPs and MSCs. While on the other side HDFs could attach to the PCL with a middle layer perfectly separating both cells apart [195].

Another study demonstrated co-culture of 3 populations of cells, MSCs, human oral fibroblasts, and keratinocytes (FNB6), which were seeded on an electrospun PCL scaffold. MSCs were seeded to one side, whilst NOFs were seeded on the other side, and FNB6 cells were seeded on top to mimic the oral mucosa tissue. After 28 days of culture, there were 2 layers of cells on both sides of the scaffold [158]. These studies show that biomaterials can support 2-3 cell types simultaneously to grow and deposit their matrices, with a possibility of craniofacial tissue regeneration support.

Co-cultured tissue as an implant

Whilst the co-culture may have many benefits as a model to study cell interactions, the use of a co-culture system as an implant is another interesting aim within regenerative medicine. There have been multiple *in vivo* studies of cartilage repair using co-culture of chondrocytes and MSCs on (1) salt-leached Poly (l-lactic acid)/poly (lactide-co-ε-caprolactone) (PLLA/PLCL), and (2) electrospun PCL to implant into animal models. It was demonstrated that MSCs co-seeded with chondrocytes on any material yielded a higher cartilaginous tissue when compared to chondrocytes alone, whilst the scaffold with MSCs alone showed no cartilaginous tissue [196, 197]. For bone tissue engineering, the co-culture technique was introduced to be used to assist in vascularisation. MSCs and MSC-derived endothelial cells were seeded on porous β-tricalcium phosphate ceramic (β-TCP) and implanted in a 1.5cm ulna defect in an animal model. The result showed vascularisation and significantly more bone formation than the group of β-TCP alone and β-TCP with MSCs [198]. Several studies found similar success in bone tissue regeneration by implanting a scaffold with MSCs and blood vessels related cells [199-201]. These results of co-culture implanted scaffolds show promising results in tissue regeneration using tissue engineering techniques. However, it requires pre-obtaining, expanding, a large storage capacity, and well-timed thawing of two types of cells, which may make tissue engineering more complicated.

Table 2.6 Examples of previous studies using co-culture.

Category of co-culture	What has been co-cultured?	Purpose or results
A study model	Cultures of various types of bacteria	***D***rug development, understanding drug resistance [179-181]
	A triculture of cardiomyocytes, smooth muscle cells, and endothelial cells.	Improving cell numbers of cardiomyocytes and endothelial cells compared to monolayer co-culture [180].
	Bone marrow endothelial cells and MSCs.	A formation of blood vessel-like tissue within 3 days of co-culture showing a synergy

		between the two cells in creating one specific tissue [181].
	Human MSCs with rat cardiomyocytes	MSCs could differentiate into cardiomyocytes [182].
	MSCs and Nucleus Pulposus (NP) from intervertebral disc	MSCs differentiated into the Nucleus Pulposus (NP) only when they were cultured in direct contact with the NP [186].
	MSCs and osteoblasts on a 3D scaffold	MSCs differentiated into osteoblasts [187].
	Co-culture of fibroblasts and osteoblasts on a tri-phasic scaffold	promoting the production of fibrocartilage tissue *via* paracrine signals [188].
	MSCs in a lower chamber with anterior cruciate ligament (ACL) cells in an insert with a permeable membrane.	MSCs cultured in a lower differentiated into ACL-like cells [189, 190]
	Using a hydrogel matrix allowed for the complete separation of osteoblasts from osteocytes in their co-culture.	A model to study their interaction via gene expression without cross-contamination of their RNAs [202].
	Osteoblasts and osteoclasts on a 3D scaffold	Testing the scaffold if it was able to support bone tissue regeneration in both bone formation and bone resorption [194].

	human dermal fibroblasts (HDFs), human embryonic stem cell-derived mesenchymal progenitor cells (hESMPs), and MSCs on a trilayer electrospun PCL scaffold	The trilayer PCL electrospun can separate the layer of MSCs and hESMPs from a layer of HDFs perfectly [195].
An implant	MSCs and chondrocytes seeded on salt leached PLLA/PLCL and electrospun PCL	MSCs co-seeded with chondrocytes on any material yielded a higher cartilaginous tissue when compared to chondrocytes alone [196, 197].
	MSCs and MSC-derived endothelial cells were seeded on porous β-TCP	Improving vascularisation and bone formation significantly [198].

However, there are currently few studies that introduce co-culture to be used for full craniofacial tissue regeneration in terms of both the bone and soft tissue. This is a gap in research that should be filled. Though implanting a biomaterial scaffold with co-culture of cells was reported to show promising results in tissue regeneration, implanting a biomaterial as a scaffold is certainly less complicated, less time-consuming, and more cost-effective. It is necessary to first study whether a PGS scaffold or PGS scaffold with a cell-derived decellularised matrix can support cell growth and matrix deposition of both bony and soft tissue parts to fulfil the aim of craniofacial tissue regeneration.

Chapter 3

Materials and methods

3.1. 3D Salt leached porous Poly(glycerol sebacate)

3.1.1. Synthesis of PGS prepolymer

Glycerol (Sigma-Aldrich, UK) and sebacic acid powder (Sigma-Aldrich, UK) were weighed equimolarly, placed in a 3-neck flask and mixed with a magnetic stirrer at 120°C using an oil bath and nitrogen gas system (1 bar or 100 kPa). The mixture was left under these conditions for 24 hours, and then a vacuum pipe was connected to the system for a further 24 hours.

3.1.2. Creating a mould for the PGS scaffold

A mould was created using SYLGARD™ 184 (DOW chemical, US) or Polydimethylsiloxane (PDMS) using silicone base and a curing agent provided in the kit mixed together (10:1 v/v) and cured at 70 ℃. A hole was punched into the crosslinked PDMS sheet (diameter = 1 cm) which later became a mould for a scaffold.

3.1.3. Fabrication of porous PGS scaffold using the salt leaching method

A known amount of PGS prepolymer was mixed with NaCl salt (ThermoFisher Scientific, UK) at a series of weight/weight ratios (*Table 3.1*). The mixture was incubated at 120°C in an oven for 1 hour. Subsequently, the oven chamber was vacuumed, and continuously incubated for further 24 hours. After 24 hours of curingunder heat and vacuum, the polymer was submerged in deionised water for 3 days to dissolve the salt grains (*Figure 3.1*). The scaffolds were initially prepared with various amounts of salt with the hypothesis that scaffolds will have more pores at a higher concentration of salt.

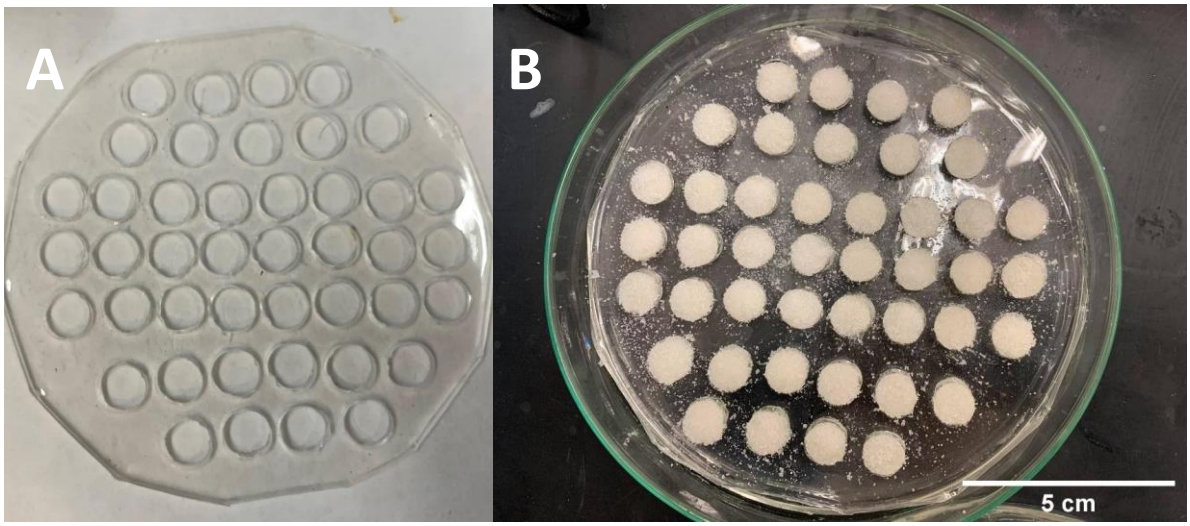

Figure 3.1 *(A) The PDMS mould prepared for fabricating a scaffold. (B) The mixture of PGS prepolymer and NaCl salt was placed into a PDMS mould.*

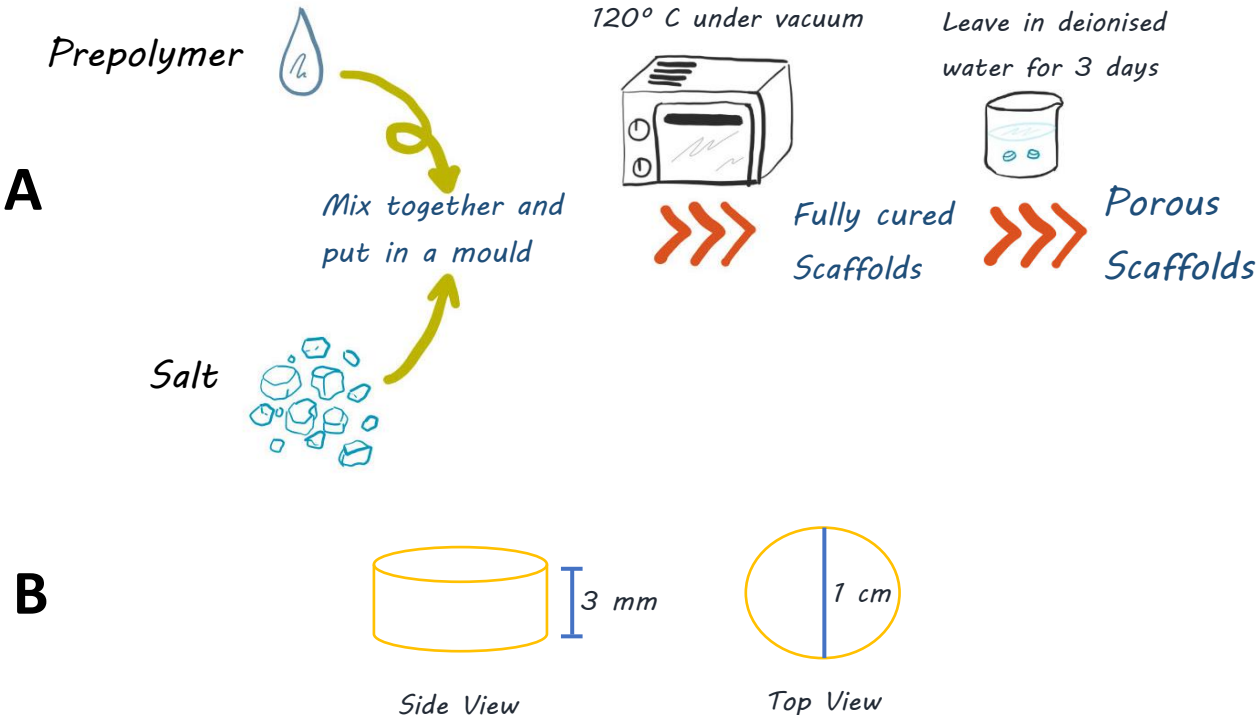

Figure 3.2 *(A) Diagram of fabrication of a salt leaching PGS scaffold. A mixture of prepolymer and NaCl salt in a mould were crosslinked in the 120°C oven under vacuum for 24 hours. Once fully cured, a scaffold was soaked in deionised water for 3 days for NaCl salt to be dissolved leaving behind pores in the PGS scaffold. (B) Diagram of a salt leaching PGS scaffold in a side and a top view, a scaffold was expected to be a disc with a diameter of 1 cm and 3 mm thick.*

Table 3.1 Porous PGS scaffolds were made at different ratios of salt to prepolymer (w/w)

Scaffold	Salt amount (g)	Prepolymer (g)
2.5	2.5	1
3.0	3.0	1
3.5	3.5	1
4.0	4.0	1
4.5	4.5	1

3.1.4. Porosity assessment of the prepared scaffolds

Drying porous scaffolds

To assess the scaffolds either physically or mechanically, the scaffold needs to be dried to prevent any harm to the machine. The porous scaffold was dried by a freeze-drying method. The scaffolds were frozen for 4 hours and incubated in a desiccator overnight under vacuum at room temperature.

Scanning electron microscopy (SEM)

The dried porous scaffold was mounted on a stainless-steel stub with a carbon sticker. The mounted sample was subsequently coated with 5-10 nm of gold (Sorby Centre, UoS) and lined by silver at the sides to enable a full electrical circuit. The coated specimens were left overnight to be dried. The images were created by using an electron beam of Inspect™ F SEM under vacuum which scanned across the surface of the scaffold to image the porosity at 5 kV. The generated SEM images were used to measure pore size and evaluate porosity using ImageJ™. Pores were selected by superimposing a grid of 9x8 and pores at the intersection were measured to ensure they were selected randomly. Each selected pore was measured by drawing a line across the widest diameter of the pore.

Porosity measurement using a pycnometer

The dried scaffold was weighed using a balance. Then, the scaffold was put into the designated sample chamber of the pycnometer (Micromeritics AccuPyc™ 1340). Pore volume, material

volume and material density were calculated by the equipment using the pressure of helium gas which had diffused into the pores of the scaffold.

$$Porosity = \frac{V_0 - (\frac{m}{d})}{V_0}$$

The equation was used to calculate porosity of a scaffold where V_0 is the scaffold volume calculated as measured using callipers, m is the scaffold weight, measured on a high precision balance, and d is the scaffold density which was assessed using the pycnometer.

3.1.5. Mechanical assessment of the scaffolds

Scaffold fabrication for mechanical testing

To get the best data for the scaffold tensile strength, the material should be in a 'dog bone' shape which was required to reduce the influence of grip force [198]. So, the scaffold was fabricated as a large sheet with the same thickness as the discs (3 mm).

Laser cutting scaffolds as a designated shape

The scaffold was dried prior to cutting. The scaffold was cut as into dog bone shapes using a Laserscript® LS3040 Desktop. This laser cutter was a high-power laser beam created by electric discharge with an excitation from a mixture of gas medium inside a closed container. The cutting pattern was designed using software and controlled by a computer numerical control (CNC). A jet of air was released to blow any burnt or melted polymer from the cutting surface.

Tensile strength testing

A dog bone shape scaffold with 3 mm x 10 mm in size at the test compartment (*Figure 3.2*), was mounted with both grips of Mecmesin® MultiTest 2.5-dV. The force and the distance were recorded by the software VectorPro. Once the scaffold was ripped apart, the force immediately fell to zero, this indicated the failure point (*Figure 3.3*).

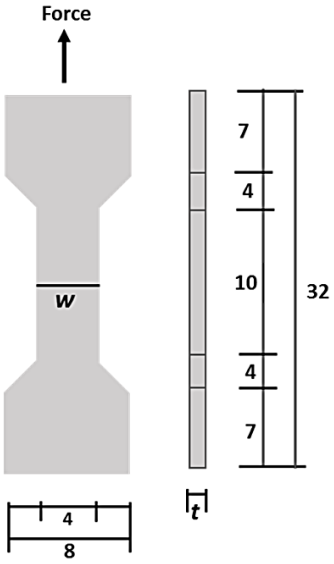

Figure 3.3 *A scaffold in bone shape required for a tensile strength test to reduce the influence of the grip force. Length and width of each compartment as shown were used following the previously studies (All dimensions were in mm). While the thickness (t) and width (w) were of our scaffold, 3 and 10 mm respectively. The diagram was reproduced from A. I. Pangesty and M. Todo, "Improvement of Mechanical Strength of Tissue Engineering Scaffold Due to the Temperature Control of Polymer Blend Solution," Journal of Functional Biomaterials, vol. 12, no. 3, p. 47, 2021-08-14 2021 under Creative commons license [203].*

3.2. Cell culture

3.2.1. Cells

Human telomerase reverse transcriptase MSCs (Y201)

Human bone marrow-derived stromal cells (MSCs) contain cells that are heterogenous in terms of their differentiation ability, and are donor-dependent [51]. Human telomerase reverse transcriptase (hTERT) MSCs, immortalised clonal cells have been previously developed by our collaborators to understand differentiation of Primary MSCs. James et.al. from the University of York created a subclonal line of cells called “Y201”, the cells were demonstrated to have multipotent properties, including the potential to differentiate into osteoblasts, and express of specific bone markers such as RUNX2, osteopontin and ALP genes expression, and deposit mineralised matrix [52, 53] Immortalised cells are attractive for use in this project because the aims require a consistent batch of cells which can be frequently passaged and tested under a range of conditions.

Human gingival fibroblasts (NOF343) and hTERT buccal keratinocytes (FNB6)

Since craniofacial tissue repair doesnot only require bone tissue but also covering soft tissue to prevent soft tissue invade into bone area, therefore co-culturing mimicking both bone tissue and soft tissue is important for testing whether a material supports craniofacial tissue regeneration. Fibroblasts and keratinocytes are the essential cells for epithelial soft tissues including skin and oral cavity mucosa. Human gingival fibroblasts (NOF343) and hTERT buccal keratinocytes (FNB6) have frequently been used in the past used in oral mucosa model construction in our colleague's group.

Table 3.2 Cell lines and primary cells being cultured in this thesis.

Cells	Tissue description	Source
Y201	hTERT bone marrow mesenchymal stem cell line	University of York
NOF343	Normal gingival fibroblast	Buccal fibroblasts isolated at Charles Clifford Dental School, The University of Sheffield with with written consent. Ethical Approval No. 09/H1308/66.
FNB6	hTERT atypical immortalised buccal keratinocyte cell	Beatson Institute for cancer research, UK (McGregor *et al.,* 2002)

3.2.2. Cell cultivation

General Cell culture proceedures

- **Expansion medium for Y201 cells**

Expansion medium or basal medium for Y201 composed of 89% of Dulbecco's Modified Eagle Medium (DMEM)(Sigma-Aldrich, UK), 10 % of foetal bovine serum (ThermoFisher scientific, UK) and 1% of penicillin-streptomycin (Sigma-Aldrich, UK)(*Table 3.3*).

Table 3.3 A list of components of basal medium for Y201 and NOF343 cells.

Components	Volume added	Final concentration
DMEM (high glucose)	445 ml	89%
FBS (Thermo Fisher, UK)	50 ml	10%
Penicillin-streptomycin	5 ml	100 I.U/ml penicillin, 100 µg/ml streptomycin

- **Osteogenic medium for Y201 cells**

Y201 can be driven to have osteogenic differentiation by supplemented basal medium with 50 µg/ml of Ascorbic acid (Sigma-Aldrich, UK), 5 mM of β-Glycerolphosphate (Sigma-Aldrich, UK), and 100 nM of Dexamethasone (Sigma-Aldrich, UK) at 1% each. The final concentration of each supplement was shown in *Table 3.4*.

Table 3.4 A list of components for osteogenic differentiation medium for Y201.

Components	Volume added	Final concentration
Basal medium	485 ml	N/A
Ascorbic acid 5 mg/ml (stock conc.)	5 ml	50 µg/ml
β-Glycerolphosphate 500 mM (stock conc.)	5 ml	5 mM
Dexamethasone 10 µM (stock conc.)	5 ml	100 nM

- **Green's medium for NOF343 and FNB6**

Green's medium was formulated to culture keratinocytes. The media is composed of components as shown in a *Table 3.5* below.

Table 3.5 A list of components for Green's medium for FNB6.

Component	Volume added	Final concentration
DMEM (Sigma-Aldrich, UK)	330 ml	66%
Ham's F12 (Sigma-Aldrich, UK)	108 ml	21.60%
FBS (Sigma-Aldrich, UK)	50 ml	10%
EGF (Invitrogen, UK)	50 µl of 100 µg/ml	10 ng/ml
Insulin (Sigma-Aldrich, UK)	2.5 ml of 1 mg/ml	5 µg/ml
Hydrocortisone (Sigma-Aldrich, UK)	80 µl of 2.5 mg/ml	0.4 µg/ml
Penicillin/Streptomycin (Sigma-Aldrich, UK)	5 ml	100 i.u./ml penicillin and 100 µg/ml streptomycin
Amphotericin B (Sigma-Aldrich, UK)	1.25 ml of 250 µg/ml	0.625 µg/ml
Adenine (Sigma-Aldrich, UK)	2 ml of 6.25 µg/ml	0.025 µg/ml
T/T (Sigma-Aldrich, UK)	0.5 ml of 1.36 µg/ml T3 and 5 mg/ml Apo-T	1.36 ng/ml T3 and 5 µg/ml Apo-T

- **Cell cryopreservation**

Cells previously frozen in cryovials containing freezing medium consisting of FBS with 10% Dimethyl sulfoxide (DMSO)(Sigma-Aldrich, UK) were removed from long-term storage in liquid nitrogen. The frozen cells were defrosted in a water bath at 37°C. Warmed basal media for

Y201 and NOF343/Green's media for FNB6 was then added to dilute the DMSO. Cells were centrifuged at 1000 rpm for 5 minutes, then the supernatant removed. The cell pellet was resuspended in fresh basal media and the solution transferred to a T-75 culture flask and incubated at 37°C and 5% CO_2 in a humidified environment. Cell culture media (Basal media for Y201 and NOF343/ Green's media for FNB6) was changed on the day after thawing and every 2-3 days. Cells were incubated at 37°C and 5% CO_2 in a humidified environment until reaching 80-90% confluency.

For culturing a monolayer of Y201 on tissue culture plastic (TCP), the TCP surface was prepared by coating with 0.1% gelatine for 1 hour before rinsing excess liquid out as recommended by a previous work in the lab. Gelatine solution was made from dissolving 0.1% (w/v) of Sigma-Aldrich, UK Gelatine from porcine skin with deionised water and autoclaving. While NOF343 and FNB6 didn't need any coating according to the standard protocol.

- **Cell expansion and subculture in general**

After reaching the optimum confluency (no flask was left beyond 80% confluency to avoid contact inhibition), cells were subcultured by detaching the cells from the tissue culture flask and incubating with 0.25% trypsin EDTA (Sigma-Aldrich, UK) at 37°C for 5-10 minutes. Cells were then inspected for cell detachment using a light microscope. Once the cells were detached, the trypsin solution with a concentration of 0.25% was deactivated by adding warmed media (basal media for Y201 and NOF343/Green's media for FNB6). Cells were centrifuged at 1000 rpm for 5 minutes to remove supernatant liquid and resuspended in a known volume of fresh media (basal media for Y201 and NOF343/Green's media for FNB6). Cells were then counted under a light microscope using a haematocytometer.

For sub-culturing, a known number of cells were transferred into a fresh flask. To freeze down for long-term storage, cells were resuspended in freezing medium (FBS with 10% DMSO, v/v) at $1x10^6$ cells/ml of freezing medium. A cryovial with cells were transferred into a freezing container and kept in -80°C freezer overnight before transferring into liquid nitrogen for long term storage.

Monolayer culture

For monolayer '2D' experiments, approximately $4x10^4$ cells per well were seeded in 24 well plate (Corning® Costar, UK) (cell density = $2.11x10^4$ cells/cm^2) with 0.5 ml of basal media. The plate was then incubated at 37°C and 5% CO_2 in a humidified environment. In this thesis, monolayer culture was performed to demonstrate cell growth, differentiation, and mineralisation of Y201. Therefore, on day 1^{st} after cell viability assay using Resazurin was done to assess cell viability, basal media was replaced with osteogenic media and was refreshed every 2 days. A resazurin assay was continuously performed to monitor cell viability on day 7^{th},14^{th}, and 21^{st}.

3D culture

- **Sterilisation of porous scaffold**

  Porous scaffolds were sterilised by autoclaving at 121°C for 30 minutes. After cooling down, the scaffolds were transferred into sterile FBS solution overnight prior to further use. However, no characterisation on changes in mechanical properties after autoclaving was done.

- **Y201 cell culture on 3D salt leached porous PGS for short term analysis (cell attachment, growth)**

  Briefly, $4x10^4$ cells of Y201 were seeded on one side of a PGS scaffold (N = 1, n = 3) in small volume, 20 µl (cell density = $5.1x10^4$ cells/cm^2 of a top surface of scaffold). The cells were left for 1 hour at 37°C to allow the cells to attach, before being submerged with 1 ml of basal media or enough to cover the top surface of a scaffold. The culture media was replaced every 2 days. A resazurin assay was performed to monitor cell viability on day 1^{st},7^{th}, and 14^{th}.

- **Y201 cell culture on 3D salt leached porous PGS for long term analysis (ECM production of cells)**

  To yield sufficient matrix production by Y201 cells to be enough for cell-derived matrices, the experiment was adapted from Berning et.al. [199]. Briefly, Y201 were seeded on a PGS scaffold ($5x10^5$ cells in 20 µl) and then the seeding was repeated on day 3^{rd} and 5^{th} by seeding on top of the previous seeded cell layer (*figure 3.4*). A resazurin assay was

performed to monitor cell viability on day 1^{st},5^{th}, 7^{th}, 14^{th}, and the last day of an experiment. To induce a production of bone-like matrix, basal medium was replaced with osteogenic media on day 7^{th} and replaced every 2 days.

- **NOF343 cell culture on 3D salt leached porous PGS**

  A collagen layer was prepared by mixing collagen (rat tail) with DMEM (10X), reconstitution buffer (10X), FBS, and L-glutamine. This should be mixed in a low temperature condition (using a bucket of ice to maintain the temperature) to avoid setting prior use. The mixture was adjusted to pH 7.4 before adding NOF 343 cells. A PGS scaffold was placed in an insert prior adding 500 µl of collagen solution with NOF344 $1x10^5$ cells on top of it. The sample was incubated at 37°C for 1 hour in a humidified environment to enable the collagen to fully set (*figure 3.5*).

- **FNB6 cell culture on top of a collagen layer with oral fibroblast mimicking oral tissue**

  After a fully set of a collagen layer, $2.5x10^5$ cells of FNB6 in 500 µl of Green's media were seeded on top of a collagen layer. Green's media of 4.5 ml was added to the well below the insert enough to cover the bottom part of the insert. Culturing the model for 5 days by changing media every 2 days both an insert and a well.

  After 5 days of culture, FNB6 was raised to air-liquid interface by removing all the media in an insert to dried. The media underneath the insert, 4.5 ml was refreshed every 2 days until day 10^{th} that the model was ready to be collected (*figure 3.5*).

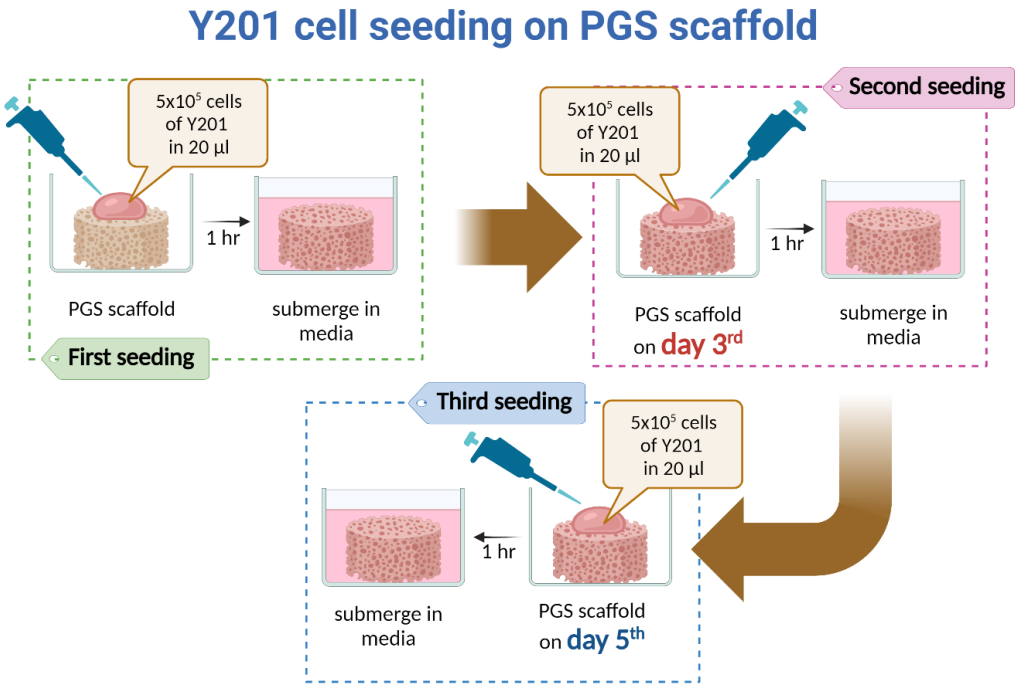

Figure 3.4 *Diagrams of Y201 seeding on PGS scaffold for long term analysis. After seeding, the cells were incubated for 1 hour before submerging with media. Seeding of Y201 was always repeated on day 3rd and 5th in this protocol. Created with BioRender.com*

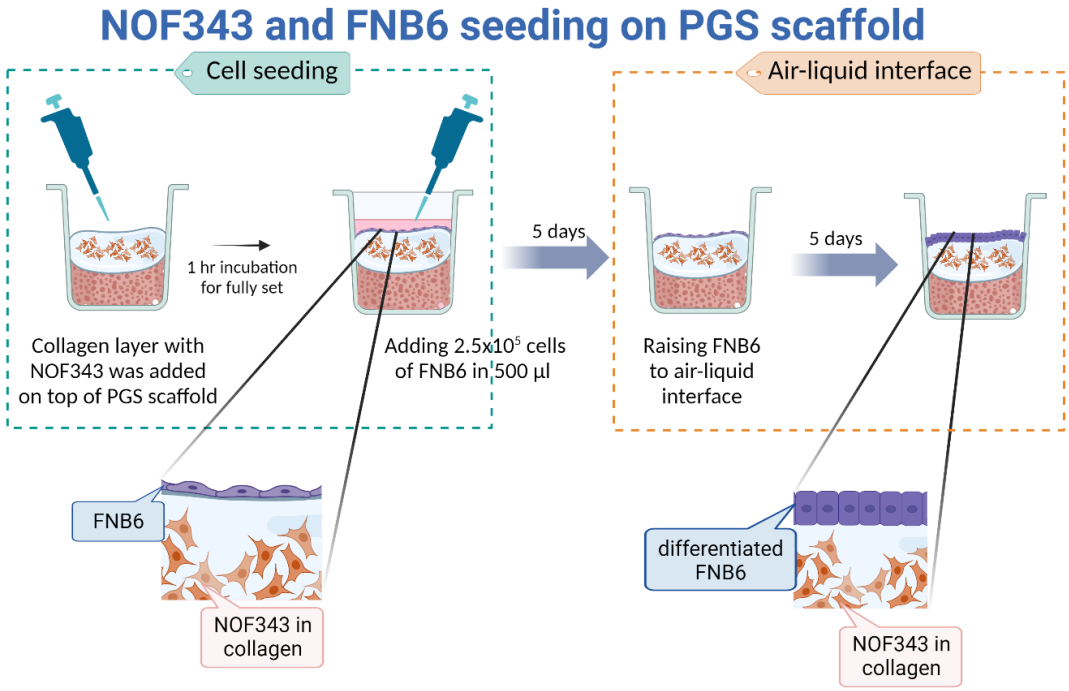

Figure 3.5 *Diagrams of seeding a collagen layer with NOF343 and a layer of FNB6 on a PGS scaffold. Created with BioRender.com*

3.2.3. Assays related to cell cultivation

Cell metabolism assay

Resazurin reduction is a cost-effective and yet simple assay used to evaluate cell metabolism which can indirectly cell viability. It is not toxic, thereby allowing multiple measurements throughout an experiment [204]. Resazurin is a blue non-fluorescent dye which can be reduced into a pink highly fluorescent resorufin by the mitochondrial respiratory chain in live cells (*Figure 3.6*) [205].

Resazurin dye (Sigma-Aldrich, UK) was dissolved in PBS solution to 0.1% (w/v) as a stock solution. Cell media was removed and replaced with 1 ml of 0.01% resazurin solution diluted with basal medium. Cells were incubated for 2 hours at 37°C and 5% CO_2 in a humidified environment. Triplicate samples (200 µl each) of the solution were transferred to a clear 96 well-plate and read at 540 nm in a fluorescent plate reader. The excess resazurin was removed from the cultures and washed with PBS before adding 0.5 ml of warmed fresh media for further culture.

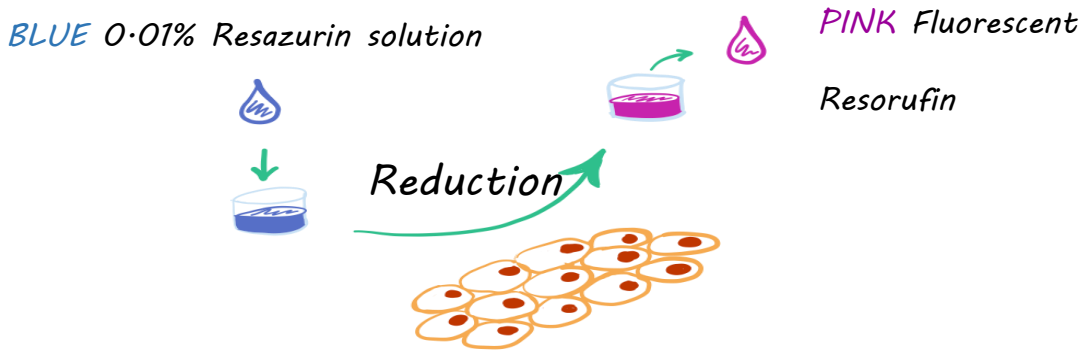

Figure 3.6 *Resazurin can be reduced to a pink high fluorescent Resorufin. This reaction can be happened only by mitochondrial activity in live cells. The solution can be measured its fluorescence intensity by a microplate reader. Therefore, demonstrating of cell metabolism which indirectly refer to cell viability.*

Cell differentiation

Osteogenic differentiation was assessed by investigation of the early bone marker alkaline phosphatase (ALP). ALP is an enzyme which is highly produced at an early stage of osteoblast differentiation. Its expression can be determined by quantitative colourimetric using p-nitrophenyl phosphate (pNPP) from Thermo-Fisher Scientific® which can be hydrolysed by ALP into a yellow solution of p-nitrophenol (pNP) (*Figure 3.7*) [206, 207].

After 14 days in culture, cells were washed with PBS twice before the addition of 1 ml of cell digestion buffer for 24 hours. Following this incubation cells were subjected to three cycles of freezing and thawing for cellular content release including the ALP enzyme. The lysates were transferred into sterile microcentrifuge tubes and centrifuged for 5 minutes at 10,000 rpm. The cell lysate 80 µl was mixed with 120 µl of ALP substrate and read at 405 nm using an absorbance plate reader for 30 cycles with 1 minute in each cycle. of the rate of activity of ALP was calculated as nanomoles of p-nitrophenol per minute (nmol pNP/min) assuming that one absorbance value equals to 19.75 nmol of pNP [206].

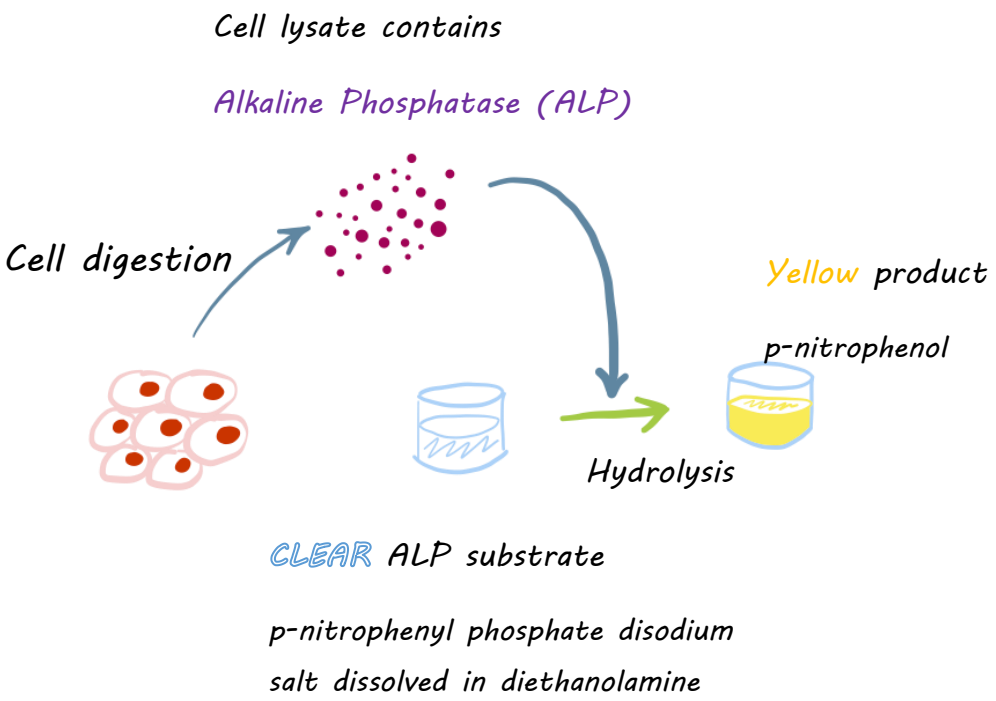

Figure 3.7 *ALP is an enzyme that can hydrolyse* p-nitrophenyl phosphate (pNPP) into a yellow solution of p-nitrophenol (pNP) *which the absorbance of this yellow solution can be measured using a microplate reader. This ALP activity can be use for Y201 differentiation assay.*

DNA detection using Quant-iT™ dsDNA High sensitivity kit

After 14 days in culture, cells were washed with PBS twice before the addition of 1 ml of cell digestion buffer for 24 hours. Following this incubation, cells were subjected to three cycles of freezing and thawing for cellular content release including the DNA. The lysates were transferred into sterile microcentrifuge tubes and centrifuged for 5 minutes at 10,000 rpm. The cell lysate 10 µl was mixed with 90 µl of DNA working solution from Quant-iT™ dsDNA

High sensitivity kit (Thermo Fisher, UK) in a black 96 well plate. The mixture was required to be shaken, rested for 10 minutes and then shaken again before being read at 485/535 nm using a fluorescence plate reader at room temperature. The detection range of the kit is 0.2-100 ng of DNA. The kit works by using PicoGreen, a fluorescent dye to bind with the target of double stranded DNA (dsDNA) and generate the signal.

Collagen deposition assay

Collagen type I was quantified colourimetrically using Sirius red staining [208]. The sulphonic acid functional group of Sirius red molecules bound to basic amino groups on the collagen chain, forming the precipitates [38].

Cells were fixed with 3.7% formaldehyde for 30 minutes. Cells were then washed with deionised water twice before the addition of a solution of 0.1% Direct Red 80 powder (Sigma-Aldrich, UK) in Picric acid (Sigma-Aldrich, UK) and left for 30 minutes. Samples were washed with deionised water until the water ran clear to wash out the excess stain and left to air dry. Stained cells were submerged with 1 ml 0.2 M NaOH:Methanol (1:1) (Sigma-Aldrich, UK) for 30 minutes to de-stain and triplicate 100 µl samples of the resultant solution transferred to a 96 well-plate and read at 540 nm absorbance using a plate reader.

Calcium deposition assay

To quantify calcium deposition Alizarin red staining assay was used [209]. Alizarin binds with the calcium cation through a chelation bond, forming an orange to red precipitate [210]

Cells were fixed with 3.7% formaldehyde for 30 minutes and washed twice with deionised water and 1% Alizarin red solution was added (Sigma-Aldrich, UK) from After 30 minutes of being submerged, the excess stain was removed, and cells were washed with deionised water until the water ran clear. The samples were left to air dry before the addition of the de-staining solution, 5% Perchloric acid for 30 minutes. Triplicate 100 µl samples were transferred to a 96 well plate and the optical density determined at 405 nm using an absorbance plate reader.

BCA assay

To lyse the cells, samples were minced and submerged in RIPA buffer (SERVA) with protease inhibitor added (Roche) The mixture was homogenised using a Qiagen Tissueruptor® II. In

order to quantify the amount of protein being used to test each time, the Bicinchoninic acid (BCA) assay was used. Briefly, the reduction of Cu2+-protein gives Cu+ as a product which can be chelated with BCA and gives a purple end product which can be detected with spectrophotometry at 595 nm. The high absorbance value can be translated as a high amount of protein in that sample. The protein content of the samples and a standard were tested using a BCA kit (ThermoFisher Scientific, UK) and a standard curve was used to calculate how much protein was present. .

Western blot

After BCA was undertaken, the homogenised lysate was loaded as a calculated volume of 10 µg of each (calculated from the result of BCA assay) onto a polyacrylamide gel and proteins were separated according to the size by electrophoresis in sodium dodecyl sulphate (SDS) solution at 150 kV for 1 hour. The proteins were then transferred to a nitrocellulose membrane and the non-specific proteins blocked using 5% skimmed milk powder in 0.1% Tween-20 in tris-buffered saline incubated at room temperature for 1 hour. The blot was washed with 0.1% Tween-20 TBS 3 times and then incubated overnight at 4°C with a primary antibody (*Table 3.6*). The blot was washed to remove any unbound antibody with 0.1% Tween-20 TBS 3 times before being incubated with secondary antibody conjugated with horseradish peroxidase (HRP) antibody (See *Table 3.6*) for 1 hour to bind the primary antibody enhancing the signal for detection of a specific protein. The blot then washed and the signal enhanced using Clarity™ Western Enhanced chemiluminescence (ECL) Substrate (Bio-Rad®. LI-COR™ Odyssey CLx imaging system was used to capture the image of the fluorescent signal of the bound protein.

Table 3.6 List of primary antibodies used for binding the proteins of interest present in the Y201 MSCs cellular matrix cultivated on salt leached porous PGS scaffolds.

Protein of interest	Collagen type I	Fibronectin	Osteopontin	Integrin binding Sialoprotein or Bone sialoprotein II (IBSP)
Gel used	3-8 % Tris-acetate Invitrogen® NUPage™ precast gel	3-8 % Tris-acetate Invitrogen® NUPage™ precast gel	10% SDS PAGE gel	10% SDS PAGE gel
Primary antibody and its dilution	Collagen I monoclonal antibody (5D8-G9) Invitrogen®, UK	Fibronectin monoclonal antibody (FBN11) Invitrogen®, UK	Osteopontin monoclonal antibody (7C5H12) Invitrogen®, UK	IBSP polyclonal antibody Invitrogen®, UK
	1:1000	1:2000	1:1000	1:1000
Secondary antibody and its dilution	Anti-rabbit IgG secondary antibody (HRP)	Anti-mouse IgG secondary antibody (HRP)	Anti-mouse IgG secondary antibody (HRP)	Anti-rabbit IgG secondary antibody (HRP)
	1:3000	1:5000	1:5000	1:3000

3.3. Decellularisation and recellularisation

3.3.1. Decellularisation methods

Freeze-thaw method

After the culture period (which was typically 21 days unless otherwise stated), scaffolds containing Y201 were washed twice using PBS, then soaked in deionised water and kept at-80°C for 1 hour. The scaffold was thawed at 37°C for another 1 hour and washed with deionised water to complete one cycle of freeze-thaw. The cycle was repeated for three complete cycles of freeze-thaw decellularisation.

Ammonium hydroxide with Triton X-100 method

After the culture period scaffolds were washed twice with PBS and submerged in decellularisation reagents following a protocol of Kusuma, et al. [40]. Briefly; scaffolds were first submerged in a solution of 20 mM Ammonium hydroxide (Sigma-Aldrich, UK) with 0.5% Triton X-100 (Sigma-Aldrich, UK) in PBS and incubated at room temperature. Herein, some studies were undertaken at different duraitons of ammonium hydroxide submersion (see section 5.2.2.).

1. Submerging a sample in ammonium hydroxide with triton x-100 for 10 minutes before moving to next step.
2. Submerging a sample in ammonium hydroxide with triton x-100 for 24 and 48 hours on a shaker. Every 24 hours the scaffold was washed twice with PBS and the solution refreshed.

Tributyl phosphate

At the end of the culture period cell-seeded scaffolds were washed twice with PBS and soaked with a solution of 10 mM Tris buffer (pH8.0) (ChemCruz®, The Netherlands) + 5mM Ethylenediaminetetraacetic acid disodium salt dihydrate (EDTA) from + 1% of Tri(n-butyl)phosphate (TBP) for 48 and 72 hours on a shaker Every 24 hours the scaffold was washed twice with PBS and the solution refreshed.

3.3.2. Washing of scaffolds to remove all trace of reagents

Any scaffolds that had been immersed with chemical or detergent reagents in a decellularisation process needed washing to remove any residue of the reagents. This was to reduce any further harm to cells. After the time point of being decellularised was reached, different washing steps were tested to find the best one for the purpose of the following experiments(see section 5.2.3.):

1. Washed twice with PBS and soaked in with PBS for 10 minutes before moving to the next step.
2. Washed twice with PBS and submerged in the cold media (4°C) on a shaker for 30 minutes each day before being put into the fridge to prevent any microbial growth. This was done for 3 days consecutively.

3. Washed twice with PBS and submerged with the cold media (4°C) on a shaker for 60 minutes each day before putting back to the fridge to prevent any microbial growth. Every 24 hours, the scaffold was washed twice with PBS and the media was replaced.

3.3.3. DNA removal using DNase I

After washing, scaffolds were submerged with 0.2 mg/ml DNase I (Sigma-Aldrich, UK) in deionised water for 24 hours on a shaker at room temperature to ensure removal of DNA. The decellularised scaffold was then washed twice with PBS and incubated with cell culture media for 24 hours on a shaker at 4°C

3.4. Recellularisation

3.4.1. Recellularisation steps

After the decellularisation and washing steps were completed, a new set of cells could be seeded onto the scaffolds containing decellularised matrix. $5x10^5$ cells per a whole disc shaped scaffold were seeded with a small volume of media (20 µl). The cells were left to adhere for 1 hour before the working volume of media was added gently to a final volume of 1 ml or enough to cover the top of the scaffold. Resazurin reduction assay was performed the next day to evaluate viability of cells.

3.5. Co-culture

3.5.1. Bone cell layer as a co-culture on 3D salt leached porous PGS

Y201 were seeded on a PGS scaffold ($5x10^5$ cells in 20 µl) and then the seeding was repeated on the 3rd and 5th days of culture by seeding on top of the previous seeded cell layer. The cells were cultured to day 7th before beginning the culture of the soft tissue part.

3.5.2. Oral tissue layer as a co-culture on 3D salt leached porous PGS

Construction of a collagen layer with oral fibroblast cells

The bone scaffold was flipped over and gently placed into a polycarbonate cell culture insert (*Figure 3.8*). The collagen layer with NOF343 was prepared as described in section 3.2.2.,

"NOF343 cell culture on 3D salt leached porous PGS". 500 µl of collagen solution containing NOF344 $1x10^5$ cells was then added on the reverse side of the bone scaffold. The constructs were incubated at 37°C for 1 hour in a humidified environment to enable the collagen to fully set.

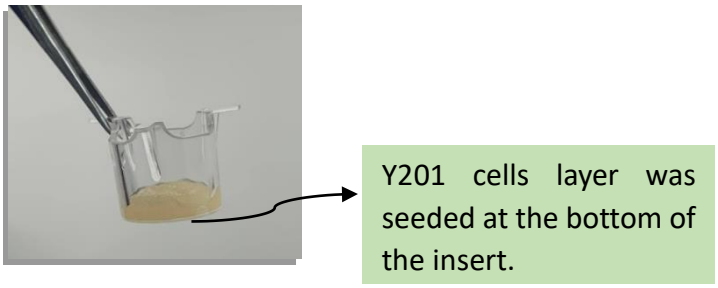

Figure 3.8 *The scaffold with Y201 cells layer was flipped over and placed into a polycarbonate cell culture insert. So, the reverse side could be used for seeding of an oral tissue layer.*

Generation an oral tissue layer by adding keratinocytes

FNB6 cells $2.5x10^5$ in 500 µl were prepared and added as described in section 3.2.2., "FNB6 cell culture on top of a collagen layer with oral fibroblast mimicking oral tissue". The scaffold was lifted to an air-liquid interface on day 5 and the co-culture was carried on to day 10. The full co-culture model is illustrated in *figure 3.9*.

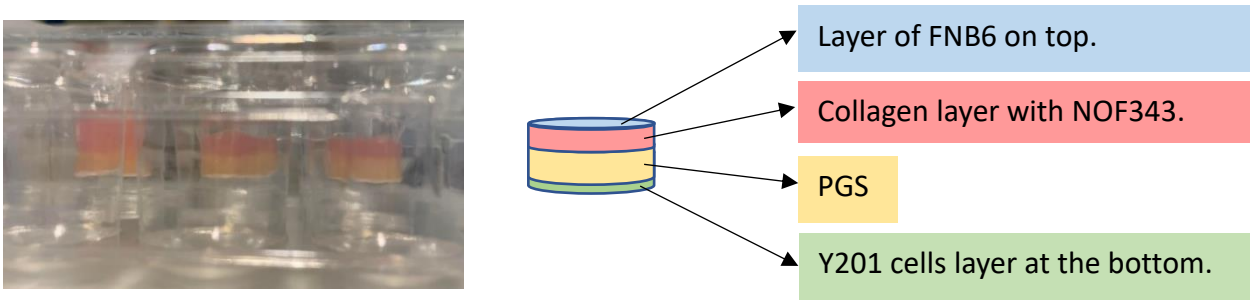

Figure 3.9 *A co-cultured model of FNB6, NOF343, and Y201 on 3D salt leached porous PGS scaffolds which aimsto mimic the complex layers of craniofacial tissue.*

3.6. Histology

3.6.1. Paraffin embedding sectioning

All scaffolds were washed and fixed with 3.7% formaldehyde or 10% formalin for 30 minutes overnight on a shaker in preparation for histology. Two methods of sectioning the sample were tested which are paraffin embedding and cryosection.

For paraffin embedding the sample was transferred into a cassette before being processed in a tissue processor (Thermo-Fisher Scientific® Epredia™ Citadel 2000 Tissue Processor). The tissue processor was left to run its 3 sequential steps: dehydration using ethanol, clearing the ethanol using xylene, and infiltration with paraffin wax. The water in the sample was replaced by paraffin at the end. The sample was then embedded in a paraffin block and cooled down using a Leica® EG1150C cold plate. The paraffin block was then mounted on a microtome (Leica® RM2235 microtome) to cut. The sample was cut at 5-10 µm thick and placed gently in a water bath. The sample was collected using a glass slide and left to dry.

However, there were no paraffin embedded sections which could be successfully cut as a whole sample. The scaffold was ripped off into several pieces (*Figure 3.10*).

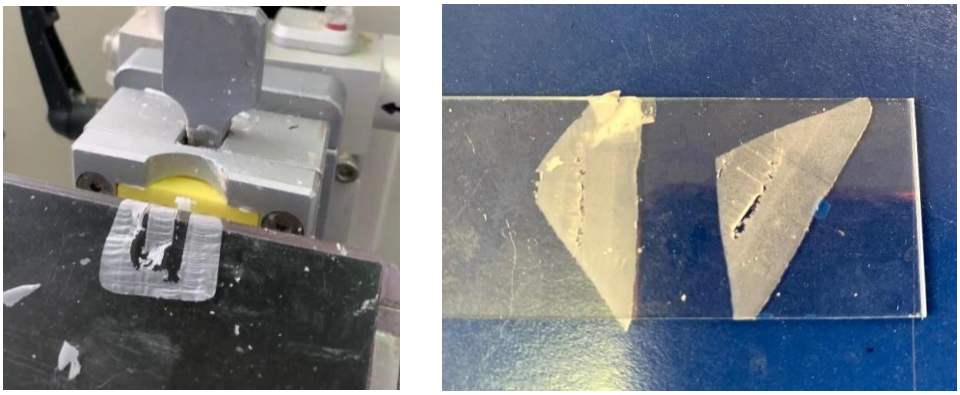

Figure 3.10 *The section of a PGS scaffold after being embedded with paraffin showed that the specimens were ripped whilst cutting.*

3.6.2. Cryosectioning

For cryosectioning the sample was submerged into an optimal cutting temperature (OCT) medium overnight. The samples were mounted on a cryostat chuck in OCT medium and rapidly frozen down to -24°C. The frozen sample was then cut at a thickness of 20-50 µm using

a Leica® CryoStar™ NX50 Cryostat and collected on a Epredia® Superfrost™ glass slide (Epredia, UK).

3.6.3. Staining with hematoxylin and eosin (H&E)

H&E staining is used for general histology staining. Haematoxylin which is a basic dye binds to acidic nucleic acid and gives a purplish-blue stain, while eosin is an acidic dye and binds to extracellular matrix and cytoplasmic proteins, which are basic and it gives a pink colour. Samples on glass slides were stained using a Leica® ST4040 automatic stainer. The cryosectioned samples were washed with deionised water and stained with haematoxylin (45 seconds). The samples were then submerged in running tap water to wash before being submerged in eosin (45 seconds), washed again and then dehydrate with ethanol and cleared with xylene. The samples were then mounted in DPX medium and covered a coverslip to preserve the section. For cryosections, the samples did not need to be rehydrated so the staining sequence started with deionised water.

3.7. Statistical analysis

All experiments were performed using triplicates (n=3) of each sample and one repeated experiment unless otherwise stated (n indicates the number of experimental repeats performed within the experiment and N indicates the number of times the experiment was repeated). The data was reported as mean ± standard deviation (±SD). The statistical analysis was performed using GraphPad Prism 9®. One-way and two-way analysis of variance (ANOVA) were used to analyse the difference between treatment groups. A difference was considered to be statistically different if $p < 0.05$ because at that value or probability the null hypothesis that two sets of data were not different was rejected.

Chapter 4

The effect of different salt concentrations used in porogen leached porous scaffolds on Y201 cell matrix production.

4.1. Introduction

In order to repair craniofacial bone defects, an appropriate material needs to be designed. Poly(Glycerol Sebacate) is an elastomer frequently used in experimental soft tissue engineering but rarely used in bone tissue engineering. However, its biocompatibility and biodegradability are very promising for use as tissue engineering scaffolds and recently it has been demonstrated that PGS scaffolds have the potential to support bone cell mineralisation of murine pre-osteoblasts [14]. To address this ability better, human Y201 cells were chosen to investigate the osteo-conductive properties of PGS scaffolds. Y201s are immortalised mesenchymal stem cells (MSCs), it was established that Y201s have a promising property of differentiating into osteoblasts and mineralising [158]. In this chapter salt -leached porous PGS will be investigated for use as a scaffold to support Y201 cells to secrete bone matrix. To my knowledge this is the first time these Y201 cells are used in combination with PGS.

Research Objectives

1. To determine whether salt leached PGS scaffolds will be suitable to support bone ECM production suitable for craniofacial bone tissue engineering.
2. To investigate the porosity of the scaffolds using several comparative methods.
3. To elucidate if different salt concentrations, used in porogen leaching to fabricate porous scaffold, affect cell attachment, proliferation or matrix production.

In this chapter all scaffolds were fabricated as described in section 3.1.3. with salt added in a w/w ratio. Whereby 2.5 = 2.5 g of salt to 1 g of polymer and 4.5 is 4.5 g of salt to 1 g of polymer. The expectation was that the 4.5 ratio would provide a higher porosity.

4.2. Results and discussion

4.2.1. SEM images analysis of salt grain size

NaCl salt purchased from ThermoFisher Scientific® (UK) was used as a porogen for this entire thesis. Since the salt is going to be the basis of the pore size of the scaffold, measuring salt grains was undertaken to evaluate if the salt can be a good porogen to work with. SEM images of salt grain size were analysed using ImageJ and plotted as a histogram (*Figure 4.1*). Salt particles were shown to range from very small sub-micron to 500 µm with most of the salt in the range of 100-350 µm which should create pores of that range. This matched the suggested size of pores described in the literature as in the range that enable bone cells to attach and grow [111].

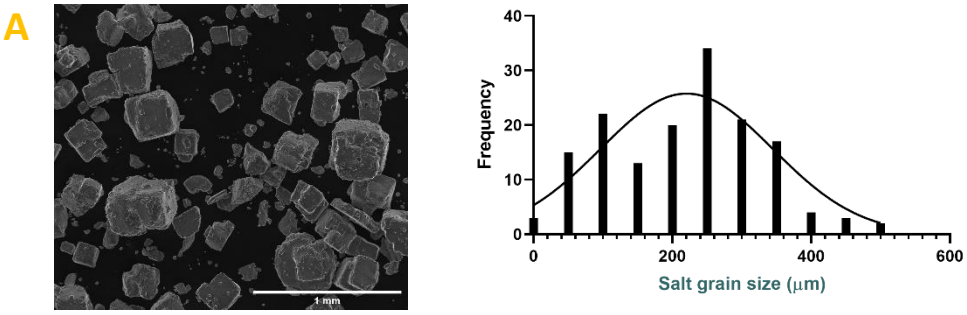

Figure 4.1 *SEM images of salt grain (A) which will be used in fabrication of salt leached porous PGS were analysed by ImageJ, representative image of 3 samples (N=3) (B) The histogram of salt grain size distribution (N=3, n=50) with a bin centre of 50 fitted with the Gaussian curve.*

4.2.2. Scaffold production

All salt concentrations attempted did produce a porous scaffold. However, at 2.5 salt the scaffold was the most difficult to handle since the material was leaked out of the mould. The density of salt and PGS polymer is 2.16 g/cm^3 and 1 g/cm^3 respectively. The volume of polymer contained of the highest salt used scaffold (4.5) is 35%, while of the lowest salt (2.5) is 46%.

4.2.3. SEM of Salt leached PGS scaffold with porosity measurements

All scaffold preparations using the method described in section 3.1.3. formed highly porous scaffolds with good handling properties. Scaffolds were then examined under SEM as described in section 3.1.4. The wall thickness and porosity were also measured using ImageJ™ by placing a grid of 9x8 squares on each image to select which pores were measured (methods

section 3.1) (*Table 4.1)*. The use of the grid and the reporting of only the largest diameter was aimed at reducing operator effects on the measurements.

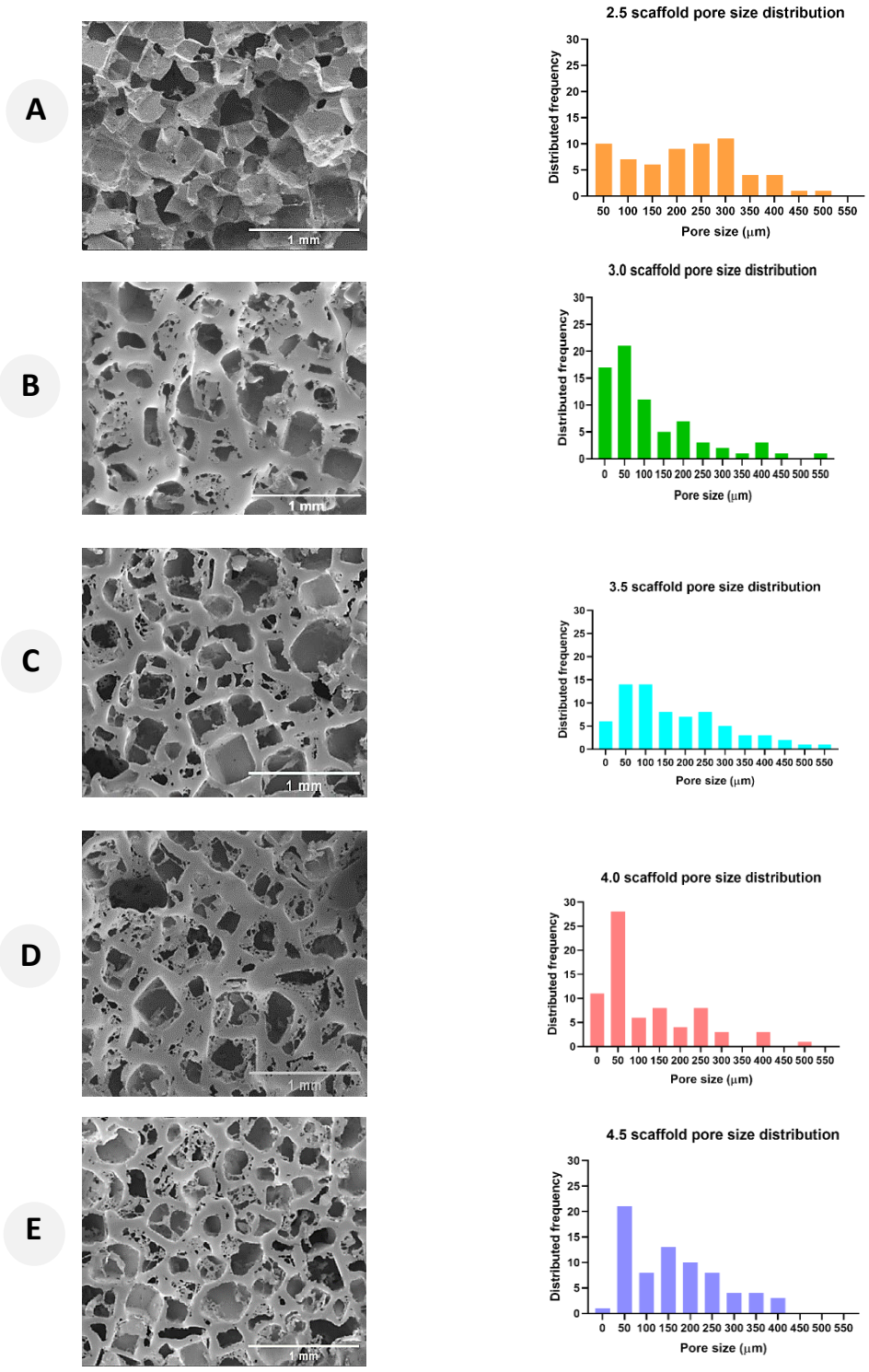

Figure 4.2 *Surface morphology of different porous salt leached PGS scaffolds according to the amount of salt: prepolymer used (A=2.5, B=3.0, C=3.5, D=4.0, and E=4.5). The second column is the pore size distribution of each scaffold measured by ImageJ™ (Bin centre = 50, N=1, n=72)*

Table 4.1 Wall thicknesses of the scaffold measured and calculated using ImageJ™. (N=1, n=72, Mean ± 1SD)

Scaffold	Average wall thickness (µm)
2.5	66.45 ± 34.31
3.0	95.57 ± 42.09
3.5	98.25 ± 33.12
4.0	117.86 ± 41.95
4.5	78.13 ± 27.95

Visual inspection of SEM images indicated that the higher salt content (ranging from 4.5 salt:polymer to 2.5 salt:polymer) created a higher proportion of opened pores to enclosed pores which is consistent with previous studies investigating porous salt leached scaffold [112, 211, 212]. The pore size range was between 50-400 µm (*Figure 4.2*) which was in the reported ideal range for cells to attach and proliferate [111]. Also, this range of pore sizes is similar to as reported in previous studies where researchers were successful in growing bone matrix on scaffolds [112]. The lowest salt concentration (2.5) had a more even distribution of pore sizes (*Figure 4.2*), while the others tended to have a higher percentage of small pores. The small pores are likely to have formed where salt grains were previously touching to create smaller interconnect 'windows'. Increasing volume of salt may increase a chance of salt grains were packed in one area and increase a chance of the windows to be created, therefore the surface of each condition was different as shown in *figure 4.2*. Wall thickness of pores within each scaffold were measured and recorded. *Table 4.1* demonstrated that the lowest amount of salt (2.5) used created overall thinnest walls compared to the others. ($p<0.05$, one way ANOVA with Tukey's pair-wise comparisons). Like pores and windows, the wall thickness difference were created from how salt grain touch and not touch each other. The space between the salt was filled with polymer and become a wall of a pore.

Automated porosity analysis using image thresholding

Thresholding of microscopy images is one of the easiest ways to perform porosity analysis. The principle is to convert pixels on any colour or grayscale image into binary images, i.e., black-white images. ImageJ™ was used to adjust this threshold of the SEM images and convert the image to binary, therefore the area of the material and its pores was distinguishable. Those white-black areas were calculated as a percentage of the two colours.

Table 4.2 Porosity evaluated using image thresholding.

Scaffold	Porosity from SEM (%)
2.5	27.92
3.0	30.39
3.5	36.94
4.0	31.37
4.5	38.44

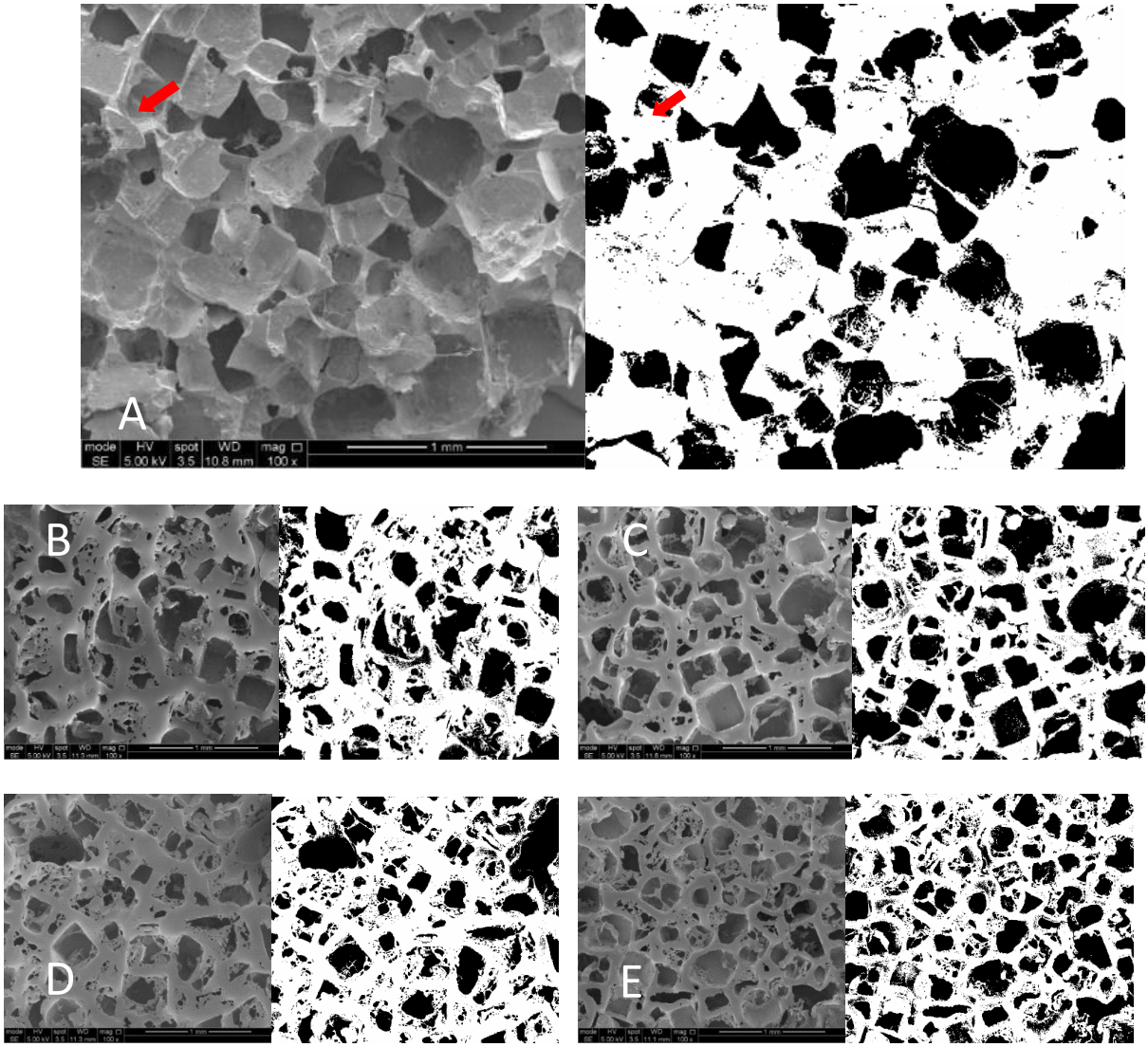

Figure 4.3 *Surface morphology of different porous salt leached PGS scaffolds according to the amount of prepolymer: salt using (A=2.5, B=3.0, C=3.5, D=4.0, and E=4.5). The right image of each scaffold showed threshold adjusted using ImageJ™ to analyse the porosity of scaffold.*

The % porosity of the lowest salt content scaffold (2.5) as measured by this technique was estimated to be very low *(Table 4.2)* and as noted on the raw images the thresholded images also presented little visual evidence of interconnectivity of pores (*Figure 4.3-A*). While other scaffolds which had a higher proportion of salt had higher % porosity (*Table 4.2*). However, the porosity may be underestimated by this technique because the ImageJ threshold was only able to detect pores that open to the surface. While the pores which had a back wall closed to the surface were not selected by the thresholding tool as indicated by the red arrows on *Figure 4.3*. Hence, the % porosity calculated using this technique may be an underestimate of the overall volumetric porosity.

Porosity analysis using pycnometry

Porosity of a porous scaffold can also be estimated using a physical method of measuring pore volume. The pore space in each scaffold group was evaluated by measuring pore volume using a Micromeritics AccuPyc™ 1340.

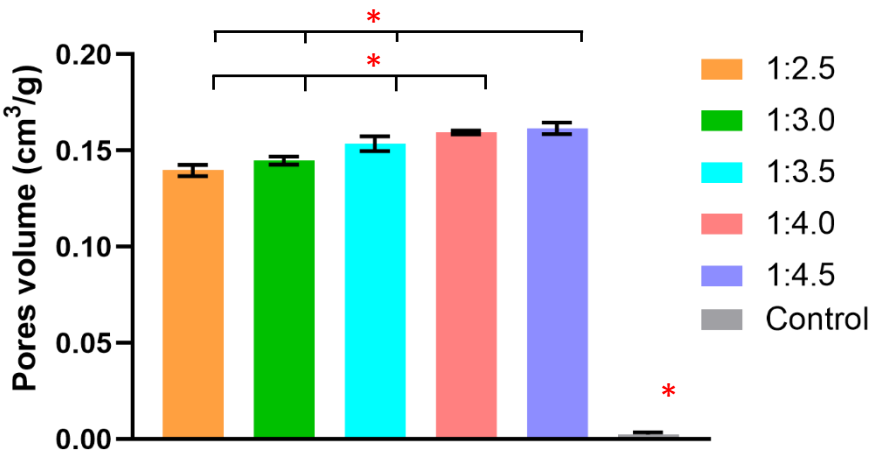

Figure 4.4 *Pore volume of salt leached porous PGS measuring with pycnometer of scaffolds fabricated with different amounts of salt. The largest amount of salt was shown to create a higher volume of pores. Mean ± SD (n=10). *p < 0.05, one way ANOVA with Tukey's pair-wise comparisons.*

The result of volumetric porosity (*Figure 4.4*) followed a similar pattern to that yielded from the SEM with the higher amount of salt causing higher pore volume. All the conditions were statistically different from the others, except between the 4.0 and 4.5 scaffolds which were not significantly different.

A linear relationship between the porosity and the amount of salt confirmed that different amounts of salt used in the salt leaching method can display different porosity and pore volume in porous scaffolds. This was similar to those reported in previous studies [112, 211, 212].

Volumetric porosity calculated from pycnometry data

To confirm the outcome of porosity yielded from different concentrations of salt used, a method of calculating this was performed [58]. The porosity was calculated based on the mass of polymer and the overall volume of the porous material. To yield a volume of pore space divided by overall scaffold volume.

The polymer density within the scaffold was calculated the Micromeritics AccuPyc™ 1340. The geometric volume - the space occupied by the polymer provides the volumetric porosity of the scaffold. The porosity for each scaffold condition was calculated as a percentage of volume of pores per overall volume of a scaffold, shown in *Table 4.3*

$$Porosity = \frac{V_0 - (\frac{m}{d})}{V_0}$$

- V_0 = geometric volume of the scaffold ($\pi r^2 h$) (cm^3)
- m = mass of polymer (g) weighed from the balance after drying.
- d = density of polymer from pycnometer (g/cm^3)
- $\frac{m}{d}$ = volume of the polymer (cm^3)

Table 4.3. Porosity percentage and measured parameters of scaffolds.

Scaffold	Radius ®	Height (h)	Mass (m)	Density	Porosity
	cm	cm	g	g/cm^3	%
2.5	0.56	0.9	0.2854	1.1976	72.59
3.0	0.60	0.9	0.3048	1.1854	74.52
3.5	0.61	1.1	0.3829	1.1912	75.21
4.0	0.58	1.04	0.3551	1.198	72.91
4.5	0.57	0.9	0.2863	1.2008	74.86

Noted: Since a pycnometer requires its chamber to be filled as much as possible, therefore scaffold height (h) was referred to a total height of all scaffolds being put in.

The mathematically calculated volumetric porosity (*Table 4.3)* was higher than that reported by the SEM imaging with ImageJ thresholding method. From SEM images it can be seen that porous salt leached PGS scaffolds have irregular shaped pores generally and enclosed pores

in some regions, so the ImageJ™ software was not able to perfectly convert those pores into binary images. All methods confirmed that the lowest amount of salt provided the lowest amount of porosity. While increasing the salt amount raised the porosity.

However, the porosity percentages and the parameters were random among the condition. This could imply that this range of salt amount difference was not enough to make a huge difference in scaffold's porosity. In addition, the lowest amount of salt (2.5) not only had the lowest pore volume and porosity but was also observed to have the thinnest wall between its pores. This was contradictory from what has been previously reported that the strong and significant inverse relationship between porosity and wall thickness was observed during a characterisation of a composite scaffold between poly(ester urethane) (PU) and hydroxyapatite nanoparticle. It meant the thinnest wall thickness scaffold should give the highest porosity [213].

4.2.4. Biological analysis

In this project, it was aimed to demonstrate that porous salt leached PGS scaffolds would be suitable to support bone matrix for in vitro culture of MSCs. For this purpose, we tested the scaffolds using an immortalised MSC cell line (Y201)

Cell attachment

The reduced resazurin fluorescence method was used to determine the viability of Y201 cells on each group of scaffolds (section 3.2.3.).

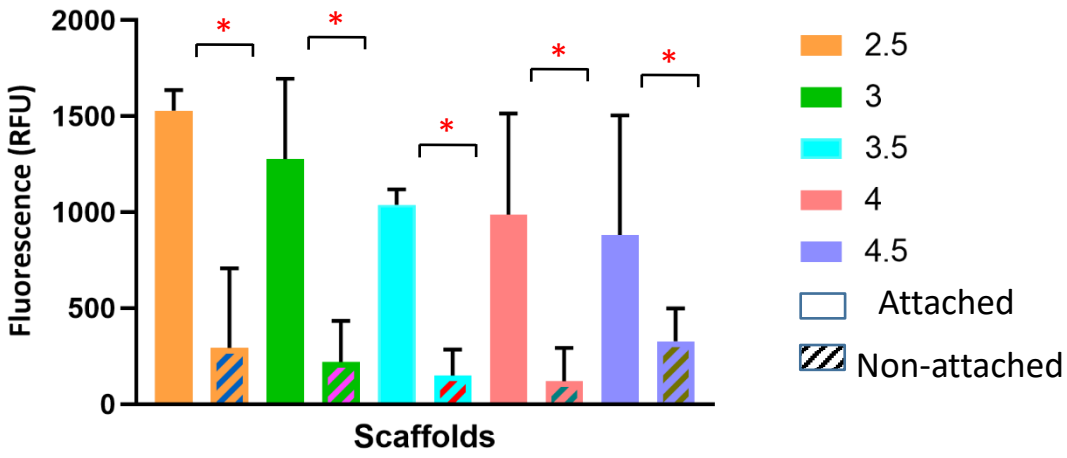

Figure 4.5 *Cell viability of Y201s cultured on scaffolds fabricated with different amounts of salt (seeding of* 5x10^5 cells). *The viability of cells on day 1 was compared between cells that had attached to the scaffold and those that had fallen to the well surface. The results showed that salt leached porous PGS is compatible, but there was no significant difference between scaffolds. Mean ± SD, N=1, n=3, * = p<0.05, one way ANOVA with Tukey's pair-wise comparisons.*

Table 4.4 Percentages of attached cells viability fluorescence mean value ± 1SD.

Scaffold	Cell viability fluorescence (Mean ± 1SD)
2.5	86.6 ± 18.9
3.0	83.9 ± 16.4
3.5	88.7 ± 10.1
4.0	92.5 ± 10.6
4.5	68.4 ± 10.4

At day 1st of culture there were more cells attached to the scaffold than on the base of the well as indicated by resazurin fluorescence. This meant the majority of cells were able to attach to the scaffolds with all porosities investigated. There was no difference among the conditions. The percentages of attached cells to all cells were calculated (*Table 4.4)*. All conditions of scaffold fabrication supported more than 65% cell attachment. The 4.5 scaffold seemed to have fewer cells attached compared to the others. However, there was quite high variability in each condition which might reflect cell distribution during seeding. The floating cells were not measured since Y201 cells are adherent cells, means that they grow as they attach only.

The experiment was planned to be 3 repeats (N=3) but as an effect from the pandemic, the experiments were unfortunately cut down to proceed to the next step as soon as possible.

Cell number changes over time in culture

After 14 days of cultivation scaffolds fabricated with the lowest amount of salt were found to have the highest fluorescence value, indicating more viable cells although this was not statistically different from the others (*Figure 4.6*). However, the results do indicate that porous salt leached PGS scaffolds are compatible with Y201 cells to attach and undergo metabolic activity.

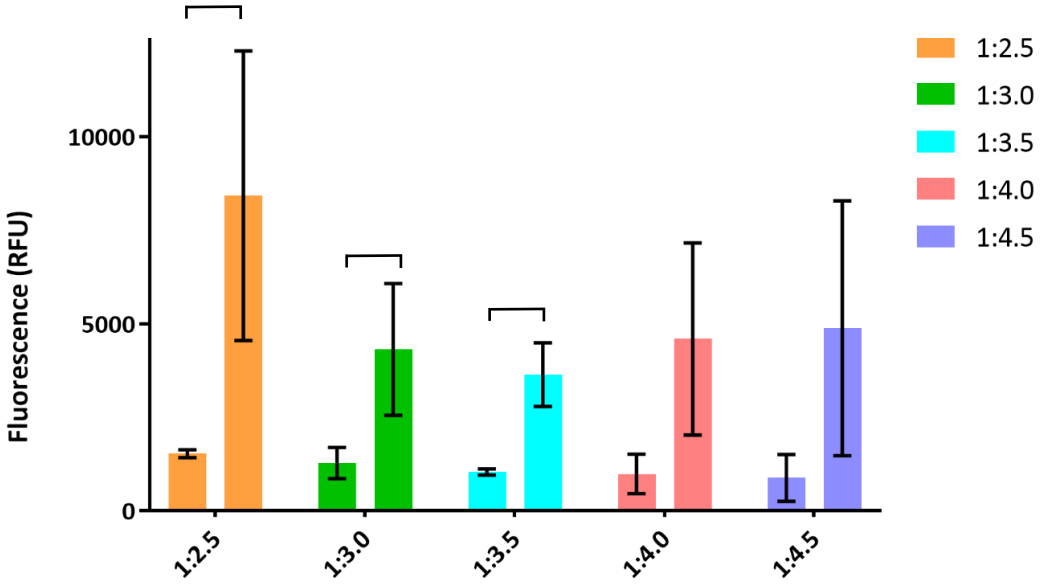

Figure 4.6 *Viability of cells on day 1st (the first bar of each group) and day 14th (the second bar of each group) on different conditions of scaffold showed cell proliferation had occurred on the scaffolds. Mean ± SD, N=1, n=3, * = p<0.05, one way ANOVA with Tukey's pair-wise comparisons.*

After 14 days of culture there were no observable differences in cell number between the scaffolds of different porosities, but all scaffolds showed much higher cell viability than on day 1 indicating that cells underwent net growth and therefore proliferated during the culture period.

The porosities of these scaffolds calculated by pycnometry was in the range of those published in the previous papers. Using various types of material, it has been demonstrated that above 70% porosity was suitable for cell culture [67, 103, 214]. However, the difference in porosity between different salt amounts used didn't seem to play any significant role when it comes to biological assay (in terms of cell number) unlike a previous published study of salt leached PCL-PLLA scaffold which showed that a higher porosity and bigger pores resulted in higher metabolic activity of cells [112]. Also, 3D printed porous titanium scaffold and foam replica zirconia scaffold were both reported the same way that a higher porosity could support a higher cell viability [67, 215]. This could be from the difference of materials selection, pore shape, or porosity of a scaffold. These published studies were noted of having the difference of porosity between each group at least 10%. While the result from this chapter demonstrated a smaller range of difference in porosity which this may be too small to cause any difference in cell viability. However, the high cell attachment and increase in cell number over time

deemed the scaffolds suitable for culture of cells and therefore they were taken forward to create a full tissue-engineered model.

Matrix production

Since preliminary results indicated that the cells attached and proliferated to a similar extent regardless of the different amount of salt used in scaffold fabrication, the conditions were narrowed down to three scaffolds for subsequent work. The cells were grown for 28 days to allow the cells to deposit a matrix.

Protein quantifying assay

The samples were analysed for their total protein quantity by using BCA technique (described in section 3.2.3.).

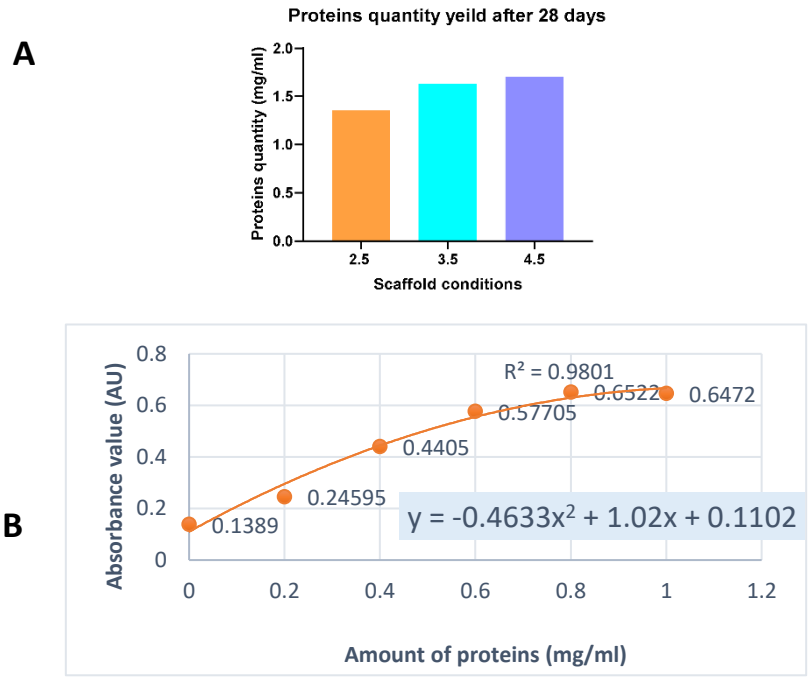

Figure 4.7 *Protein quantity per scaffold as measured by BCA assay after Y201 had been cultured for 28 days (A). The amount of protein was calculated using a standard curve of protein concentration (B).*

The BCA protocol and standard curve was done following a group's protocol in dental school. The scaffold made with the highest amount of salt at 4.5:1 (higher porosity) was found to support more matrix deposition despite there being no evidence of higher cell numbers on this scaffold (*Figure 4.7*). This higher volumetric porosity leads to more space and this space

might enable cells to build up their matrix more than in the lower porosity scaffolds. The higher porosities of polymer scaffold have been previously noted to yield a higher protein concentration when compared to lower porosity [216, 217]. Unfortunately, for this chapter this was not verified with statistical analysis as only one scaffold was tested for each group.

Western blot protein analysis

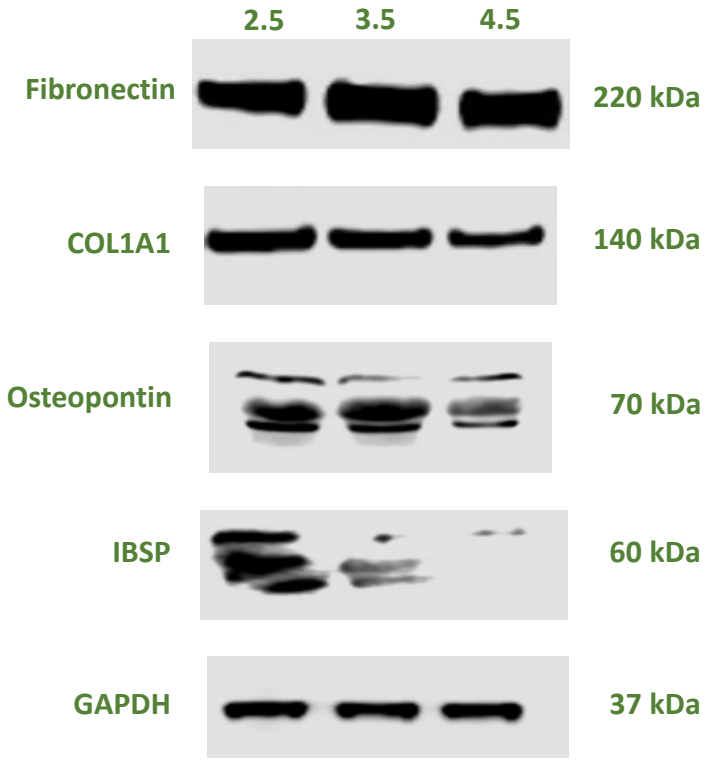

Figure 4.8 *Western blots of specific protein in cellular matrix on different scaffolds (N=1, n=1).*

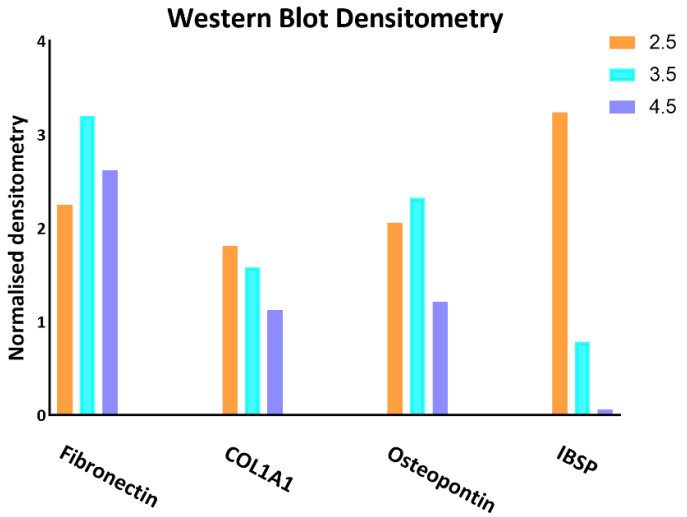

Figure 4.9 *Each band of bone matrix related proteins yielded from western blot technique was semi-quantified as a densitometry. Each band was normalised using a band of GAPDH (N=1, n=1).*

The blots showed probed protein bands in every scaffold. This meant that every condition of scaffold allowed Y201 cells to lay down bone-like matrix. The study showed bone cell matrix proteins were secreted from Y201 cells. It is the first study demonstrating Osteopontin in MSCs cultured on PGS scaffold, which has not been assessed in the previous published study of this polymer [13]. The amount of protein was able to be analysed using a semi-quantitative method by measuring each band as shown in *Figure 4.9*. From four target proteins, the scaffold with a higher concentration of salt (4.5) demonstrated lower protein production of the bone specific proteins although not of fibronectin. The scaffold made with the lowest salt (2.5) seemed support the highest protein production with high levels of osteopontin, collagen and bone sialoprotein. There was little observable difference between the 2.5 and the medium porosity (3.5) scaffold in most proteins examined except for IBSP.

The BCA result showed a lot of protein was collected from the scaffolds cultures for 28 days. Bone specific proteins assessed using Western blot technique were found to have quite a similar density among conditions, except for IBSP which seem to be more prominent in the lowest salt concentration used. As discussed earlier the scaffolds at 2.5 salt concentration had visually more closed pores creating more of an intact surface with less open porosity for cells to migrate into. It would be interesting to investigate whether the surface properties of the scaffold do influence IBSP secretion specifically, however there is no specific evidence of this to date.

As stated, though the very prominent IBSP showing during the Western Blot the lowest salt was cut off since its difficulty in handling. The low salt amount referred to a higher proportion of prepolymer which was liquid. High viscous liquid in a mixture could trap a lot of air inside which resulted as a burst when air was removing under vacuum condition making the scaffold outcome less predictable than the others. While the other scaffolds contained more salt proportion making it was easier for the air to get out via the salt space.

4.2.5. Mechanical analysis

Tensile mechanical analysis was undertaken for 5 samples of each scaffold with different porosities.

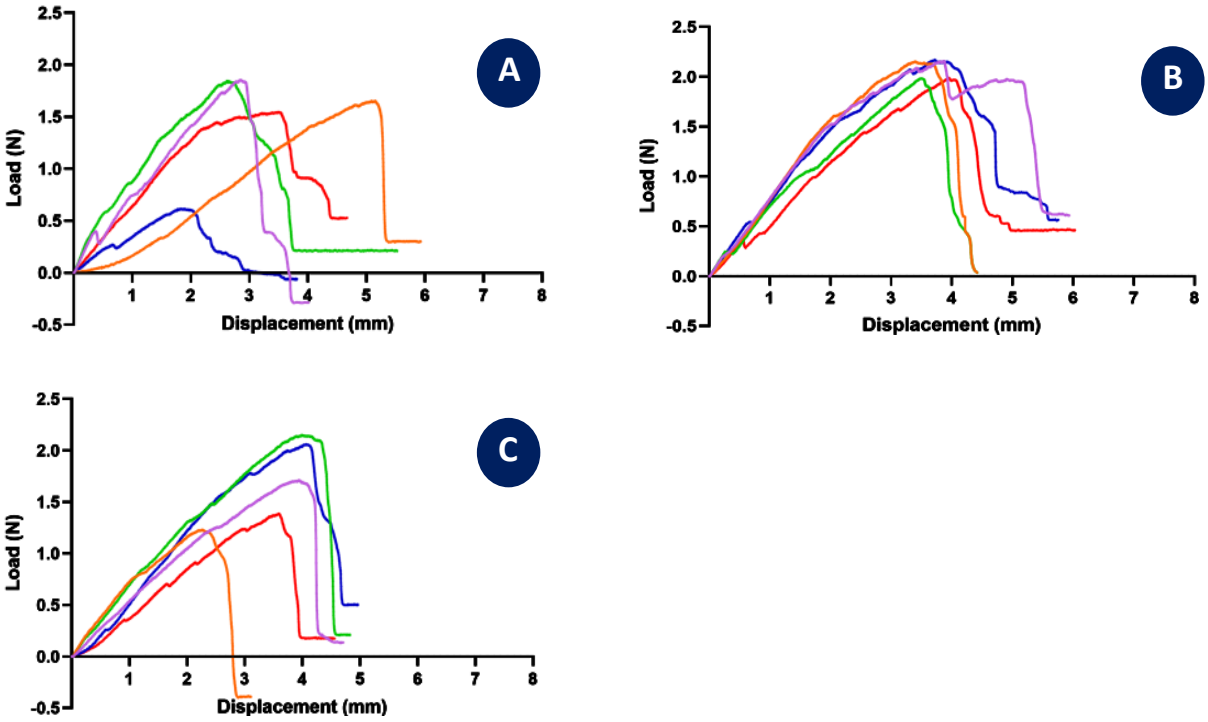

Figure 4.10 *The relationship line graph between loading force and scaffold's displacement (A=2.5, B=3.5, C=4.5) (N=1, n=5). The different colour of each graph represents one sample in each group.*

For all scaffold groups the mechanical data was quite variable, as would be expected for a soft, porous polymer, and the scaffold with the least salt (2.5) showed the greatest variation as shown in *Figure 4.10*. The failure point just after maximum load, which is also the ultimate tensile strength appeared the most variable for the 2.5 scaffolds.

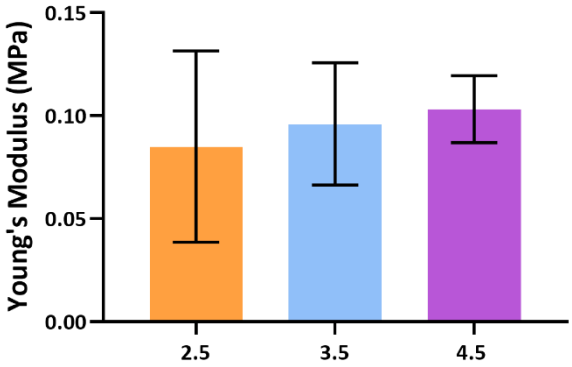

Figure 4.11 *Young's modulus showed no difference between the groups of scaffolds. Mean ± SD, n=5 of each group (2.5, 3.5, and 4.5 scaffold).*

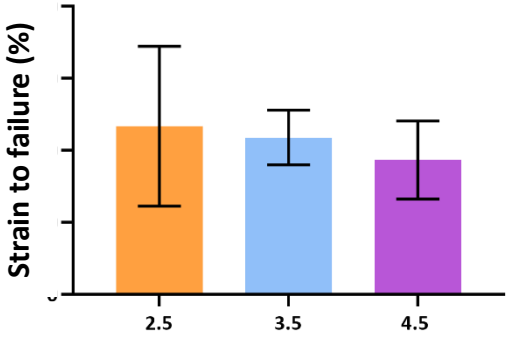

Figure 4.12 *Strain to failure (%) was calculated. The result showed no difference between the scaffold condition. Mean ± SD, n=5 of each group (2.5, 3.5, and 4.5 scaffold).*

Both Young's modulus and strain to failure from 3 groups of samples (*Figure 4.11, 4.12*) were similar between the 3 groups of samples tested with no significant difference. These results indicate that there is not sufficient difference in structural properties as seen in wall thickness and porosity, to cause any significant difference in mechanical properties. Within this range of 2.5-4.5 ratios of salt scaffolds, seem to behave in a fairly similar way within the outcomes tested here. As mentioned in Literature review that PGS was reported to have a mechanical property in a wide range from 0.004-0.28 MPa. Zaky et.al. found their salt leached PGS (90% porosity) had a Young's modulus around 0.038±0.03 MPa similar to that of osteoid tissue, which is approximately 0.03 MPa [101]. It was discussed that these were in a range of matrix properties previously shown to induce osteogenesis(0.025-0.04 MPa) a material with elasticity that falls in this range is expected to have the ability to direct stem cells to differentiate into bone cell lineage [218]. Gao et.al. found their 80% porosity salt leached PGS

scaffold had a young's modulus at 0.004±0.001 MPa which was between osteoid tissue and bone marrow (0.0002 MPa) [94].

While the Young's moduli of the scaffolds in this study were observed to be 0.085±0.04 MPa (2.5 scaffold), 0.096±0.02 MPa (3.5 scaffold), and 0.103±0.01 MPa (4.5 scaffold) which were all higher than reported in the literature. Briefly, in the literature a range of Young's Moduli foreach tissue from highest to lowest were found to be: Cortical bone (100-200 MPa), Cancellous bone (2-12 MPa), Cartilage (0.5-0.9 MPa), Bone osteoid (0.03 MPa), and Bone marrow (0.0002 MPa) [101]. Therefore, the scaffold produced here had its Young's modulus between bone osteoid and cartilage.

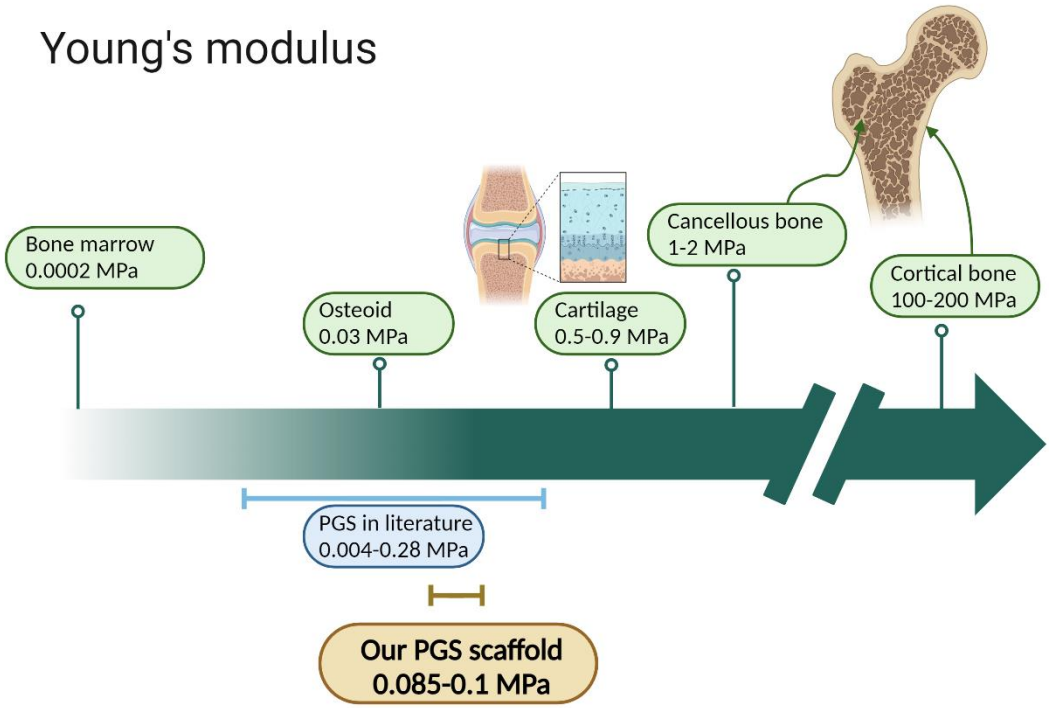

Figure 4.13 *A diagram showing of where salt leaching PGS scaffold of this thesis falls in a range of various tissue. It apparently fell between osteoid tissue and cartilage tissue. It was also in the range of those from previous studies. The diagram was created with BioRender.com.*

All experiments in this chapter were intended to be repeated (N=3) but due to the very strict restrictions during the pandemic, and the small differences between scaffolds examined at this point it was decided to use the data and analysis to narrow down the scaffold to a single preparation condition. The 3.5 condition was selected as a scaffold to work with in further

experiments since the mechanical properties, the attachment and proliferation of cells showed no difference among scaffolds, but 3.5 showed promising results in terms of supporting key proteins. Although the lowest amount of salt (2.5) also supported bone matrix protein deposition these scaffolds usually leaked from moulds during fabrication which meant that the thickness of the scaffold was a not always as intended . This instability is likely to be the reason that the 2.5 scaffold was quite variable, for example in mechanical properties. Also, in future applications the lowest porosity and high proportion of enclosed pores may not allow many cells to attach inside and much nutrient to get through to, for example blood vessel invasion would likely be limited.

4.3. Chapter Summary

These studies of Y201 cells on different scaffolds showed no significant difference in attachment and proliferation which can imply that this range of difference in salt amount used in scaffold fabrication did not strongly affect cell attachment, cell proliferation, or protein production. Overall, all the PGS scaffolds provided promising support for cell attachment, proliferation, and protein production including bone-specific matrix proteins such as osteopontin and bone sialoprotein II. This indicates that salt leached porous PGS scaffolds can provide support for the growth of osteogenic precursors for bone tissue engineering. Because there were no significant differences between the scaffolds in terms of mechanical properties and cell support the medium-porosity scaffolds were chosen for the next block of work in the thesis, the one containing 3.5 g of salt per 1 g of PGS prepolymer.

Chapter 5

Decellularisation and recellularisation of extracellular matrix on Poly(glycerolsebacate) scaffolds for bone regeneration.

5.1. Introduction

It was observed in the previous chapter that salt leached PGS scaffolds were able to support cell attachment, cell growth, and matrix secretion. However, although it has good cell compatibility, PGS is not known as a bioactive or osteogenic polymer and thus PGS alone may not be enough to support good bone regeneration. Adding extracellular matrix (ECM) to a synthetic scaffold may enhance cell differentiation and mineralization, as ECM is well known to contain abundant proteins related to most important cellular activities. Previous work, including from our own group [133, 219], has demonstrated enhanced osteogenesis on scaffolds containing ECM, but to my knowledge this has never been attempted in combination with PGS. In order to identify whether there would be any benefit of the components of extracellular matrix, the decellularisation of a cell-derived matrix was introduced into this project. The first step was to create a protocol for cell derived matrix deposition followed by a decellularisation procedure rigorous enough to wash off the native cells but gentle enough to preserve the extracellular matrix. The final step was to recellularise the scaffold to determine the effects of ECM on the new cells.

Research Objectives

1. To evaluate an appropriate method of decellularisation to be able to remove cellular content as well as preserve the extracellular matrix.
2. To evaluate an appropriate method of washing steps in order to wash out chemical reagents as much as possible to support cell attachment and growth.
3. To compare the PGS scaffold alone with the PGS scaffold containing decellularised matrix in terms of its effects on cell attachment, growth, and mineralisation.

5.2. Results and discussion

5.2.1. Developing the cell seeding protocol

Y201 cells were cultured on 3.5:1 PGS scaffolds for 2 and 4 weeks to evaluate collagen production over time. Y201 were seeded on a PGS scaffold ($5x10^5$ cells in 20 µl) and then the seeding was repeated on day 3rd and 5th by seeding on top of the previous seeded cell layer. (Section 3.2.2) which only one sample was assessed for cell viability (section 3.2.3.) and 3 samples were fixed and stained for collagen deposition with Sirius red staining (section 3.2.3.).

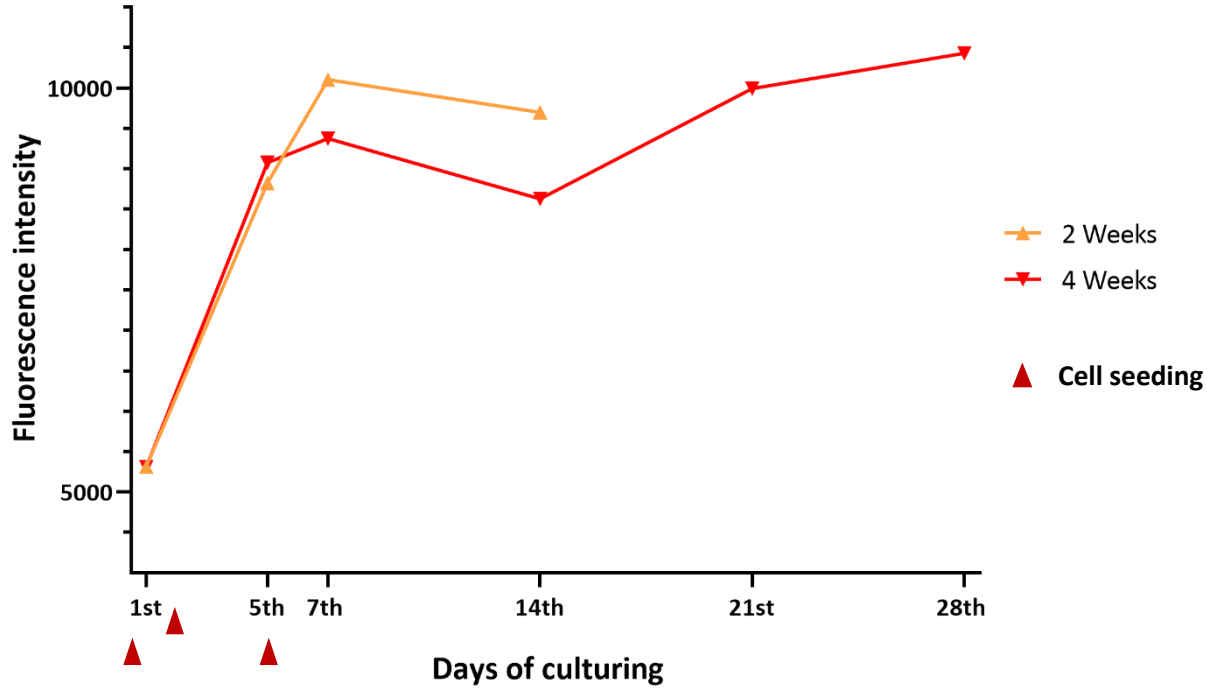

Figure 5.1 *Cell viability of Y201 growing on a PGS scaffold. Each red arrow represented cell seeding on day 0, 2nd, and 5th. The scaffold was divided into two groups which were cultured for 2 weeks and 4 weeks before undergoing decellularisation. Single scaffolds were assessed for cell viability at the time point (n=1).*

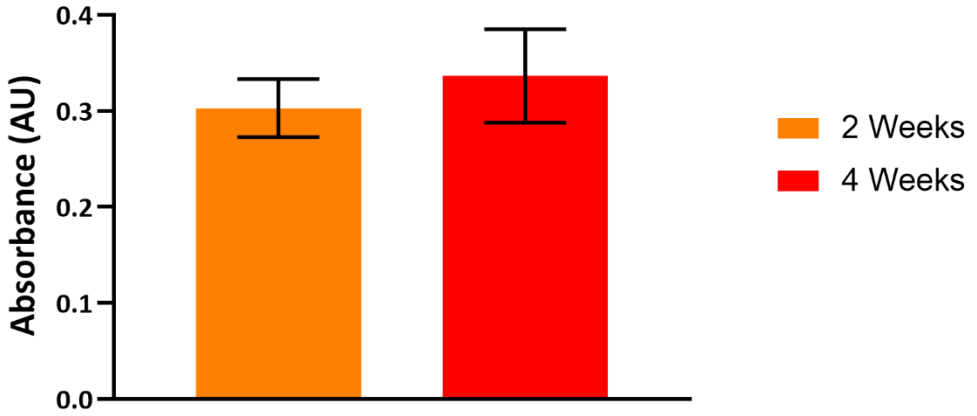

Figure 5.2 *Absorbance of eluted stain from Sirius red stained collagen in groups which were cultured for 2 weeks and 4 weeks. No difference was observed (Mean ± SD, N=1, n=3, * = p<0.05, one way ANOVA with Tukey's pair-wise comparisons).*

As seen from the resazurin data (*Figure 5.1*), the number of cells were observed to increase after each seeding step and reach a plateau from day 7th onwards. The absorbance from stained collagen demonstrated no difference between 2 and 4 weeks of culture. This meant the matrix has reached equilibrium between matrix production and matrix degradation in this environment after 14 days.

5.2.2. Optimising the decellularisation protocol

The first decellurisation study

Since it was demonstrated in the previous experiment that 2 and 4 weeks did not create a significant difference in terms of secreted matrix, the construct model was cultured with Y201 for 19 days before decellularisation. Two methods of decellularisation were compared initially which were new to our research groups [102, 133]. The ability of different methods in removing the DNA and maintaining the matrix was evaluated (Section 3.3.1.). The DNA content and collagen staining were analysed (as written in section 3.2.3.) and compared to the non-decellularised scaffold (a control group).

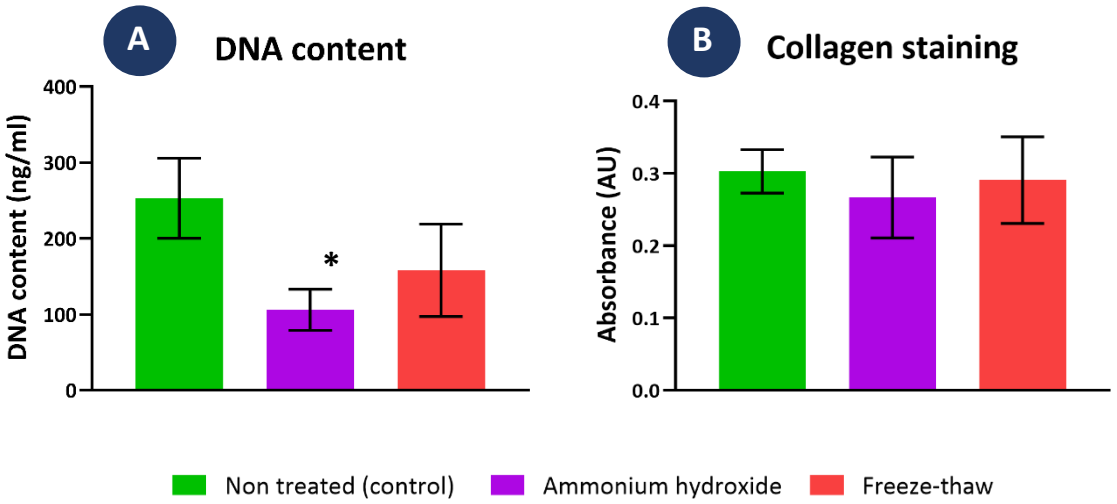

Figure 5.3 (A) *DNA content of scaffolds after 19 days of cell growth. Scaffolds were either collected directly from culture (non-treated) or decellularised with either ammonium hydroxide or a freeze-thaw process.* ***(B)*** *Collagen content of the same scaffold groups (after formaldehyde fixation). Mean ± SD, n=3, N=1, * = p<0.05 (Compared to a control group). One-way ANOVA with Tukey's pairwise comparisons.*

It was demonstrated that using ammonium hydroxide for 10 minutes could significantly reduce DNA content with a slight effect on the collagen content of the matrix, but no significant difference compared to the control group (*Figure 5.3*). In parallel, multiple freeze-thaw cycles showed a similar non-significant difference in collagen content when comparing before and after decellularisation but did not remove DNA content. Even though the DNA content was significantly reduced after treating with ammonium hydroxide for 10 minutes, only 58% relative DNA amount was removed. So, it was decided to seek for a better method to remove dsDNA more efficiently.

The second decellurisation study

One method was modified from the previous study, and another was obtained from the literature which had been used previously to remove cells from tendon and bone tissue [124]. These protocols were introduced to be harsh enough to wash out DNA but gentle enough to preserve the extracellular matrix. They were designed to undertake a longer time and with mechanical force added (with a shaker). Prior to the decellularisation process cells were grown for 19 days to be consistent with the previous study. A single scaffold was grown in parallel for the cell viability to be monitored. The DNA and the collagen content after decellularisation was analysed by comparing with the control group (non-treated).

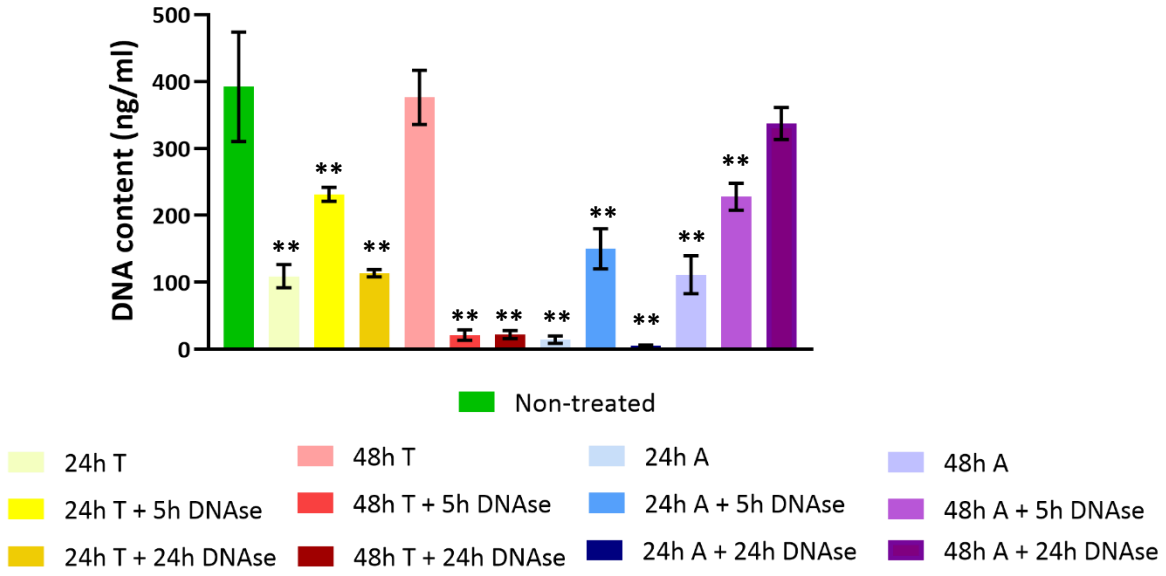

Figure 5.4 *The DNA content of the group of non-treated (control) on the left and those treated with TBP (T) or ammonium hydroxide (A) with or without DNAse at different time points. Almost every group after treatment had significantly reduced DNA (ng/ml). Mean ± SD, n=3, N=1, ** = p<0.01. One-way ANOVA with Tukey's pairwise comparisons compared to control.*

Every group treated with the combined chemical and physical protocol had significantly less DNA than the non-decellularised controls, especially those treated with ammonium hydroxide for 24 hours. DNA was efficiently removed with 3% left in the group treated with ammonium hydroxide alone and only 1% left when this was combined with 24 hours DNAse treatment. However, the group treated with 5 hours DNAse after ammonium hydroxide was not efficient in removing DNA for unknown reasons. The groups treated with TBP for 48 hours gave a satisfactory result after being incubated with DNAse, about 95% DNA (only about 5% left) was removed at both time points. The necessity of incubating with DNAse after treating with chemical reagents was still unclear since some helped in reducing DNA, while some didn't help.

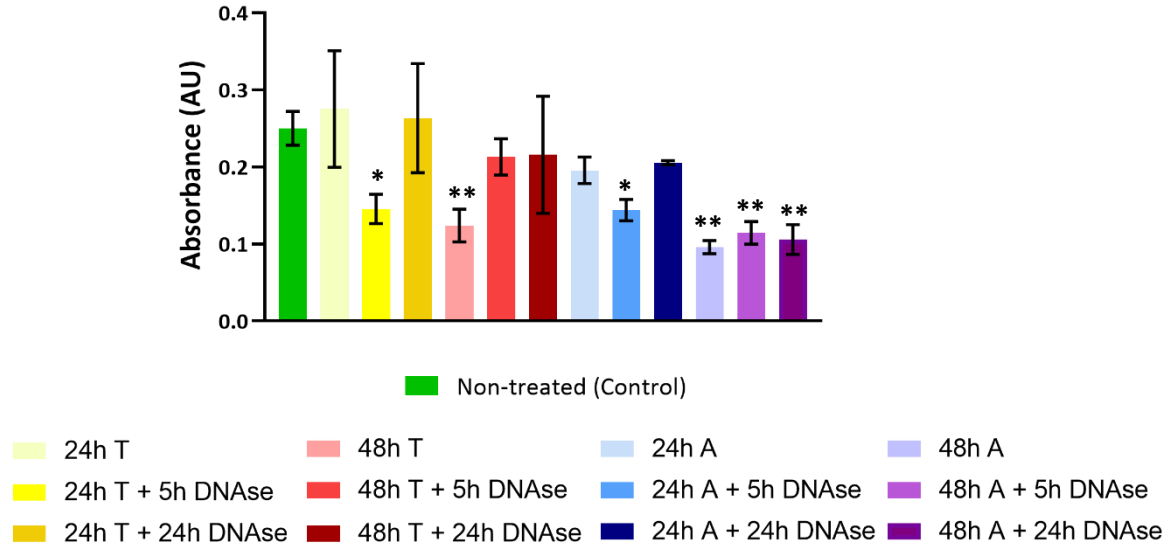

Figure 5.5 *Stained collagen absorbance value of the non-treated group (control) on the left and those treated with TBP (T) or ammonium hydroxide (A) with or without DNAse at different times points were shown. Every treated group was compared to the control group. Mean ± SD, n=3, N=1, *= p<0.05, ** = p<0.01. One-way ANOVA with Tukey's pairwise comparisons.*

Collagen staining demonstrated the groups that could maintain similar amounts of collagen to the control group, were 24 hours of both reagents (24h T, 24h A) and 48 hours of TBP. There was an exception with 24h of both T and A with 5h DNAse, and 48h T that the collagen was significantly different from the control group. While 48 hours of being treated with Ammonium hydroxide (48h A) with or without DNAse seemed to be too harsh for collagen preservation.

According to DNA content results (*Figure 5.4*), four groups with very low DNA content (48h T + 5h DNAse, 48h T + 24h DNAse, 24h A, and 24h A +24h DNase) appeared to have the same amount of collagen when compared to the control group, which fits the key aim of minimising DNA content while maximising ECM content. While the group that gave unexpected and unclear results in DNA analysis also, seemed to have significantly less collagen. Overall, this group did not yield promising results and this method was not pursued. The conditions were then narrowed down to identify the best protocol. Considering the best representative for both chemical reagents, soaking with TBP for 48 hours seemed more efficient than 24 hours in removing DNA but had no difference in maintaining the cellular matrix. While treatment with ammonium hydroxide for 24 hours seemed enough to remove DNA and not too harsh

for the collagen compared to the 48 hours. On the other hand, the shorter protocol would be better to avoid any contamination.

The third decellularisation study

Treatment with TBP at 48 hours was compared with ammonium hydroxide at 24 hrs. Due to the variable advantages of DNAse in combination with the chemical treatments it was deemed still necessary to compare plus/ minus DNAse treatment groups. Investigating the effect of DNAse was another issue to study in this experiment. The study was carried out in the same way as previous studies before decellularisation with four different methods (two chemicals with and without DNAse) comparing their DNA and collagen content with the control group (non-treated).

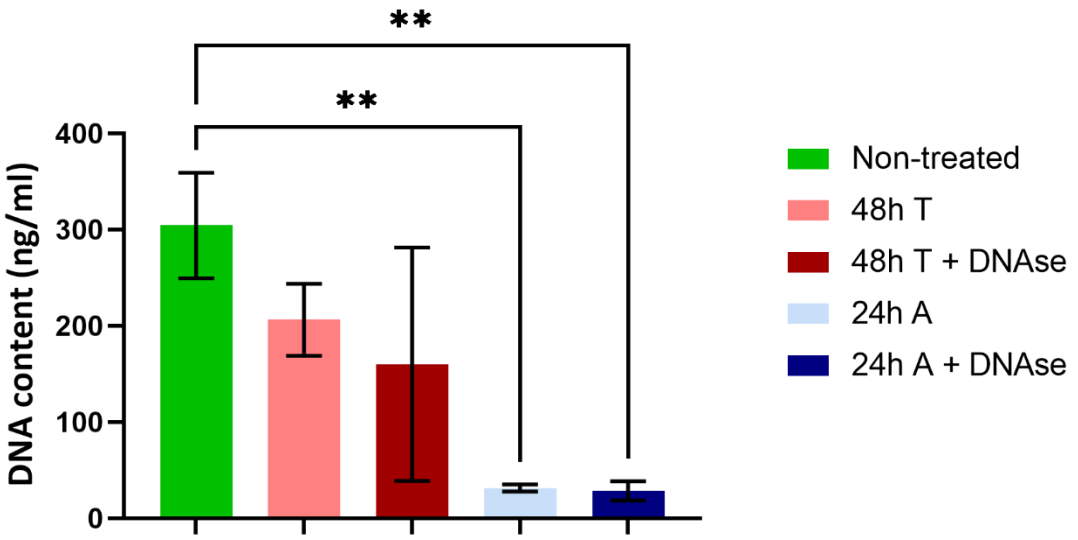

Figure 5.6 *The DNA content of 4 groups of chemically treated and a group of control were shown. Each bar represented three biological replicates. The groups being treated with ammonium hydroxide were found to be significantly different from the control group. Mean ± SD, n=3, the mean of each experiment was used to provide the individual value presented, the N=3, ** = p<0.01. One-way ANOVA with Tukey's pairwise comparisons.*

The experiments were repeated with further batches of cells. The results (*figure 5.6*) showed that both groups using ammonium hydroxide removed DNA content to a statistically significant extent leaving about 9% of DNA on average. Also, those treated with TBP alone seemed to have the same result as the previous experiment since there was no significant difference compared to the control groups. While the group treated with TBP and DNAse

seemed to be contrary to the last experiment since they didn't give any significant difference from the control group.

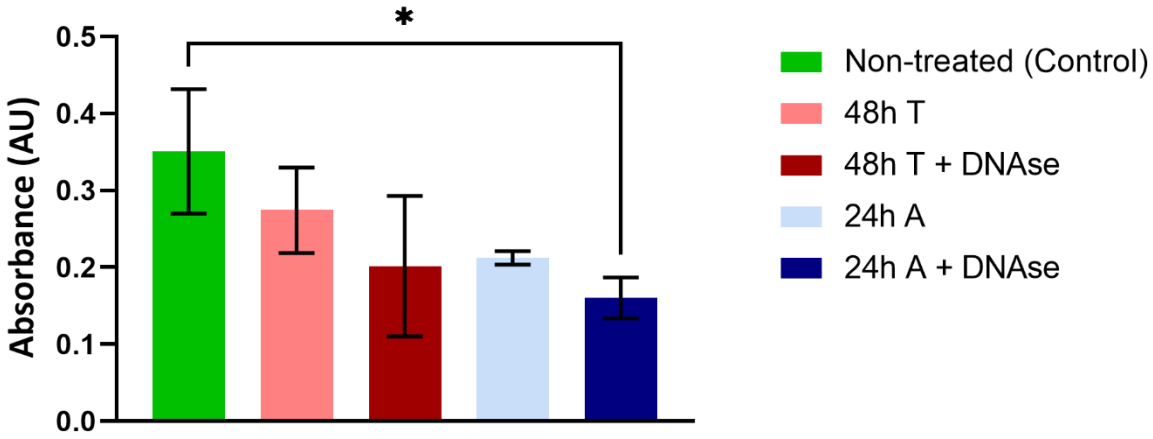

Figure 5.7 *Comparing stained collagen absorbance values between the control group and the treated groups. Mean ± SD, N=3, * = p<0.05. One-way ANOVA with Tukey's pairwise comparisons.*

From *Figure 5.7,* It was found that almost every group was not different from the control group except for the group treated with ammonium hydroxide with DNAse ($p<0.05$). However, no significant difference was noted between all treated groups. Based on DNA removal efficiency, the protocol treating the sample with a combination of ammonium hydroxide and triton x-100 for 24 hours was chosen. Despite having the lower collagen content after being decellularised when compared to the control group, it was discussed that having a sample being incubated with another 24 hours of DNAse was included in the finalised protocol. This was to ensure maximum capability of DNA removal.

Double stranded DNA (dsDNA) is believed to be the key molecule that can trigger the adverse effect of immune system in the recipient's body which then may lead to a failure of an implant. Because the decellularised matrix is aimed to be used as a part of an implant, it is important to maximise the removal of DNA and minimise the disruption of ECM. In a previously published study, it was established that using freeze and thaw followed by DNAse I to decellularise an MLO-A5 derived matrix on 3D printed Polycaprolactone (PCL) could remove DNA content by about 95% [109]. Another study found treating MSCs matrix on Poly(lactic-co-glycolic acid) (PLGA) membrane with freeze-thawed cycles and DNAse I could remove DNA by about 93% which was not significantly different from treating with ammonium hydroxide and triton x-100 [220].

While in this chapter, only 37% of DNA was removed when using the freeze and thaw method followed by DNAse I and 58% of DNA was removed when using ammonium hydroxide with triton x-100. This different ability of removing DNA of the methods might be due to the different methods of fabrication of the scaffolds that creates different shapes and sizes of pores and differing volumetric porosity and interconectedness. As previously discussed in the literature review, decellularisation success in removal of cell content can be affected by time exposure of the tissue to the decellularisation agent(s). However, being exposed to a strong chemical agent for too long can increase the risk of matrix being destroyed. Therefore, mechanical agitation is usually introduced to help the chemical solution to diffuse throughout the tissue.

In the current work an agitation was also introduced in the second experiment of this chapter [221, 222]. From the results of the second and the third studies, Y201 derived matrix being treated with TBP for 48 hours with another 24 hours of DNAse I had 55±38% of DNA content removed. This was the first time that TBP was introduced to be used for decellularisation in bone derived matrix on a 3D scaffold. It is surprising that this didn't wash DNA out successfully, as it did remove 84% of DNA in patellar tendon, in the previously published study (3 x 1.5 x 0.3 cm^3) which seemed to be a denser tissue [137]. Treatment with ammonium hydroxide with triton x-100 for 24 hours followed by another 24 hours of DNAse did remove 93±4% of DNA content and this seemed to be very similar to previously mentioned studies, in which ammonium hydroxide combined with triton x-100 could wash out around 93% of DNA from MSCs matrix on Poly(lactic-co-glycolic acid) (PLGA) membranes [220]. Even though treatment with 24 hours of ammonium hydroxide with another 24 hours of DNAse I resulted in the lower collagen outcome compared to the control group, there was no difference when compared to the other treatment groups. There was not sufficient evidence to conclude that DNAse I affected ECM. Additionally other studies have demonstrated that DNAse I had no effect on the ECM, neither tissue-derived nor cell-derived [119, 223-225]. So, this method was chosen to be used as the protocol for the further experiments.

5.2.3. Optimising washing steps after decellularisation protocol

The first washing study: PBS wash

The aim of this study was to elucidate whether a scaffold with decellularised cell-derived matrix (d-scaffold) would have potential to support cell attachment and cell growth when compared to a PGS scaffold alone. Y201 cells were cultured on a PGS scaffold for 19 days before undergoing a decellularisation procedure as optimised previously. Every d-scaffold was washed with PBS after decellularisation. d-scaffolds were then cultured with a new set of Y201 cells for 21 days compared with d-scaffolds without any cells (as a negative control group) and scaffolds with cells (as a positive control group). Cell viability assays were performed to assess the scaffolds' ability to support cell attachment and cell growth.

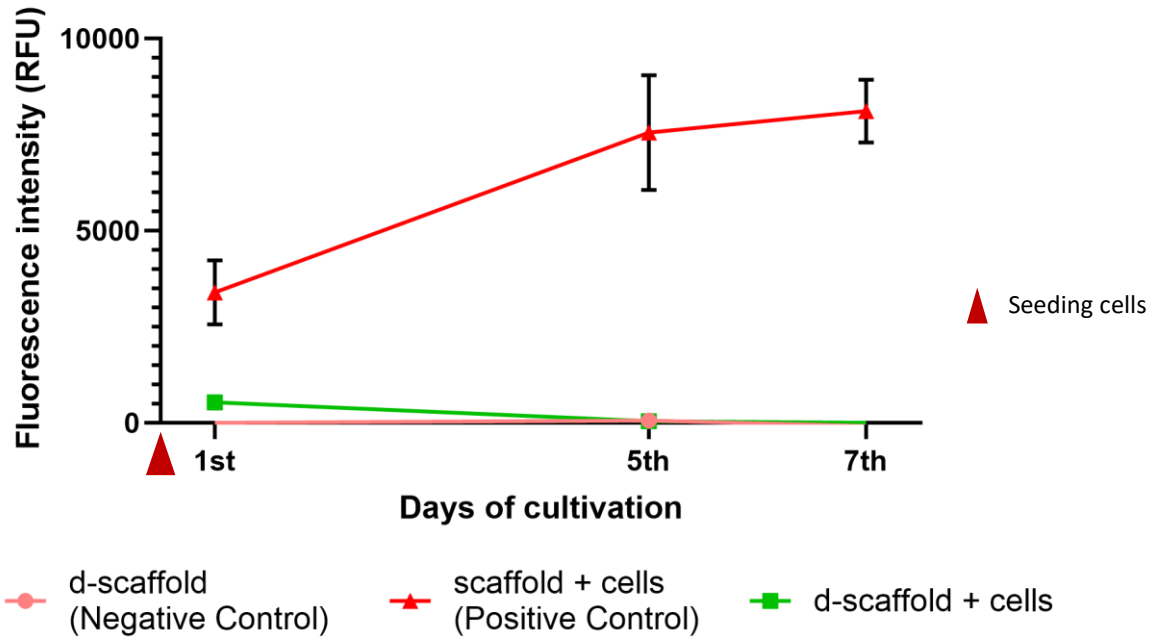

Figure 5.8 *Cell viability of Y201 cells cultured on a d-scaffold and a scaffold (positive control) compared to a d-scaffold without any cell (negative control group) on day 1, 5 and7 of culturing. Mean ± SD, n=3, N=1.*

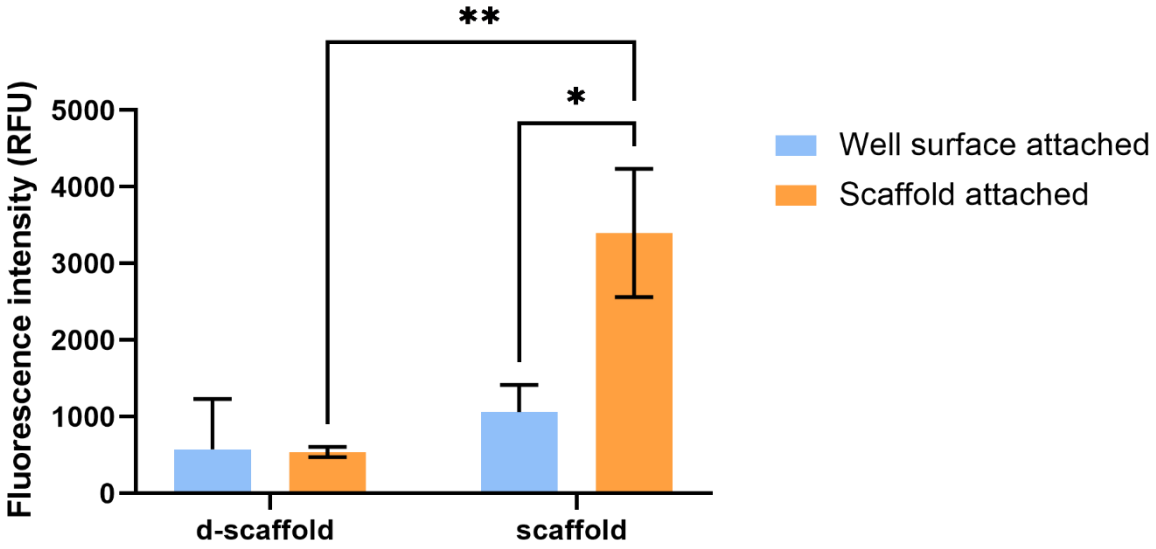

Figure 5.9 *Cell viability on day 1 on the d-scaffold and the scaffold alone. It was noted that the d-scaffold supported very low cell attachment. Mean ± SD, n=3, * = p<0.05, ** = p<0.01. One-way ANOVA with Tukey's pairwise comparisons.*

After being decellularised and washed with PBS. Both cell attachment and growth of Y201 on the d-scaffold were very low *compared to the scaffold alone. By the 5th day of culture there was no evidence of viable cells on the d-scaffold. While the cells on the scaffold kept growing until day 7* (*Figure 5.8*). Considering that even when taking into account cells that fell off the scaffold and landed on the well surface, as shown in *Figure 5.9*, there were fewer cells overall in the culture wells containing d-scaffold. Therefore, it is likely that the d-scaffold was toxic to the cells. Hence, washing thrice with PBS for only 10 minutes clearly didn't wash chemical reagents out properly.

The second washing study: media wash

The original protocol stated that the scaffold should be soaked in fresh media at 4°C for 72 hours on a shaker and then for another 24 hours after being treated with DNAse [226]. This study was modified from the original as I did not have access to a shaker eligible to be used in a fridge. The scaffold was soaked in the cold media on a shaker for 30 minutes each day before being put into the fridge. After washing, the d-scaffold was then taken to analyse biologically by growing the new set of Y201 cells on it and comparing this to those grown on a scaffold alone.

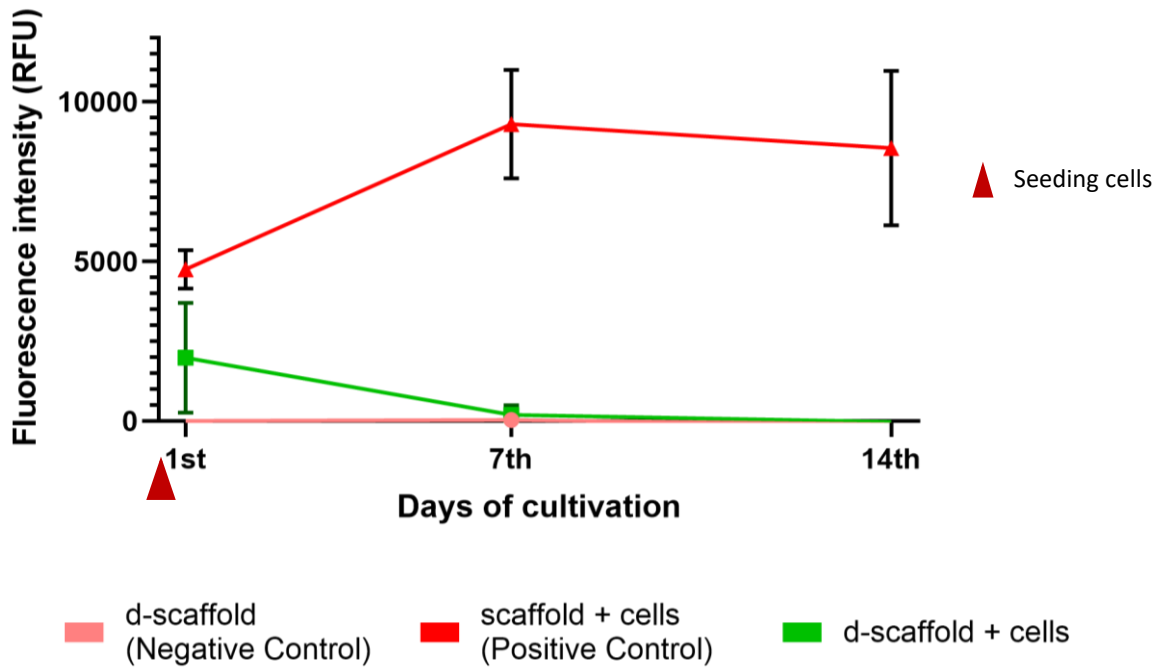

Figure 5.10 *Cell viability of Y201 cells cultured on a d-scaffold and a scaffold (positive control) compared to a d-scaffold without any cells (negative control group) on day 1, 7, and 14 of culture. Mean ± SD, N=2.*

The results in *figure 5.10* demonstrated a similar trend to the previous experiment, the fluorescence showed a lower value on a d-scaffold compared with a scaffold alone (positive control) on the 1st day and very low, equivalent to the negative control group by day 5. The cells seemed to not survive on the d-scaffold. The d-scaffold after being left for only 30 minutes a day on a shaker was shown not able to support good cell attachment or cell growth on the scaffold.

The third washing study

The procedure of washing the scaffold was adjusted by placing on a shaker for 10 minutes and then back to the fridge. This cycle was repeated 6 times a day to increase the time of the samples being on the shaker from 30 to 60 minutes a day. The action of undertaking this in multiple cycles was to improve movement of the fluid. After being washed, the scaffolds were cultured with Y201 for 21 days. Cell viability was assessed for d-scaffolds with cells and d-scaffolds without cells (negative control group), and scaffolds with cells (positive control group).

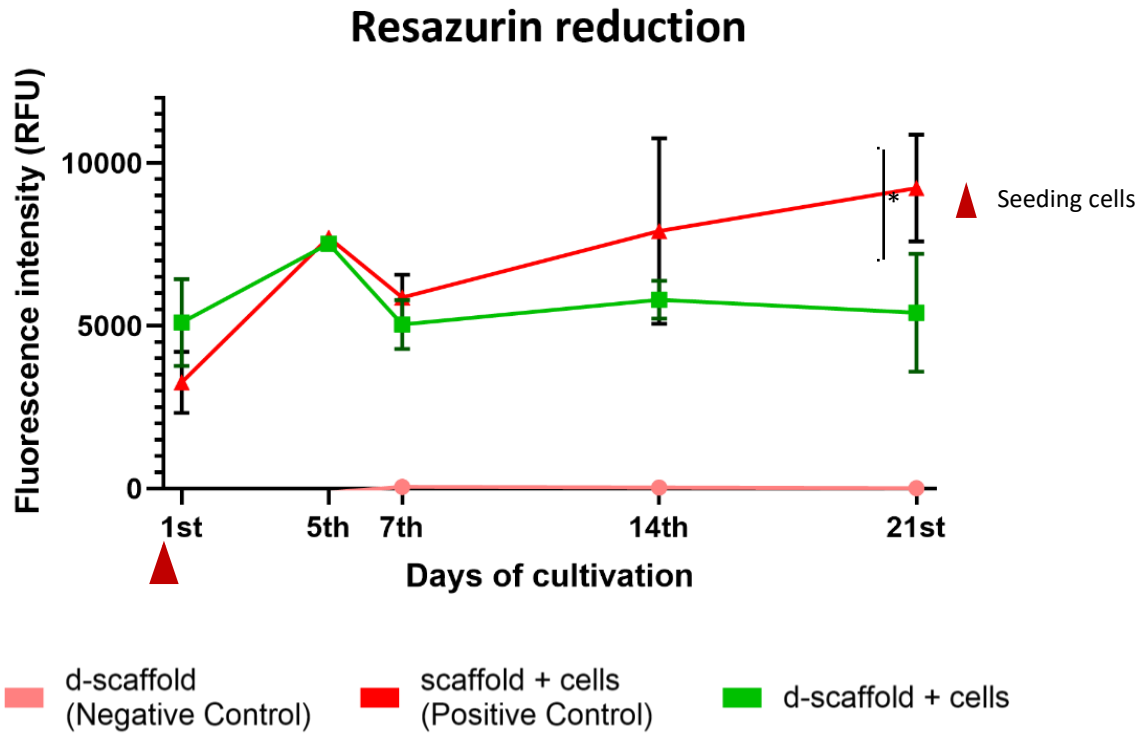

Figure 5.11 *Cell viability of Y201 cells cultured on a d-scaffold and a scaffold (positive control) compared to a d-scaffold without any cell (negative control group) on day 1, 7, 14 and 21 of culture. Mean ± SD, n=3, N=3, * = p<0.05. One-way ANOVA with Tukey's pairwise comparisons.*

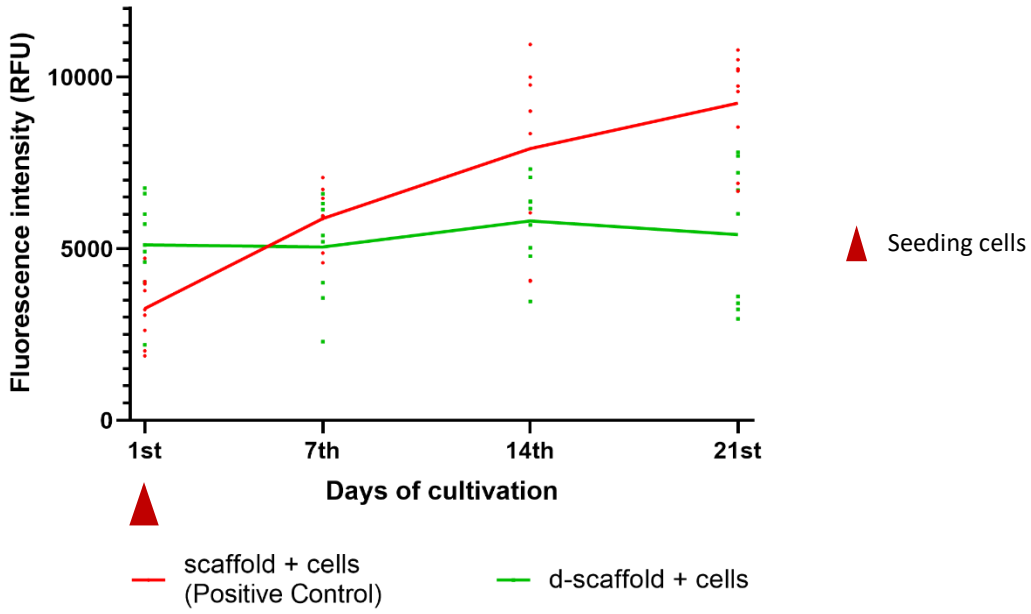

Figure 5.12 *Individual scaffold cell viability (presented as dots) for each time point with a line between the means for the d-scaffold group and the scaffold-only group indicated. Mean ± SD, n=3, N=3.*

The result seen from *figure 5.11-5.12* showed that a d-scaffold washed with the full protocol was able to support cell attachment and growth. Therefore, it can be interpreted that time exposure to mechanical force (a shaker) was an important factor to be considered in washing chemical reagents out of the decellularised scaffold. It was shown that the d-scaffold was slightly better than a scaffold-only in cell attachment, although this was not statistically significant. However, the scaffold alone seemed to support the cell growth better than the d-scaffold as seen by day 14th and 21st. The overall increase in mean viability (*figure 5.11)* demonstrated that the cell numbers on the scaffold alone seemed to keep increasing from the first day, and the d-scaffold did support steady cell numbers for the whole experiment but not an increase in cell viability (which can be interpreted as lack of cell proliferation). However, it was established that there was a significant difference between the scaffold alone and the d-scaffold only by day 21st ($p<0.05$). This could be interpreted as the d-scaffold had limited space for cells to grow compared to the scaffold alone.

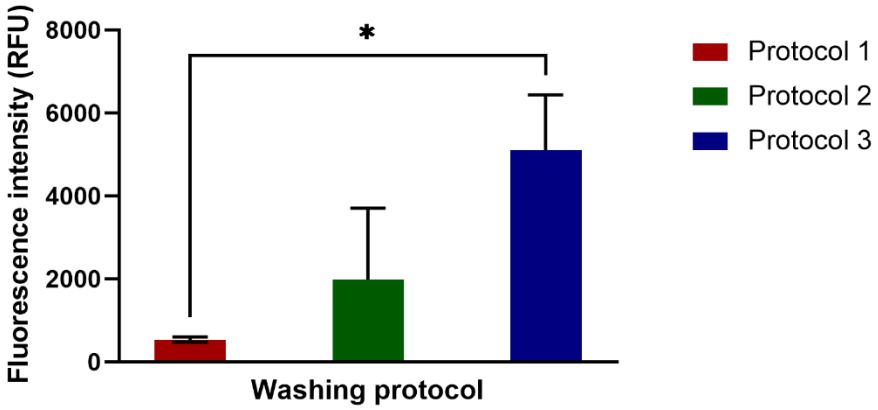

Figure 5.13 *The fluorescence intensity values (indicator of cell viability) on the 1st day of the d-scaffold groups between 3 different washing protocols were shown. Mean ± SD, n=3, * = p<0.05. One-way ANOVA with Tukey's pairwise comparisons.*

The fluorescence intensity of viable cells on day 1st was used to compare the three washing protocols in terms of the scaffolds' ability to support cell attachment. *Figure 5.13* showed the washing protocol 3 supported the highest cell attachment to the hybrid scaffolds after decellularisation (d-scaffold). It also showed success in keeping the cells alive until day 21st while the others failed to do that.

5.2.4. Osteo-conductive property assessment of the d-scaffolds

As a promising result of recellularisation and growing Y201 cells for 21 days on d-scaffolds was shown, the d-scaffold was then analysed for its ability to support the cells to differentiate, deposit collagen and mineralise.

Osteogenic differentiation

To assess cell differentiation, the d-scaffolds were collected and lysed after growing for 14 days and then tested for ALP enzyme activity (section 3.2.3.) compared to scaffolds with cells.

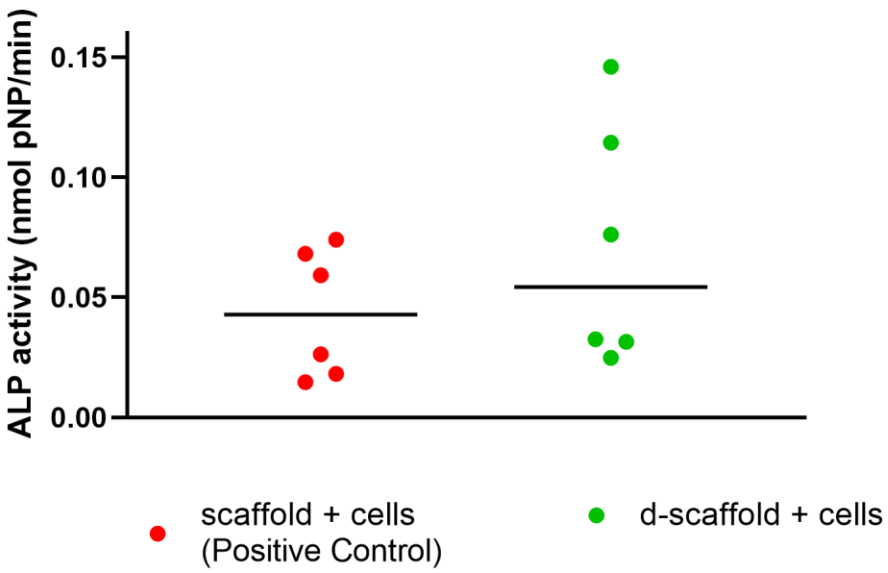

Figure 5.14 *The ability of Y201 to differentiate into bone cells was assessed. The calculated ALP activity (nmol pNP/min) was normalised using the amount of DNA contained (ng). No significant difference was observed. Mean ± SD, N=2, n=6. Unpaired parametric t-test.*

The ALP activity (nmol pNP/min) was normalised using DNA content (ng). Data on figure 5.14 demonstrated that d-scaffold and the plain PGS scaffold were not different in supporting Y201 cells to differentiate into a bone cell lineage using ALP as a marker. The d-scaffold group was found to have a high variability in its ALP response.

Collagen and calcium deposition

After being cultured for 21 days, scaffolds were collected and fixed to assess collagen and calcium content using Sirius red and alizarin red staining (Section 3.2.3.). The d-scaffold was compared to the scaffold alone (a positive control) and the d-scaffold without any cells (a negative control).

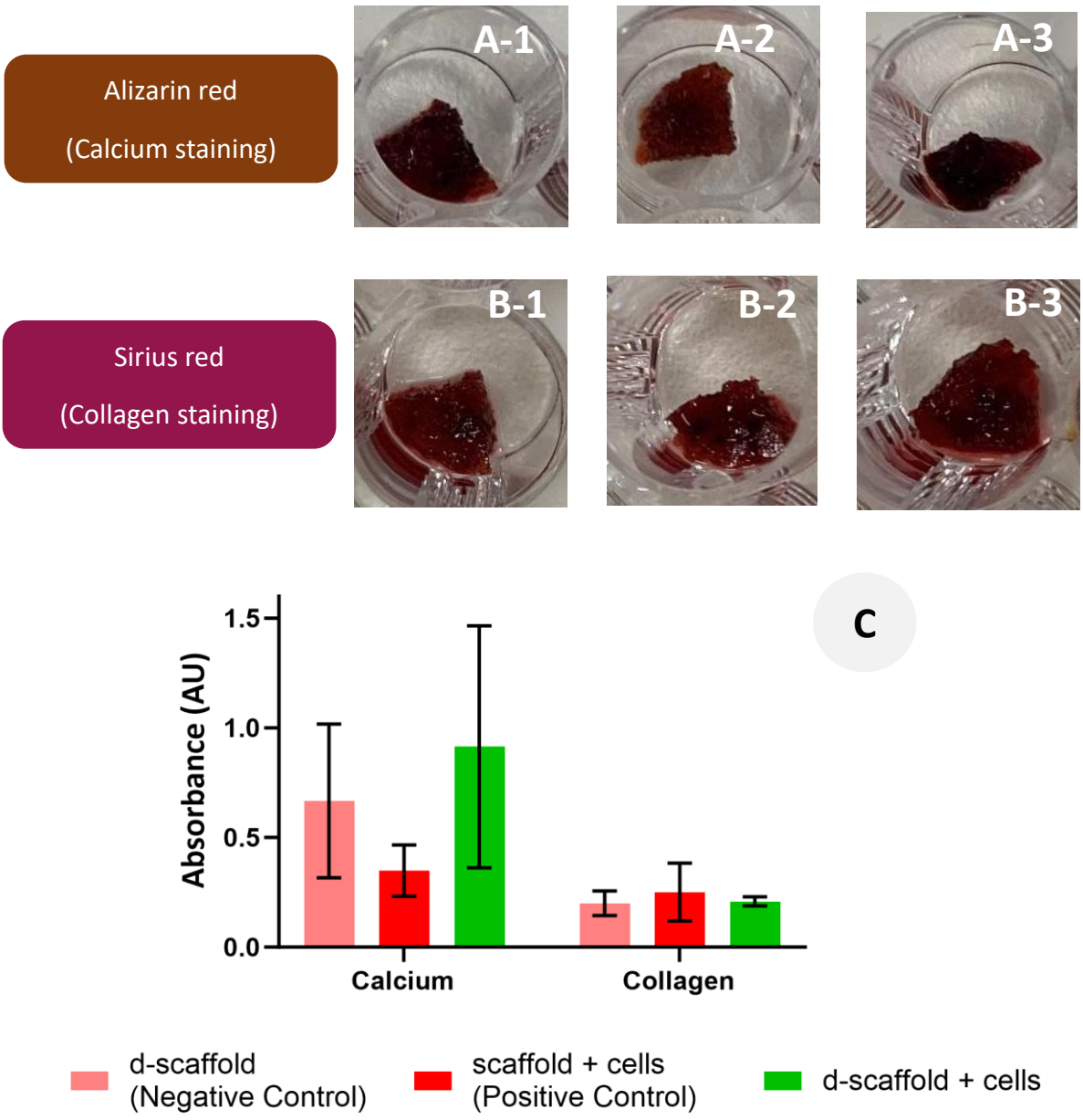

Figure 5.15 *The samples were fixed and stained on day 21. [A-1 – A-3] A representative photograph after collagen staining of a d-scaffold (A-1), a scaffold alone + cells (A-2), and a d-scaffold + cells (A-3). [B-1 – B-3] Representative photographs of calcium staining of a d-scaffold (B-1), a scaffold alone + cells (B-2), and a d-scaffold + cells (B-3). [C] The colourimetric absorbance of stained calcium and collagen between 3 different groups is shown. Mean ± SD, N=3.*

Reseeding the new set of Y201 onto the d-scaffold seemed to result in a slightly higher content of calcium compared to the scaffold alone. And cells seeded in a fresh plain PGS scaffold seemed to have lower overall calcium content than both the d-scaffold groups (with and without cells) as seen from the photos of the stained scaffolds (*figure 5.15A*). However, no statistical difference was observed between the groups. There was a large variability in calcium deposition profiles in the d-scaffold with cells (*figure 5.15C*). The collagen amount among the groups was similar to each other both visually and statistically (*figure 5.15B-C*).

A good decellularised implantable tissue for tissue replacement does not only have to demonstrate removal of cells and preservation of ECM, but also needs to be biocompatible to new cells migrating into the hybrid construct. Washing steps are very important to remove any residual decellularisation agents as much as possible. The results in this study showed that washing with DMEM for 72 hours after decellularisation and another 24 hours after DNAse when agitating with an orbital shaker worked well to improve cell attachment.

A previously published study reported that decellularised human periodontal ligament matrix supported the growth of re-seeded cells better than human periodontal ligament (hPL) seeded on a commercial collagen membrane. The membrane was washed with distilled water for 60 minutes after decellularisation [227]. This implies that the key factor might not be the media to help washed off the chemicals, but rather the length of time for the washing steps which has to be suitable for the type, the size, and the thickness of tissue to be able to wash out the solution.

Decellularised ECM was reported to aid cell attachment. Hoshiba et.al. found more human epithelial cells attached onto 3D printed PLLA with decellularised matrix compared to PLLA alone [129]. Deustch et.al. observed differently, the DNA content of MSCs reseeded on ECM/PCL was lower than those seeded on collagen coated PCL. It was discussed that the hydrophobicity after decellularisation of the matrix could be the reason for that since, both scaffolds became similar in terms of overall cell content 1 week later [29].

The result in this chapter indicated that decellularised scaffold could attract a slightly more cells (but not significantly) than the PGS only. However, differently from the other studies was that on day 21st the cell viability on decellularised ECM was significantly lower than the scaffold alone whereas in a previously published study decellularised ECM was reported to

enhance cell growth. Deutsch et. al. found that culturing MSCs on bone ECM on PCL yielded higher mineralised content than the MSCs on PCL alone after both were supplemented with osteogenic media for 4 weeks [29]. Thibault et.al. even demonstrated that decellularised bone ECM on PCL scaffold could support reseeded MSCs to deposit calcium more than those on PCL alone regardless of having dexamethasone. It was discussed by the authors that this might be because of the osteogenic factors present in the ECM which were retained even after decellularisation [121].

Unfortunately, in this present study, the calcium content, collagen content, or ALP activity yielded from Y201 cultured on decellularised bone matrix on PGS scaffold was not significantly different from PGS alone. This may be because the space was packed by the decellularised matrix and there was not much room for the cells to grow which may lead to less interaction between the cells and result less osteogenic function or it is possible that the cells need more time to mineralise.

5.3. Chapter Summary

Treating with ammonium hydroxide and triton x-100 for 24 hours and another 24 hours of DNAse I seemed to be a satisfactory method of cell removal and matrix preservation of Y201 cell-derived matrix on salt leached PGS scaffolds. Washing in DMEM with several bouts of agitation was the method that seemed to wash out the decellularisation agents the best in this study, which resulted in quite promising cell attachment. The work in the previous chapter demonstrated that salt leached PGS scaffold could support good Y201 attachment, growth, and bone matrix deposition.

In this chapter I showed that adding decellularised matrix onto PGS scaffolds didn't seem to enhance cell attachment, growth, differentiation, or mineralization for a fresh batch of Y201 cells, and therefore my hypothesis was not supported. However, it might be too soon to conclude that the Y201 matrix combined with PGS scaffold couldn't make any difference at all since here I have only used one specific porosity and one fabrication method for the scaffold construction. Using a different fabrication method of PGS, in particular one with a higher and more interconnected porosity may lead us to more interesting results. Ongoing work by others in the research group is investigating different ways of fabricating porous scaffolds with PGS

and once this is optimized the combination of scaffold with ECM could still be further investigated.

Chapter 6

Salt leaching Poly(glycerol sebacate) tested with co-culture of fibroblasts, oral keratinocytes and osteogenic precursors for craniofacial tissue repair.

6.1. Introduction

In chapters 4 and 5, it was demonstrated that the salt leaching scaffolds showed promising support to Y201 attachment, growth, bone-like matrix deposition. However, since the craniofacial tissue consists of both bone and soft tissue, repairing only bone tissue might not successfully regenerate the whole craniofacial tissue. Not enough soft tissue to cover the whole defect, if this is forced to be closed, then there are consequences. If it is closed improperly, then it surely risks underneath tissue contamination which can become an infection which affects success in regeneration. While if it's closed properly, but the tension of it is too high it can easily cause a fibrosis scar which affects the tissue aesthetically and functionally [168-172].

In this chapter, it's going to be an examination of the potential to support co-culture of the bone part (Y201) and soft tissue part which comprises of a fibroblast layer (NOF343) and keratinocytes layer (FNB6) of craniofacial bone tissue. This was done using the plain PGS scaffold without cell-derived decellularised ECM because the result in chapter 5 showed decellularised ECM couldn't enhance Y201 attachment, growth, differentiation, or mineralisation when compared to PGS scaffold alone. Also, a process of generating a PGS scaffold with decellularised ECM is time consuming. Therefore, it is interesting to study co-culture of Y201, NOF343, and FNB6 on salt leached PGS scaffold to elucidate whether PGS scaffold can support these cells being co-culture for craniofacial tissue regeneration use.

Research Objectives

1. To assess whether Y201 growth, differentiation, and collagen and calcium deposition can be supported in media used for oral keratinocyte growth.
2. To demonstrate whether PGS scaffolds can support the co-culturing of NOF343, FNB6 and Y201 cells and maintain the cell types in a layered structure similar to that of the bone/oral mucosa structure.

6.2. Results and discussion

6.2.1. Observing Y201 cell proliferation in Green's media

Both fibroblasts (NOF343) and oral keratinocytes (FNB6) are generally cultured in Green's media in our laboratories. Green's media is supplemented with compounds such as EGF which of course raise the cost of growing oral keratinocytes, but the growth factor is essentially needed for oral keratinocytes differentiation. So, using Green's media is unlikely to be replacable with basal media for growing oral keratinocytes. However, there is no evidence to date that Y201 cells can grow and survive in Green's media. Therefore, the first step of the co-culture experiments was to examine how Y201 cells perform in Greens media compared to the basal media used in the previous chapters and previous work with these cells.

Y201 cells were cultured in monolayer and divided into four groups of media: BM, BM with osteogenic supplements, Green's media, and Green's media with osteogenic supplements which are 50 µg/ml ascorbate, 5 mM β-Glycerolphosphate and 100 nM Dexamethasone. The cells were cultured for 21 days with cell viability measured on day 1st, 7th, 14th and 21st. ALP enzyme activity was assessed on day 14th (see section 3.2.3.). On day 21 all samples were stained with Sirius red and alizarin red to evaluate collagen and calcium deposition (see section 3.2.3.).

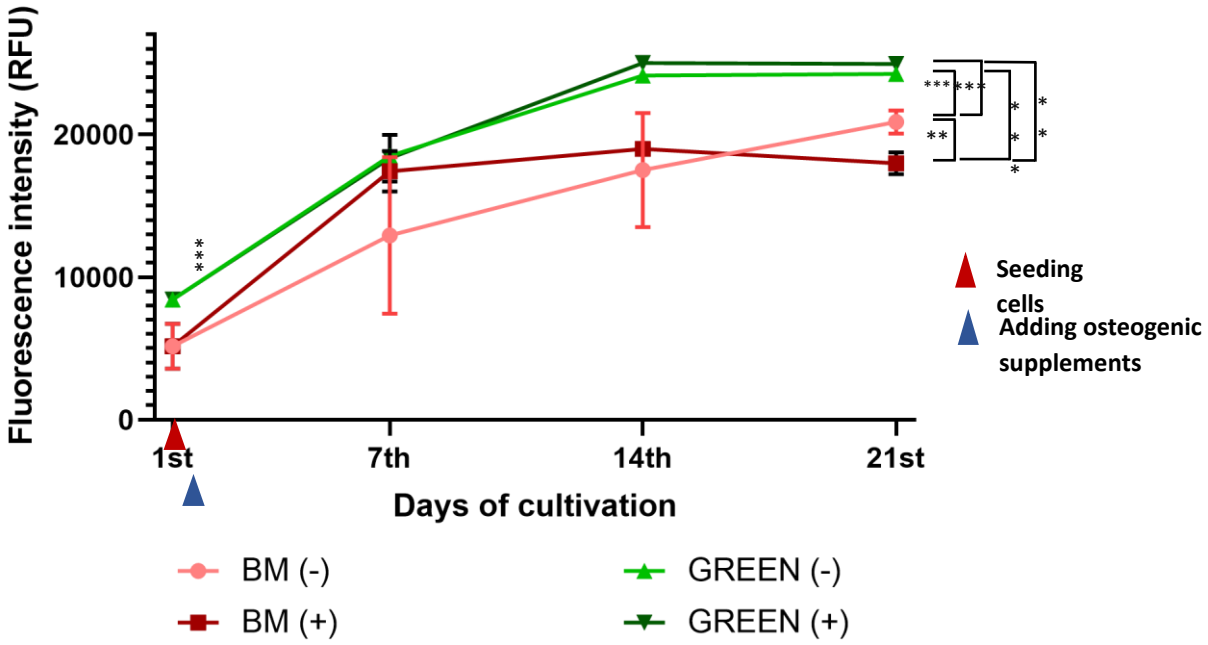

Figure 6.1 *Y201 cell viability on days 1, 7, 14 and 21 of culture in four different media: BM, BM with osteogenic supplements, Green's media, and Green's media with osteogenic supplements. Data is presented as mean ± SD, n=3, N=1, ** = p<0.01, *** = p<0.001, **** = p<0.0001. One-way ANOVA with Tukey's pairwise comparisons.*

One day after seeding, there was a significant difference noted between the group fed with BM and the group with Green's media. Green's media fed cells gave a higher metabolism ($p<0.01$). The osteogenic supplements were added on day 1st, after the cell viability assay had been performed. Fluorescence intensity increased over time, indicative of an increase in metabolic activity showing that cell proliferation did occur. After culture for 21 days, it was evident that cell viability of cells cultured in Green's media was significantly higher than the cells cultured in BM ($p<0.001$, $p<0.0001$). There was no difference between the groups those being grown in Green's media. On the other hand, for the group being cultured in BM [BM (-)] was significantly higher than the group of BM with osteogenic supplements [DMEM(+)]($p<0.01$). Culturing Y201 in Green's media with osteogenic supplements resulted as a 1.2-fold increase of cell metabolism when compared to those cultured in BM [BM(-)]($p<0.001$), and a 1.4-fold increase to those in BM with supplements [BM(+)]($p<0.0001$) (*Figure 6.1*).

There are various components in Green's media as listed in Chapter 3 which are added for specific reasons related to cell growth. For example, Epidermal growth factor (EGF) is well known to play an important role in cell mitogenesis (including mesenchymal cells), therefore

cell proliferation [228]. There was a previous experiment comparing cell numbers after 3 days of MSCs culture between standard basal media and media with EGF added at a different concentration. The result demonstrated that media with EGF could increase cell numbers higher than culturing MSCs in normal media. After 3 days of culture, media with EGF could enhance cell growth for 11.9±7.4% (at 5 ng/ml of EGF), 20.2±6.9% (at 25 ng/ml of EGF), and 29.4±14.4% (at 50 ng/ml of EGF) [229]. While another experiment carried out similarly by culturing MSCs with normal media and 10 ng/ml EGF added media. Numbers of MSCs on day 5 were counted and compared with day 1. After culturing for 5 days, MSCs fed with normal media were expanded for 5.5-fold, while adding 10 ng/ml could expand MSCs numbers up to 8.5-fold [228].

Insulin is also present in Green's media and was suggested to be a key regulator of seeding, proliferation, and mRNA transcription of human pluripotent stem cells [230]. Some published papers also stated that Insulin and EGF have a synergistic effect on mitogenesis and therefore cell proliferation. Insulin was suggested to activate EGF receptors at the early stage of the EGF signaling pathway of cell mitogenesis in fibroblast cells [231, 232]. These positive effects on cell mitogenesis can provide an explanation for the cell viability being significantly higher in Y201 cultured in Green's media. However, cell proliferation was not the only factor to be considered in order to further the creation of the bone layer of the model. Cell differentiation, collagen deposition and mineralisation should also be taken into account.

6.2.2. Observing Y201 cell differentiation, collagen deposition, and mineralisation in Green's media

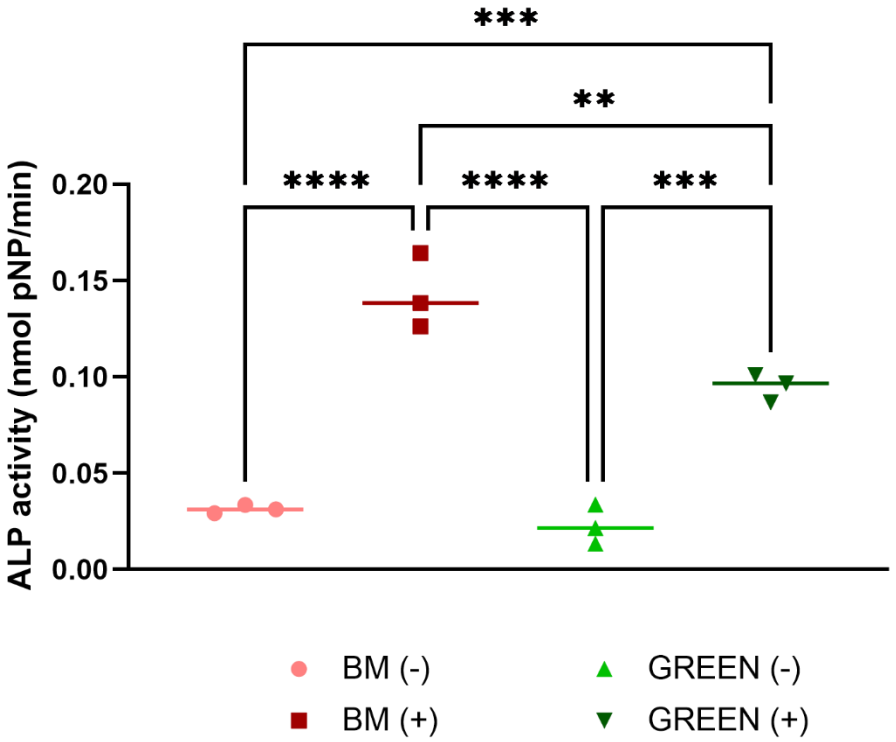

Figure 6.2 *ALP activity on day 14 of Y201 cultured in four different media: BM, BM with osteogenic supplements, Green's media and Green's media with osteogenic supplements. ALP activity values (nmol pNP/min) were normalised to DNA amount (ng). Mean ± SD, n=3, N=1, ** = p<0.01, *** = p<0.001, **** = p<0.0001. One-way ANOVA with Tukey's pairwise comparisons.*

Results in *Figure 6.2* showed the ALP activity of both groups without osteogenic supplements were significantly lower than their respective comparison media which contained osteogenic supplements ($p<0.001$ in Green's and $p<0.0001$ in BM). The group cultured in BM with osteogenic supplements was shown to have the highest ALP activity of Y201. When comparing the groups containing osteogenic supplements, culturing Y201 in BM showed a 1.5-fold increase in cell differentiation compared to Green's media ($p<0.01$). EGF seemed to suppress ALP activity in MSCs on day 14^{th} of culture when compared to basal media without EGF added.

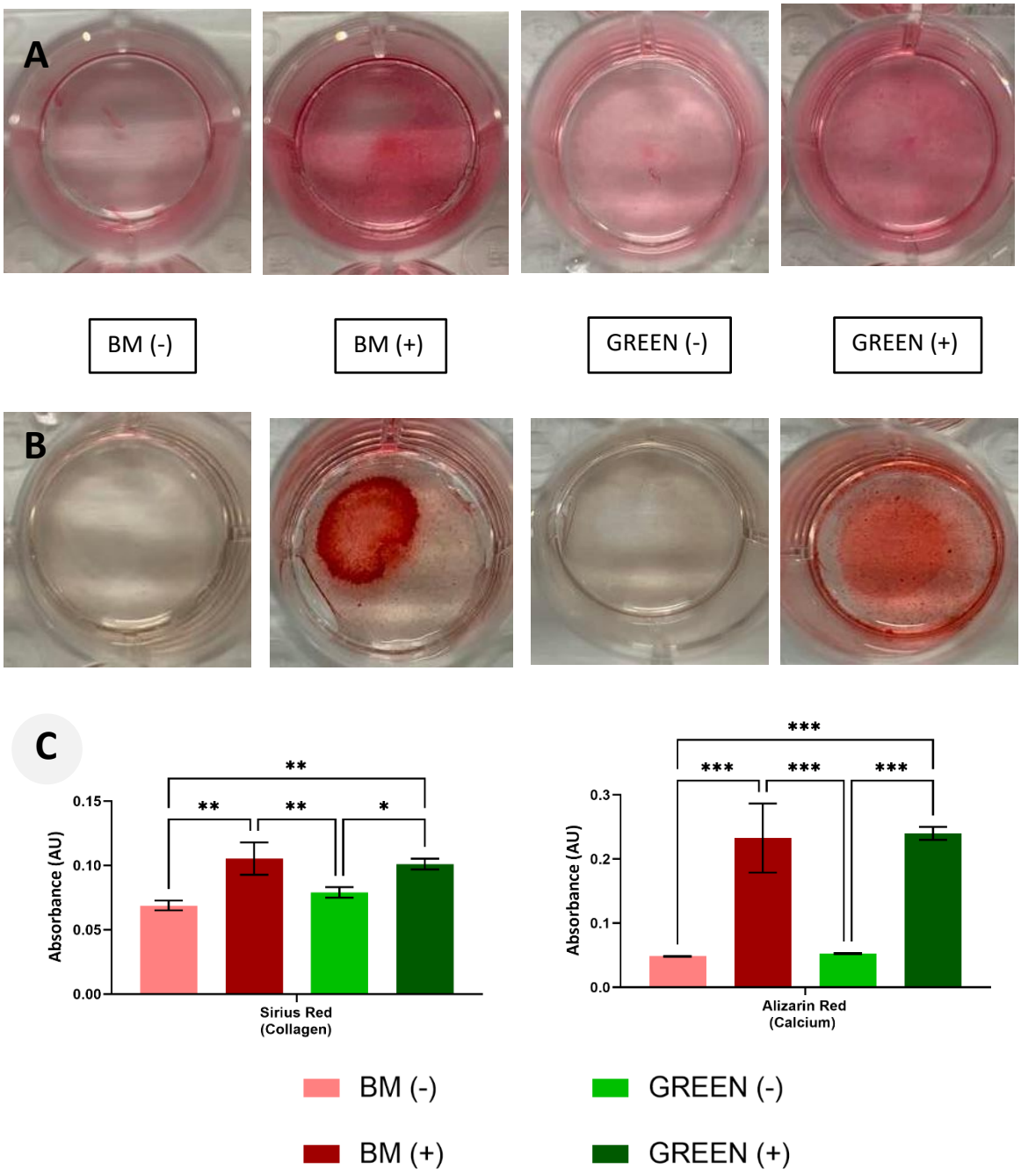

Figure 6.3 *Representative images and quantitative analysis of Sirius red and Alizarin red staining. Y201 cells on day 21 of culture in four different media: BM, BM with osteogenic supplements, Green's media and Green's media with osteogenic supplements. (A) Sirius red staining revealed collagen deposition in each sample. (B) Alizarin red staining to show calcium deposition by the cells. (C) Absorbance value of Sirius red and Alizarin red staining. Mean ± SD, n=3, N=1, * = p<0.05, ** = p<0.01, *** = p<0.001 One-way ANOVA with Tukey's pairwise comparisons.*

The quantitative analysis of Sirius red staining (*Figure 6.3-C)* showed that the groups with osteogenic supplements had significantly higher (1.2-fold for Green's ($p<0.05$) and 1.5-fold for BM ($p<0.01$)) collagen deposition when compared to the groups without the supplements.

While comparing the groups containing the supplements [BM (+) versus GREEN (+)] there was no significance difference. Calcium deposition followed a similar pattern as observed for the collagen deposition. The cells cultured in osteogenic media demonstrated a significantly higher absorbance value (4.6-fold for Green's and 4.8-fold for BM ($p<0.001$)) than the group lacking the supplements. Likewise, there was no statistically significant difference observed when comparing the groups with the supplements [BM (+) versus GREEN (+)].

Apart from dexamethasone, osteogenic differentiation of MSCs can be influenced by various types of molecules such as growth factors or hormones. EGF is a growth factor that was reported to have an effect on MSCs osteogenesis. Krampera et.al. reported that 14 days of human MSCs cultured in osteogenic media added with 50 ng/ml of EGF showed little sign of bone marker gene expression compared to those being cultured using osteogenic media without EGF. This demonstrated that EGF seemed to preserve MSCs multipotency and suppress cell differentiation [229]. While Tamama et.al. suggested that adding 10 ng/ml of EGF did not inhibit but also did not enhance osteogenic differentiation of human MSCs [228]. In addition, Kratchmarova et.al. supported that adding EGF (the concentration was not listed) enhances bone cell differentiation and mineralisation both for in vitro (human MSCs) and in vivo experiments [233].

From the results above in is possible that EGF added in Green's media might have suppressed or slowed down Y201 ability to differentiate into osteoblasts compared to BM (+). However even if components of green media did slow down the early differentiation process it was encouraging to see that they didn't interfere with the cell's ability to deposit collagen or to mineralise. Overall, because the composition of Green's media is reported to be necessary for growing NOF343 and FNB6 and Green's media didn't seem to cause any negative effects on Y201 proliferation or ability to deposit bone-relevant extracellular matrix, it was decided that Green's media with osteogenic supplements was the media of choice for the co-culture of Y201, NOF343 and FNB6.

6.2.3. 3D co-culturing for craniofacial repair

A pilot model of a collagen layer on a PGS scaffold

PGS scaffolds were initially cultured just with FNB6 keratinocytes to see if the scaffolds can support a collagen layer and epithelial stratification. Also, to demonstrate if the scaffold with a collagen layer can be sectioned intact for histological analysis. A scaffold without any bone layer was created by adding a layer of collagen seeded with FNB6 on top of the PGS scaffold (see section 3.2.2., "3D culture"). After culturing for 10 days, the scaffold was fixed, sectioned using a cryostat, and stained with H&E (3.6.2. & 3.6.3.).

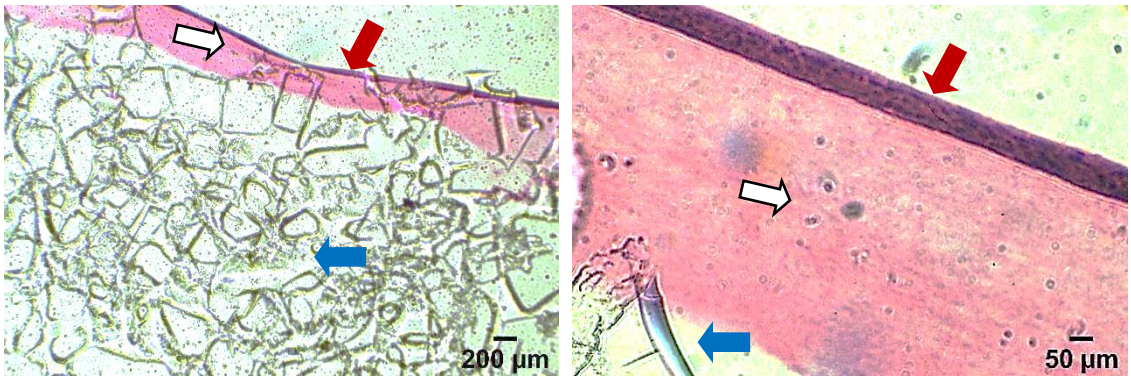

Figure 6.4 *A collagen layer on a PGS scaffold with a layer of FNB6 stained with H&E. Red arrows demonstrated a layer of oral keratinocytes. White arrows showed a collagen layer (which will be where oral fibroblasts are). Blue arrows represent the PGS scaffold.*

The H&E-stained scaffold with a layer of collagen and FNB6 cells demonstrated that a salt-leached PGS scaffold can support full thickness epithelial growth. It was also demonstrated that the scaffold could be sectioned as a full thickness model with the collagen layer as an intact structure. The FNB6 epithelial layer was completely distinguishable from the collagen layer.

A full thickness 3D model of oral tissue with an attached bone component

Y201, NOF343 and FNB6 were seeded onto a PGS scaffold to create the 3D oral tissue model as described in section 3.5 and cultured in Green's media with osteogenic supplements as previously optimised. Y201 were seeded on a PGS scaffold and cultured to day 7 before the scaffold was flipped over to be fit in a NUNC insert (the Y201 layer became the bottom side of

the scaffold). A collagen layer with NOF34 was set. The co-culture was carried for 10 days before fixing, sectioning with cryostat and staining with H&E.

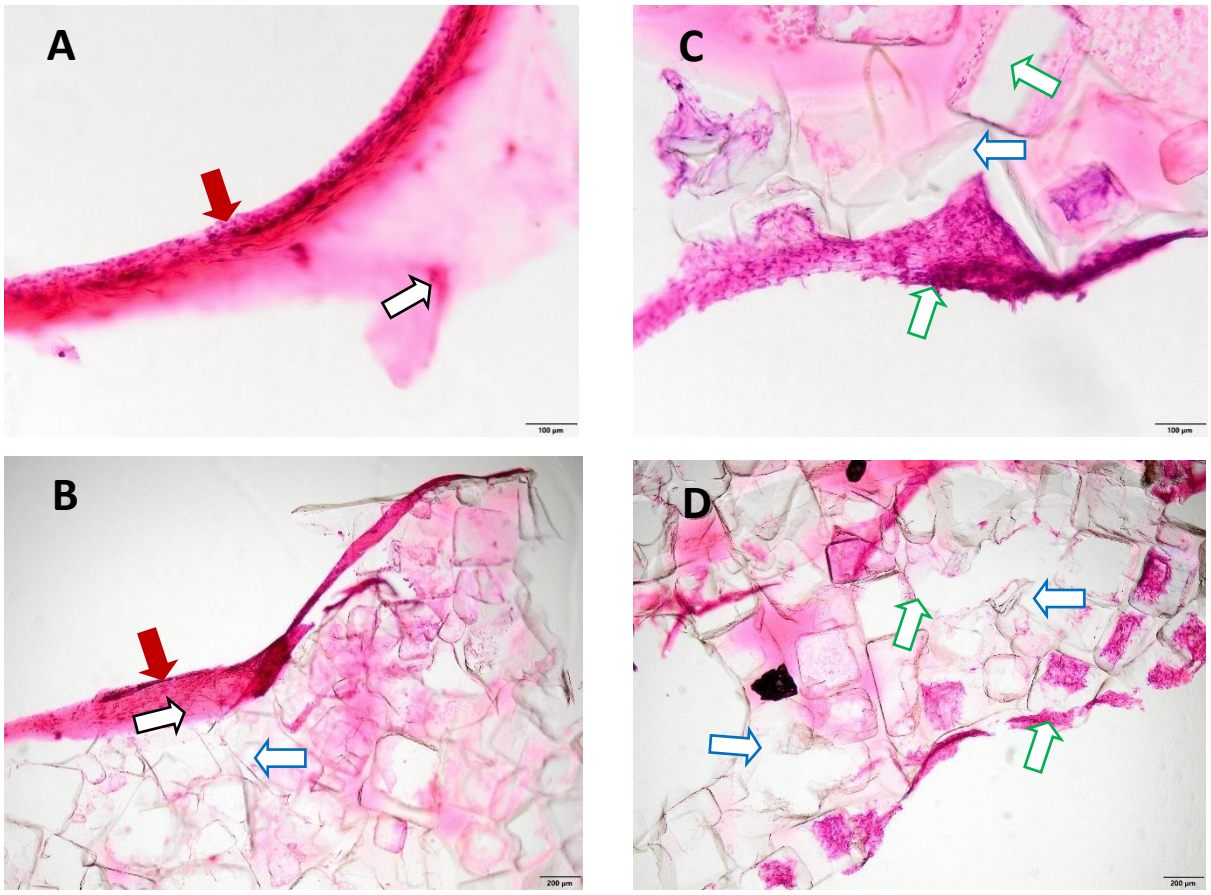

Figure 6.5 *Representative images of the full thickness 3D model of after co-culture. A collagen layer seeded with NOF343 on a PGS scaffold (A-B; red arrows = oral keratinocytes, black striped = a collagen layer with oral fibroblasts) and Y201 co-cultured on the other side of the PGS scaffold (C-D; green arrows with square pattern = Y201 layer) was stained with H&E. While blue arrows with wavy pattern demonstrated PGS scaffold.*

Images of a stained model obtained by light microscopy (Figure 6.5) showed that a salt leaching PGS scaffold could support a layer of collagen with NOF343 and FNB6 and a layer of Y201 to grow. There was cell infiltration into the pores of the scaffold. It seemed to address the possibility of co-culturing these 3 types of cells together which led to a 3D oral tissue model.

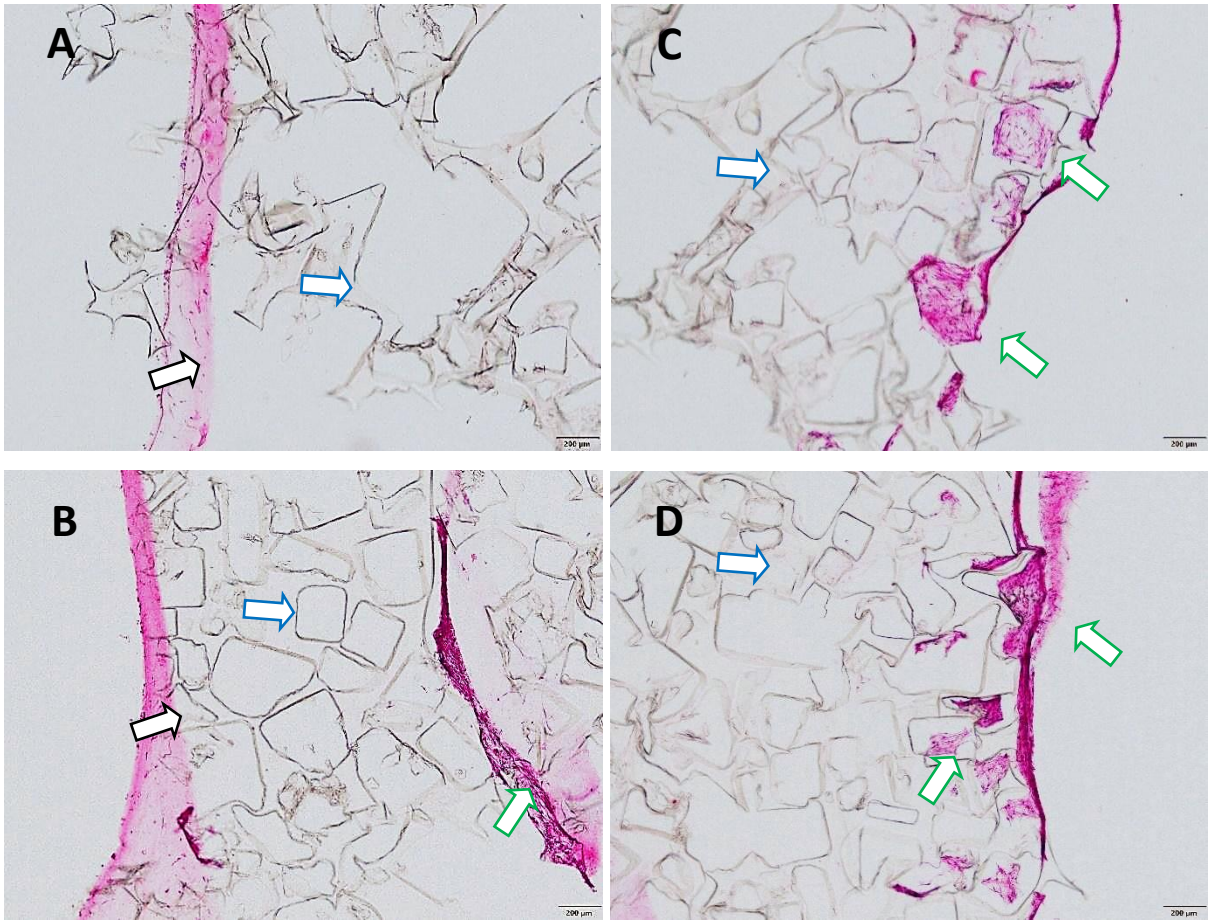

Figure 6.6 *Collagen layer with NOF343 on a PGS scaffold (A-B; black striped = a collagen layer with oral fibroblasts) and a layer of Y201 on the other side of the PGS scaffold (C-D; green arrows with square pattern = Y201 layer) was stained with H&E. Blue arrows with wavy pattern demonstrated PGS scaffold. However, a layer of oral keratinocytes was not observed in any section.*

The stained oral tissue model in *Figure 6.6* showed that a PGS scaffold could support both layers of Y201 and NOF343 in collagen. However, no trace of the FNB6 layer was observed as in the previous experiment.

There's a couple of previously published studies using a co-culture technique to culture 2 or more populations of cells for bone regeneration with both bone and soft tissue compartments. In 2016, Puwanun et.al. demonstrated that a trilayer could be created with electrospun PCL and a co-culture of MSCs and human dermal fibroblasts (HDFs). After 21 days, layers of seeded HDFs and mineralised tissue of seeded MSCs were observed with a complete separation of both cell types. The mineralised tissue was interestingly noted even without culturing dexamethasone [234]. Similarly, Qassim et.al. found that a trilayer of electrospun

PCL could support co-support of 3 populations of cells: (1) MSCs, (2) human oral fibroblasts (NOFs), and (3) oral keratinocytes (FNB6) with FNB6 seeded on top of NOFs. The result showed a completely separated layer of MSCs and NOFs with FNB6 after 28 days. Unfortunately, the study didn't show if the MSCs layer was mineralised [158]. These results demonstrated that a trilayer of electrospun PCL has a potential of supporting craniofacial tissue both soft tissue and bone tissue.

Another study was carried out using a bilayer composed of electrospun PCL and polymerised high internal phase emulsion (polyHIPE) made of photocurable PCL. Murine Long-Bone Osteocytes (MLO-A5) seeded onto electrospun PCL layer and HDFs seeded onto polyHIPE PCL were co-cultured for 28 days without use of dexamethasone. HDFs were found to grow on the electrospun PCL. The ECM with calcium deposition of MLO-A5 was observed on the polyHIPE PCL scaffold and also observed deep within the scaffold layer. These results demonstrated that a scaffold combining of polyHIPE PCL with a layer of electrospun PCL was able to support a bone-like ECM and a layer of oral fibroblasts with a complete separation between 2 cell types [235].

Apart from being able to support bone-like ECM and soft tissue ECM, a scaffold to be used in craniofacial tissue regeneration should also demonstrate a capability to provide a barrier between 2 different layers of tissue. This is to prevent an ingrowth of soft tissue due to an ability of soft tissue to regenerate at a faster rate [1-5]. Our study showed that salt leach PGS has a capability to support a layer of Y201 and a collagen layer with NOFs and FNB6 and a possibility of separating the 2 layers similarly to previously published studies. However, it is still unclear if a layer of MSCs secreted tissue is bone-like ECM as observed in some of the previously published studies. Also, an investigation on how deep both cells can penetrate into a scaffold needs to be conducted to elucidate the ability of salt leached PGS scaffolto be a cell barrier.

The novelty of this project is that salt leached PGS has the potential to be used as a biomaterial scaffold for craniofacial tissue regeneration since it can support both the bony part and soft tissue part.

6.3. Summary

This chapter showed a good result of media used for keratinocytes (Green's media) could support Y201 growth from the first day after seeding compared those being grown in basal media. Although it seemed that a component added in Green's media such as EGF might suppress or slow down ALP activity, it didn't interfere with any other cell activity. Yet the media is needed for FNB6 in a co-culture. So, it was discussed to continuously use Green's media for the co-culture system. Y201, NOFs, and FNB6 were grown on a salt leached PGS scaffold before being collected, fixed, sectioned, and stained. From H&E-stained section under a light microscope, a bone-like matrix and a collagen layer of NOFs with a clearly FNB6 layer on top was observed on PGS obtained without any ingrowth of NOFs to the other side of the scaffold. This preliminary data demonstrated for the first time that a salt leached PGS scaffold has the possibility to support co-culture between these 3 cells for craniofacial tissue regeneration use. It is interesting to elucidate in the future whether a PGS scaffold can truly support Y201 differentiation andmineralisation in a co-culture and whether a PGS scaffold can truly act as a barrier and be able to separate soft tissue from bone tissue completely.

Chapter 7

Conclusion

Craniofacial tissue defects can be challenge to repair. Not only the challenge of addressing the best biomaterial to support tissue regeneration in the area but also the aesthetical and functional complications of fibrotic scar [160]. As well as soft tissue invasion into the bone area which could result as an unsuccessful bone tissue repair [171]. These were the reasons the thesis introduced salt leached PGS scaffold and decellularised cell-derived matrix to elucidate whether it can support Y201 growth leading to bone-like matrix deposition, and whether it can support a co-culture of Y201, FNB6, and NOF343 leading to a possibility of being used as a scaffold in craniofacial tissue regeneration.

7.1. PGS as a biomaterial scaffold in craniofacial tissue engineering

Poly(Glycerol sebacate) has been introduced to be used generally in soft tissue regeneration. However, it has gradually attracted attention from people working in bone tissue regeneration. As the porogen leaching technique using NaCl salt is simple and cost-effective, it was considered to be used to fabricate our PGS scaffold. This thesis showed that salt leached PGS has a potential to support the bony part of craniofacial tissue regeneration as it could support cell attachment, growth, and matrix deposition Y201. The bone-like tissue was demonstrated to contain bone -related proteins. This is the first time that Osteopontin as part of a bone-like ECM was shown to be deposited on a PGS scaffold. However, further investigation is needed to better understand the property of PGS in supporting bone tissue regeneration.

- Investigation on cell infiltration into a PGS scaffold by tagging cells with fluorescent dye and visualising under a light sheet microscope or a confocal microscope.
- Elucidating if a larger range of porosities can support cell attachment, growth, and matrix deposition differently from the range examined in this thesis. As discussed, the range in porosity difference in this study was too small to see any difference between conditions.

- Investigating whether different ratios of different sizes of porogen use in a PGS scaffolds can affect cell attachment, growth or matrix deposition.
- Investigation of the Y201 bone-like matrix comparing it's deposition with and without osteogenic supplements to determine how well osteogenic supplements can enhance Y201 osteogenic phenotypes on PGS scaffolds. This can be conducted using western blot, immunohistochemistry, or qPCR to detect bone-related proteins/genes: Collagen I, Fibronectin, Osteopontin, IBSP, and Osteocalcin.
- Investigation of different techniques used for PGS scaffold fabrication such as PolyHIPE or 3D-printing whether it can support Y201 better than salt leached PGS scaffolds since 3D printing can help maximising scaffold structural design of PGS which may lead to improving cell attachment on PGS.
- Investigation on mechanical properties to determine if a PGS scaffold with Y201 extracellular matrix has a higher Young's modulus or strain to failure than a scaffold alone.

7.2. Craniofacial tissue regeneration using cell-derived matrix on a PGS scaffold

Extracellular matrix (ECM) is known as a structural support for cells with abundant proteins and growth factors essentially needed for cells during their migration, attachment, growth, differentiation, and mineralisation. There have been several attempts trying to use this benefit from an ECM, one of these was to use decellularised cell-derived matrix on a biomaterial. Decellularisation of Y201 bone-like matrix deposited on a salt leached PGS showed good capability of cell removal and maintained collagen content. However, the decellularised cell-derived matrix didn't enhance any growth, collagen production, and mineralisation of the new set of cells compared to scaffold alone. It is very interesting to further study about cell-derived matrix on a PGS scaffold.

- Investigation on protein quantity in ECM whether it got affected after decellularisation by western blot or immunohistochemistry.
- Investigation of the "quality" of proteins in ECM on PGS scaffolds after decellularisation to investigate the processes affect the structure of bone key proteins.

- Investigation of the microstructure of cell-derived ECM for exampleit under SEM or TEM to investigate whether it is different when comparing before and after decellularisation.
- Investigation of cell penetration into a decellularised cell-derived ECM on a PGS scaffold to identify whether the decellularised ECM has an effect on cells ability to penetrate in differently from the cells ability to penetrate in a PGS scaffold.
- Elucidating if decellularised cell-derived matrix really does enhance osteogenesis of Y201 by investigating gene markers expression.

7.3. A PGS as a scaffold to support a co-culture of Y201, NOF343, and FNB6 for a craniofacial tissue regeneration

As previously mentioned, repair bone alone might not result in a successful craniofacial tissue regeneration. A complication of tissue scar, infection or graft failure can occur. Therefore, considering both soft tissue and bone tissue regeneration at the same time should be the goal of craniofacial tissue repair. The study showed that Green's media (needed to be used with keratinocytes) can enhance Y201 growth very well. Although the Green's media with osteogenic supplements didn't enhance Y201 differentiation, collagen production, or mineral deposition, it didn't interfere with it, which is promising for considering co-culture of Y201, NOF343, and FNB6.

After 10 days of co-culture of three cell populations on a PGS scaffold (Y201 were cultured 7 days prior the co-culture), it was observed that PGS can support all types of cells growing on it and can create a barrier separating a bone-like cell layer and oral mucosa-like layer. This showed a possibility of PGS being used as a biomaterial for craniofacial tissue regeneration. It's the first time using a PGS in a co-culture of three populations of cells within one scaffold. However, there were some details that should be considered for a study in the future.

- Elucidating more about each layer deposited on a PGS scaffold using a specific marker to visualise both cells.

- Investigation of a barrier property of a PGS scaffold in co-culture to identify whether there NOF343 are able to penetrate into the bone-like layer.
- Investigation of cell penetration in a thinner disc of salt leached PGS to see whether this single type of scaffold can act as a barrier between 2 layers.

Overall, the studies in this thesis showed that PGS not only provided a support to Y201 bone-like matrix deposition, but also provided support for co-culture between three populations of cells relevant to craniofacial tissues (Y201, NOF343, and FNB6). A salt leached PGS scaffold has the potential to be used as an implantable biomaterial scaffold for tissue regeneration in craniofacial defects to support both bone regeneration and a soft tissue layer.

References

[1] M. S. Ghiasi, J. Chen, A. Vaziri, E. K. Rodriguez, and A. Nazarian, "Bone fracture healing in mechanobiological modeling: A review of principles and methods," (in eng), *Bone Rep,* vol. 6, pp. 87-100, Jun 2017, doi: 10.1016/j.bonr.2017.03.002.

[2] R. G. Frykberg and J. Banks, "Challenges in the Treatment of Chronic Wounds," *Advances in Wound Care,* vol. 4, no. 9, pp. 560-582, 2015-09-01 2015, doi: 10.1089/wound.2015.0635.

[3] P. Kostenuik and F. M. Mirza, "Fracture healing physiology and the quest for therapies for delayed healing and nonunion," *Journal of Orthopaedic Research,* vol. 35, no. 2, pp. 213-223, 2017-02-01 2017, doi: 10.1002/jor.23460.

[4] R. Marsell and T. A. Einhorn, "The biology of fracture healing," *Injury,* vol. 42, no. 6, pp. 551-555, 2011-06-01 2011, doi: 10.1016/j.injury.2011.03.031.

[5] R. Pippi, "Post-Surgical Clinical Monitoring of Soft Tissue Wound Healing in Periodontal and Implant Surgery," *International Journal of Medical Sciences,* vol. 14, no. 8, pp. 721-728, 2017-01-01 2017, doi: 10.7150/ijms.19727.

[6] W. H. O. R. M. o. C. Anomalies, P. A. Mossey, E. E. Catilla, W. H. O. H. G. Programme, and W. H. O. M. o. I. C. R. o. C. Anomalies, "Global registry and database on craniofacial anomalies : report of a WHO Registry Meeting on Craniofacial Anomalies / Main editors: P. Mossey, E. Catilla," ed. Geneva: World Health Organization, 2003.

[7] D. Bister, P. Set, C. Cash, N. Coleman, and T. Fanshawe, "Incidence of facial clefts in Cambridge, United Kingdom," *European Journal of Orthodontics,* vol. 33, no. 4, pp. 372-376, 2010, doi: 10.1093/ejo/cjq117.

[8] A. Detpithak, R. Noochpoung, and N. Yensom, "Incidence of cleft lip and/or cleft palate of live births in Chiangmai from 2015-2019," *Th Dent PH J,* vol. 25, pp. 41-49, 2020.

[9] L. Tisase, "The Incidence of Cleft Lip and/or Cleft Palate in Newborn in Sisaket Hospital Between 2005-2007," *Medicine journal of Sisaket hospital, Surin hospital, and Buriram hospital,* vol. 3, pp. 417-428, 2007.

[10] S. M. Visram, D. Gill, J. T. Shute, and S. J. Cunningham, "Qualitative study to identify issues affecting quality of life in adults with craniofacial anomalies," *British Journal of Oral and Maxillofacial Surgery,* vol. 57, no. 1, pp. 47-52, 2019, doi: 10.1016/j.bjoms.2018.06.011.

[11] S. Warschausky, J. B. Kay, S. Buchman, A. Halberg, and M. Berger, "Health-Related Quality of Life in Children with Craniofacial Anomalies," *Plastic and Reconstructive Surgery,* vol. 110, no. 2, 2002. [Online]. Available: https://journals.lww.com/plasreconsurg/Fulltext/2002/08000/Health_Related_Quality_of_Life_in_Children_with.4.aspx.

[12] D. Payer, M. Krimmel, S. Reinert, B. Koos, H. Weise, and C. Weise, "Oral health-related quality of life in patients with cleft lip and/or palate or Robin sequence," *Journal of Orofacial Orthopedics / Fortschritte der Kieferorthopädie,* 2022, doi: 10.1007/s00056-022-00414-6.

[13] S. H. Zaky *et al.*, "Poly (glycerol sebacate) elastomer supports osteogenic phenotype for bone engineering applications," *Biomedical Materials,* vol. 9, no. 2, p. 025003, 2014, doi: 10.1088/1748-6041/9/2/025003.

[14] Y. Deng, X. Bi, H. Zhou, Z. You, Y. Wang, P. Gu, and X. Fan, "Repair of critical-sized bone defects with anti-miR-31-expressing bone marrow stromal stem cells and poly(glycerol sebacate) scaffolds," *Eur Cell Mater,* vol. 27, pp. 13-24; discussion 24-5, Jan 15 2014, doi: 10.22203/ecm.v027a02.

[15] W. Y. Lai *et al.*, "Reconstitution of bone- like matrix in osteogenically differentiated mesenchymal stem cell– collagen constructs: A three-dimensional in vitro model to study hematopoietic stem cell niche," *Journal of Tissue Engineering,* vol. 4, no. 1, 2013, doi: 10.1177/2041731413508668.

[16] H. Jeon, J. Lee, H. Lee, and G. H. Kim, "Nanostructured surface of electrospun PCL/ dECM fibres treated with oxygen plasma for tissue engineering," *RSC Adv.,* vol. 6, no. 39, pp. 32887-32896, 2016, doi: 10.1039/c6ra03840a.

[17] C. W. Lee, Q. C. Foo, L. V. Wong, and Y. Y. Leung, "An Overview of Maxillofacial Trauma in Oral and Maxillofacial Tertiary Trauma Centre, Queen Elizabeth Hospital, Kota Kinabalu, Sabah," *Craniomaxillofac Trauma Reconstr,* vol. 10, no. 1, pp. 16-21, Mar 2017, doi: 10.1055/s-0036-1584893.

[18] R. A. Alsahafi, H. A. Mitwalli, A. A. Balhaddad, M. D. Weir, H. H. K. Xu, and M. A. S. Melo, "Regenerating Craniofacial Dental Defects With Calcium Phosphate Cement Scaffolds: Current Status and Innovative Scope Review," (in English), *Frontiers in Dental Medicine,* Systematic Review vol. 2, 2021-August-30 2021, doi: 10.3389/fdmed.2021.743065.

[19] M. J. Peltola, P. K. Vallittu, V. Vuorinen, A. A. J. Aho, A. Puntala, and K. M. J. Aitasalo, "Novel composite implant in craniofacial bone reconstruction," *European Archives of Oto-Rhino-Laryngology,* vol. 269, no. 2, pp. 623-628, 2012-02-01 2012, doi: 10.1007/s00405-011-1607-x.

[20] C. M. Hurley, R. McConn Walsh, N. P. Shine, J. P. O'Neill, F. Martin, and J. B. O'Sullivan, "Current trends in craniofacial reconstruction," *Surgeon,* vol. 21, no. 3, pp. e118-e125, Jun 2023, doi: 10.1016/j.surge.2022.04.004.

[21] L. M. B. S. D. A. H. R. H. J. K. M. L. P. M. K. M.-G. D. Q. a. J. Runyeon, *Anatomy & Physiology*. Corvallis, Oregon, United states: Open stax/Oregon state university, 2019.

[22] H. Zhao, J. Feng, T.-V. Ho, W. Grimes, M. Urata, and Y. Chai, "The suture provides a niche for mesenchymal stem cells of craniofacial bones," *Nature Cell Biology,* vol. 17, no. 4, pp. 386-396, 2015, doi: 10.1038/ncb3139.

[23] N. D. Futran and E. Mendez, "Developments in reconstruction of midface and maxilla," *The Lancet Oncology,* vol. 7, no. 3, pp. 249-258, 2006, doi: 10.1016/s1470-2045(06)70616-7.

[24] R. Dimitriou, E. Jones, D. McGonagle, and P. V. Giannoudis, "Bone regeneration: current concepts and future directions," *BMC medicine,* vol. 9, no. 1, pp. 66-66, 2011, doi: 10.1186/1741-7015-9-66.

[25] M. A. Pogrel, S. Podlesh, J. P. Anthony, and J. Alexander, "A comparison of vascularized and nonvascularized bone grafts for reconstruction of mandibular continuity defects," *J Oral Maxillofac Surg,* vol. 55, no. 11, pp. 1200-1206, 1997, doi: 10.1016/S0278-2391(97)90165-8.

[26] T. M. Chen and H. J. Wang, "Cranioplasty using allogeneic perforated demineralized bone matrix with autogenous bone paste," *Ann Plast Surg,* vol. 49, no. 3, pp. 272-279, 2002, doi: 10.1097/00000637-200209000-00006.

[27] M. Artico, L. Ferrante, F. S. Pastore, E. O. Ramundo, D. Cantarelli, D. Scopelliti, and G. Iannetti, "Bone autografting of the calvaria and craniofacial skeleton: historical background, surgical results in a series of 15 patients, and review of the literature," *Surgical Neurology,* vol. 60, no. 1, pp. 71-79, 2003, doi: 10.1016/S0090-3019(03)00031-4.

[28] G. C. Finkemeier, "Bone- Grafting and Bone- Graft Substitutes," *The Journal of Bone & Joint Surgery,* vol. 84, no. 3, pp. 454-464, 2002, doi: 10.2106/00004623-200203000-00020.

[29] E. Deutsch and R. Guldberg, "Stem cell- synthesized extracellular matrix for bone repair," *Journal of Materials Chemistry,* vol. 20, no. 40, pp. 8942-8951, 2010, doi: 10.1039/c0jm01070g.

[30] T. Bauer, "Bone graft substitutes," *Skeletal Radiology,* vol. 36, no. 12, pp. 1105-7, 2007, doi: 10.1007/s00256-007-0377-4.

[31] P. Habibovic and K. de Groot, "Osteoinductive biomaterials--properties and relevance in bone repair," *J Tissue Eng Regen Med,* vol. 1, no. 1, pp. 25-32, Jan-Feb 2007, doi: 10.1002/term.5.

[32] G. Zimmermann and A. Moghaddam, "Allograft bone matrix versus synthetic bone graft substitutes," *Injury,* vol. 42, no. 2, pp. S16-S21, 2011, doi: 10.1016/j.injury.2011.06.199.

[33] C. Delloye, M. V. Cauter, D. Dufrane, B. G. Francq, P. L. Docquier, and O. Cornu, "Local complications of massive bone allografts : An appraisal of their prevalence in 128 patients," *Acta Orthopaedica Belgica,* vol. 80, no. 2, pp. 196-204, 2014.

[34] M. A. Kainer, J. V. Linden, D. N. Whaley, H. T. Holmes, W. R. Jarvis, D. B. Jernigan, and L. K. Archibald, "Clostridium Infections Associated with Musculoskeletal- Tissue Allografts," *The New England Journal of Medicine,* vol. 350, no. 25, pp. 2564-2571, 2004, doi: 10.1056/NEJMoa023222.

[35] K. Saikia, T. Bhattacharya, S. Bhuyan, D. Talukdar, S. Saikia, and P. Jitesh, "Calcium phosphate ceramics as bone graft substitutes in filling bone tumor defects," *Indian Journal of Orthopaedics,* vol. 42, no. 2, pp. 169-172, 2008, doi: 10.4103/0019-5413.39588.

[36] B. C. Jones, "Biological Basis of Fracture Healing," *Journal of Orthopaedic Trauma,* vol. 19, no. 10 Suppl, pp. S1-S3, 2005.

[37] K. Tilkeridis, P. Touzopoulos, A. Ververidis, S. Christodoulou, K. Kazakos, and G. I. Drosos, "Use of demineralized bone matrix in spinal fusion," *World journal of orthopedics,* vol. 5, no. 1, pp. 30-37, 2014, doi: 10.5312/wjo.v5.i1.30.

[38] H. Zhang *et al.*, "Demineralized Bone Matrix Carriers and their Clinical Applications: An Overview," *Orthopaedic Surgery,* vol. 11, no. 5, pp. 725-737, 2019, doi: 10.1111/os.12509.

[39] G. I. Drosos, P. Touzopoulos, A. Ververidis, K. Tilkeridis, and K. Kazakos, "Use of demineralized bone matrix in the extremities," *World journal of orthopedics,* vol. 6, no. 2, pp. 269-277, 2015, doi: 10.5312/wjo.v6.i2.269.

[40] E. Roddy, M. R. Debaun, A. Daoud-Gray, Y. P. Yang, and M. J. Gardner, "Treatment of critical-sized bone defects: clinical and tissue engineering perspectives," *European Journal of Orthopaedic Surgery & Traumatology,* vol. 28, no. 3, pp. 351-362, 2018, doi: 10.1007/s00590-017-2063-0.

[41] R. B. M. de Vries, A. Oerlemans, L. Trommelmans, K. Dierickx, and B. Gordijn, "Ethical aspects of tissue engineering: a review," *Tissue engineering. Part B, Reviews,* vol. 14, no. 4, pp. 367-375, 2008, doi: 10.1089/ten.teb.2008.0199.

[42] G. Fernandez de Grado *et al.*, "Bone substitutes: a review of their characteristics, clinical use, and perspectives for large bone defects management," vol. 9, ed. London, England, 2018.

[43] H. Capella-Monsonís and D. I. Zeugolis, "Decellularized xenografts in regenerative medicine: From processing to clinical application," *Xenotransplantation,* vol. 28, no. 4, 2021, doi: 10.1111/xen.12683.

[44] U. S. F. a. D. Administration. "PHS Guideline on Infectious Disease Issues in Xenotransplantation." Center for Biologics Evaluation and Research. https://www.fda.gov/regulatory-information/search-fda-guidance-documents/phs-guideline-infectious-disease-issues-xenotransplantation (accessed 20/10/2022, 2022).

[45] Y. Fillingham and J. Jacobs, "Bone grafts and their substitutes," *The bone & joint journal,* vol. 98-b, no. 1 Suppl A, pp. 6-9, 2016, doi: 10.1302/0301-620X.98B.36350.

[46] T. T. Roberts and A. J. Rosenbaum, "Bone grafts, bone substitutes and orthobiologics," *Organogenesis,* vol. 8, no. 4, pp. 114-124, 2012, doi: 10.4161/org.23306.

[47] B. Skovrlj, J. Z. Guzman, M. Al Maaieh, S. K. Cho, J. C. Iatridis, and S. A. Qureshi, "Cellular bone matrices: viable stem cell-containing bone graft substitutes," *The Spine Journal,* vol. 14, no. 11, pp. 2763-2772, 2014, doi: 10.1016/j.spinee.2014.05.024.

[48] M. R. Alison, R. Poulsom, S. Forbes, and N. A. Wright, "An introduction to stem cells," vol. 197, M. R. Alison, R. Poulsom, and N. A. Wright, Eds., ed. Chichester, UK, 2002, pp. 419-423.

[49] T. Nandedkar and M. Narkar, "Stem cell research: its relevance to reproductive biology," *Indian journal of experimental biology,* vol. 41, no. 7, pp. 724-739, 2003.

[50] R.-H. Fu *et al.*, "Differentiation of Stem Cells: Strategies for Modifying Surface Biomaterials," *Cell Transplantation,* vol. 20, no. 1, pp. 37-47, 2011, doi: 10.3727/096368910X532756.

[51] I. Kang *et al.*, "Donor-dependent variation of human umbilical cord blood mesenchymal stem cells in response to hypoxic preconditioning and amelioration of limb ischemia," *Experimental & molecular medicine,* vol. 50, no. 4, pp. 35-35, 2018, doi: 10.1038/s12276-017-0014-9.

[52] Y. Xiaoxue, C. Zhongqiang, G. Zhaoqing, D. Gengting, M. Qingjun, and W. Shenwu, "Immortalization of human osteoblasts by transferring human telomerase reverse

transcriptase gene," *Biochemical and Biophysical Research Communications,* vol. 315, no. 3, pp. 643-651, 2004, doi: 10.1016/j.bbrc.2004.01.102.

[53] S. James *et al.*, "Multiparameter Analysis of Human Bone Marrow Stromal Cells Identifies Distinct Immunomodulatory and Differentiation-Competent Subtypes," 2015.

[54] D. B. Musante, M. E. Firtha, B. L. Atkinson, R. Hahn, J. T. Ryaby, and R. J. Linovitz, "Clinical evaluation of an allogeneic bone matrix containing viable osteogenic cells in patients undergoing one- and two-level posterolateral lumbar arthrodesis with decompressive laminectomy," *Journal of Orthopaedic Surgery and Research,* vol. 11, no. 1, 2016, doi: 10.1186/s13018-016-0392-z.

[55] N. H. Riordan *et al.*, "Non-expanded adipose stromal vascular fraction cell therapy for multiple sclerosis," *Journal of Translational Medicine,* vol. 7, no. 1, p. 29, 2009, doi: 10.1186/1479-5876-7-29.

[56] Amp, Apos, and F. J. Brien, "Biomaterials & scaffolds for tissue engineering," *Materials Today,* vol. 14, no. 3, pp. 88-95, 2011, doi: 10.1016/S1369-7021(11)70058-X.

[57] C. M. Murphy, F. J. O'Brien, D. G. Little, and A. Schindeler, "Cell- scaffold interactions in the bone tissue engineering triad," *European Cells and Materials,* vol. 26, pp. 120-132, 2013, doi: 10.22203/eCM.v026a09.

[58] Q. L. Loh and C. Choong, "Three- Dimensional Scaffolds for Tissue Engineering Applications: Role of Porosity and Pore Size," *Tissue Engineering Part B: Reviews,* vol. 19, no. 6, pp. 485-502, 2013, doi: 10.1089/ten.teb.2012.0437.

[59] M. Peuster *et al.*, "A novel approach to temporary stenting: Degradable cardiovascular stents produced from corrodible metal - Results 6- 18 months after implantation into New Zealand white rabbits," *Heart,* vol. 86, no. 5, pp. 563-569, 2001.

[60] F. Witte, V. Kaese, H. Haferkamp, E. Switzer, A. Meyer-Lindenberg, C. J. Wirth, and H. Windhagen, "In vivo corrosion of four magnesium alloys and the associated bone response," *Biomaterials,* vol. 26, no. 17, pp. 3557-3563, 2005, doi: 10.1016/j.biomaterials.2004.09.049.

[61] T. Ghassemi, A. Shahroodi, M. H. Ebrahimzadeh, A. Mousavian, J. Movaffagh, and A. Moradi, "Current Concepts in Scaffolding for Bone Tissue Engineering," *The archives of bone and joint surgery,* vol. 6, no. 2, pp. 90-99, 2018, doi: 10.22038/abjs.2018.26340.1713.

[62] K. Das, V. K. Balla, A. Bandyopadhyay, and S. Bose, "Surface modification of laser- processed porous titanium for load- bearing implants," *Scripta Materialia,* vol. 59, no. 8, pp. 822-825, 2008, doi: 10.1016/j.scriptamat.2008.06.018.

[63] B. Stevens, Y. Yang, A. Mohandas, B. Stucker, and K. T. Nguyen, "A review of materials, fabrication methods, and strategies used to enhance bone regeneration in engineered bone tissues," *J Biomed Mater Res B Appl Biomater,* vol. 85, no. 2, pp. 573-82, May 2008, doi: 10.1002/jbm.b.30962.

[64] S. T. Kao and D. D. Scott, "A Review of Bone Substitutes," *Oral and Maxillofacial Surgery Clinics of North America,* vol. 19, no. 4, pp. 513-521, 2007/11/01/ 2007, doi: https://doi.org/10.1016/j.coms.2007.06.002.

[65] S. K. Nandi, S. Roy, P. Mukherjee, B. Kundu, D. K. De, and D. Basu, "Orthopaedic applications of bone graft & graft substitutes: A review," *Indian Journal of Medical Research,* vol. 132, no. 7, pp. 15-30, 2010.

[66] T. Kokubo, H.-M. Kim, and M. Kawashita, "Novel bioactive materials with different mechanical properties," *Biomaterials,* vol. 24, no. 13, pp. 2161-2175, 2003, doi: 10.1016/s0142-9612(03)00044-9.

[67] J. Liu, F. Jin, M. L. Zheng, S. Wang, S. Q. Fan, P. Li, and X. M. Duan, "Cell Behavior on 3D Ti-6Al-4 V Scaffolds with Different Porosities," *ACS Appl Bio Mater,* vol. 2, no. 2, pp. 697-703, Feb 18 2019, doi: 10.1021/acsabm.8b00550.

[68] J. H. Kim *et al.*, "Electrospun nanofibers composed of poly(ε-caprolactone) and polyethylenimine for tissue engineering applications," *Materials Science & Engineering C,* vol. 29, no. 5, pp. 1725-1731, 2009, doi: 10.1016/j.msec.2009.01.023.

[69] G.-M. Kim, K. Le, S. Giannitelli, Y. Lee, A. Rainer, and M. Trombetta, "Electrospinning of PCL/PVP blends for tissue engineering scaffolds," *Official Journal of the European Society for Biomaterials,* vol. 24, no. 6, pp. 1425-1442, 2013, doi: 10.1007/s10856-013-4893-6.

[70] S. Agnes Mary and V. R. Giri Dev, "Electrospun herbal nanofibrous wound dressings for skin tissue engineering," *The Journal of The Textile Institute,* vol. 106, no. 8, pp. 1-10, 2014, doi: 10.1080/00405000.2014.951247.

[71] K. Wang *et al.*, "Three-Layered PCL Grafts Promoted Vascular Regeneration in a Rabbit Carotid Artery Model," *Macromolecular Bioscience,* vol. 16, no. 4, pp. 608-618, 2016, doi: 10.1002/mabi.201500355.

[72] N. Samsudin, Y. Hashim, M. Arifin, M. Mel, H. Salleh, I. Sopyan, and D. Jimat, "Optimization of ultraviolet ozone treatment process for improvement of polycaprolactone (PCL) microcarrier performance," *Incorporating Methods in Cell Science International Journal of Cell Culture and Biotechnology,* vol. 69, no. 4, pp. 601-616, 2017, doi: 10.1007/s10616-017-0071-x.

[73] T. Hanas, T. S. Sampath Kumar, G. Perumal, and M. Doble, "Tailoring degradation of AZ31 alloy by surface pre- treatment and electrospun PCL fibrous coating," *Materials Science & Engineering C,* vol. 65, pp. 43-50, 2016, doi: 10.1016/j.msec.2016.04.017.

[74] X. H. Liu and P. X. Ma, "Polymeric scaffolds for bone tissue engineering," (in English), *Ann. Biomed. Eng.,* Review vol. 32, no. 3, pp. 477-486, Mar 2004, doi: 10.1023/B:ABME.0000017544.36001.8e.

[75] L. S. Nair and C. T. Laurencin, "Biodegradable polymers as biomaterials," vol. 32, ed, 2007, pp. 762-798.

[76] P. X. Ma, "Biomimetic materials for tissue engineering," (in English), *Advanced Drug Delivery Reviews,* Review vol. 60, no. 2, pp. 184-198, Jan 2008, doi: 10.1016/j.addr.2007.08.041.

[77] C. A. Sundback, J. Y. Shyu, Y. Wang, W. C. Faquin, R. S. Langer, J. P. Vacanti, and T. A. Hadlock, "Biocompatibility analysis of poly(glycerol sebacate) as a nerve guide material," *Biomaterials,* vol. 26, no. 27, pp. 5454-5464, 2005, doi: 10.1016/j.biomaterials.2005.02.004.

[78] D. J. Lee, R. Padilla, H. Zhang, W. S. Hu, and C. C. Ko, "Biological assessment of a calcium silicate incorporated hydroxyapatite-gelatin nanocomposite: a comparison to decellularized bone matrix," *Biomed Res Int,* vol. 2014, p. 837524, 2014, doi: 10.1155/2014/837524.

[79] F. Ghosh, W. L. Neeley, K. Arnér, and R. Langer, "Selective Removal of Photoreceptor Cells In Vivo Using the Biodegradable Elastomer Poly(Glycerol Sebacate)," *Tissue Engineering Part A,* vol. 17, no. 13-14, pp. 1675-1682, 2011, doi: 10.1089/ten.tea.2008.0450.

[80] C. K. Hagandora, J. Gao, Y. Wang, and A. J. Almarza, "Poly (Glycerol Sebacate): A Novel Scaffold Material for Temporomandibular Joint Disc Engineering," *Tissue Engineering Part A,* vol. 19, no. 5-6, pp. 729-737, 2013, doi: 10.1089/ten.tea.2012.0304.

[81] H. Park, B. L. Larson, M. E. Kolewe, G. Vunjak-Novakovic, and L. E. Freed, "Biomimetic scaffold combined with electrical stimulation and growth factor promotes tissue engineered cardiac development," *Experimental Cell Research,* vol. 321, no. 2, pp. 297-306, 2014, doi: 10.1016/j.yexcr.2013.11.005.

[82] H. I. Pryor *et al.*, "Poly(glycerol sebacate) films prevent postoperative adhesions and allow laparoscopic placement," *Surgery,* vol. 146, no. 3, pp. 490-497, 2009, doi: 10.1016/j.surg.2009.04.012.

[83] I. S. Tobias, H. Lee, G. C. Engelmayr, D. Macaya, C. J. Bettinger, and M. J. Cima, "Zero- order controlled release of ciprofloxacin- HCl from a reservoir-based, bioresorbable and elastomeric device," *Journal of Controlled Release,* vol. 146, no. 3, pp. 356-362, 2010, doi: 10.1016/j.jconrel.2010.05.036.

[84] Z.-J. Sun *et al.*, "The application of poly (glycerol– sebacate) as biodegradable drug carrier," *Biomaterials,* vol. 30, no. 28, pp. 5209-5214, 2009, doi: 10.1016/j.biomaterials.2009.06.007.

[85] R. Robergs and S. Griffin, "Glycerol," *Sports Medicine,* vol. 26, no. 3, pp. 145-167, 1998, doi: 10.2165/00007256-199826030-00002.

[86] F. Yi and D. A. Lavan, "Poly(glycerol sebacate) Nanofiber Scaffolds by Core/ Shell Electrospinning," *Macromolecular Bioscience,* vol. 8, no. 9, pp. 803-806, 2008, doi: 10.1002/mabi.200800041.

[87] I. Jaafar, M. Ammar, S. Jedlicka, R. Pearson, and J. Coulter, "Spectroscopic evaluation, thermal, and thermomechanical characterization of poly(glycerol- sebacate) with variations in curing temperatures and durations," *Full Set - Includes `Journal of Materials Science Letters',* vol. 45, no. 9, pp. 2525-2529, 2010, doi: 10.1007/s10853-010-4259-0.

[88] Q.-Z. Chen, J. M. W. Quinn, G. A. Thouas, X. Zhou, and P. A. Komesaroff, "Bone-Like Elastomer-Toughened Scaffolds with Degradability Kinetics Matching Healing Rates of Injured Bone," *Advanced Engineering Materials,* vol. 12, no. 11, pp. B642-B648, 2010, doi: 10.1002/adem.201080002.

[89] J. Ifkovits, J. Devlin, G. Eng, T. P. Martens, G. Vunjak-Novakovic, and J. Burdick, "Biodegradable Fibrous Scaffolds with Tunable Properties Formed from Photo- Cross- Linkable Poly(glycerol sebacate)," *ACS Appl. Mater. Interfaces,* vol. 1, no. 9, pp. 1878-1886, 2009, doi: 10.1021/am900403k.

[90] D. Singh, A. J. Harding, E. Albadawi, F. M. Boissonade, J. W. Haycock, and F. Claeyssens, "Additive Manufactured Biodegradable Poly(glycerol sebacate methacrylate) Nerve Guidance Conduits," 2018.

[91] M. Vert, S. Li, G. Spenlehauer, and P. Guerin, "Bioresorbability and biocompatibility of aliphatic polyesters," *Official Journal of the European Society for Biomaterials,* vol. 3, no. 6, pp. 432-446, 1992, doi: 10.1007/BF00701240.

[92] J. L. Ifkovits and J. A. Burdick, "Review: photopolymerizable and degradable biomaterials for tissue engineering applications," *Tissue engineering,* vol. 13, no. 10, pp. 2369-2385, 2007, doi: 10.1089/ten.2007.0093.

[93] Y. Wang, G. Ameer, B. Sheppard, and R. Langer, "A tough biodegradable elastomer," *Nature Biotechnology,* vol. 20, no. 6, pp. 602-6, 2002, doi: 10.1038/nbt0602-602.

[94] J. Gao, P. M. Crapo, and Y. Wang, "Macroporous elastomeric scaffolds with extensive micropores for soft tissue engineering," *Tissue engineering,* vol. 12, no. 4, pp. 917-925, 2006, doi: 10.1089/ten.2006.12.917.

[95] S. Zaky, J. Gao, K. Lee, A. Almarza, Y. Wang, and C. Sfeir, "Poly (glycerol sebacate) Elastomer Supports Bone Regeneration by Its Mechanical Properties Similar to Osteoid Tissue," *Tissue Eng. Part A,* vol. 20, pp. S7-S7, 2014.

[96] K. Yang *et al.*, "β-Tricalcium phosphate/poly(glycerol sebacate) scaffolds with robust mechanical property for bone tissue engineering," *Materials Science & Engineering C,* vol. 56, pp. 37-47, 2015, doi: 10.1016/j.msec.2015.05.083.

[97] S. Sant, C. M. Hwang, S. H. Lee, and A. Khademhosseini, "Hybrid PGS-PCL microfibrous scaffolds with improved mechanical and biological properties," (in English), *Journal of Tissue Engineering and Regenerative Medicine,* Article vol. 5, no. 4, pp. 283-291, Apr 2011, doi: 10.1002/term.313.

[98] S. H. Zaky *et al.*, "Poly(Glycerol Sebacate) Elastomer: A Novel Material for Mechanically Loaded Bone Regeneration," (in English), *Tissue Engineering Part A,* Article vol. 20, no. 1-2, pp. 45-53, Jan 2014, doi: 10.1089/ten.tea.2013.0172.

[99] J. M. Kemppainen and S. J. Hollister, "Tailoring the mechanical properties of 3D- designed poly(glycerol sebacate) scaffolds for cartilage applications," *Journal of Biomedical Materials Research Part A,* vol. 94, no. 1, pp. 9-18, 2010, doi: 10.1002/jbm.a.32653.

[100] H. Shi, Q. Gan, X. Liu, Y. Ma, J. Hu, Y. Yuan, and C. Liu, "Poly(glycerol sebacate)-modified polylactic acid scaffolds with improved hydrophilicity, mechanical strength and bioactivity for bone tissue regeneration," *RSC Advances,* vol. 5, no. 97, pp. 79703-79714, 2015, doi: 10.1039/c5ra13334c.

[101] S. H. Zaky *et al.*, "Poly (glycerol sebacate) elastomer supports bone regeneration by its mechanical properties being closer to osteoid tissue rather than to mature bone," *Acta Biomater,* vol. 54, pp. 95-106, May 2017, doi: 10.1016/j.actbio.2017.01.053.
[102] B. Aldemir Dikici, "Development of emulsion templated matrices and their use in tissue engineering applications," Doctor of Philosophy, Materials science and engineering, University of Sheffield, United Kingdom, 2020.
[103] J. M. Seok *et al.*, "Fabrication of 3D plotted scaffold with microporous strands for bone tissue engineering," *J Mater Chem B,* vol. 8, no. 5, pp. 951-960, Feb 7 2020, doi: 10.1039/c9tb02360g.
[104] J. Jang, H. G. Yi, and D. W. Cho, "3D Printed Tissue Models: Present and Future," *ACS Biomater Sci Eng,* vol. 2, no. 10, pp. 1722-1731, Oct 10 2016, doi: 10.1021/acsbiomaterials.6b00129.
[105] V. Keriquel *et al.*, "In vivo bioprinting for computer- and robotic-assisted medical intervention: preliminary study in mice," *Biofabrication,* vol. 2, no. 1, p. 014101, Mar 2010, doi: 10.1088/1758-5082/2/1/014101.
[106] M. J. Sawkins, P. Mistry, B. N. Brown, K. M. Shakesheff, L. J. Bonassar, and J. Yang, "Cell and protein compatible 3D bioprinting of mechanically strong constructs for bone repair," *Biofabrication,* vol. 7, no. 3, 2015, doi: 10.1088/1758-5090/7/3/035004.
[107] H. Leonards *et al.*, "Advantages and drawbacks of Thiol-ene based resins for 3D-printing," vol. 9353, ed, 2015, pp. 93530F-93530F-7.
[108] A. Koroleva *et al.*, "Two- photon polymerization- generated and micromolding- replicated 3d scaffolds for peripheral neural tissue engineering applications," *Biofabrication,* vol. 4, no. 2, p. 025005, 2012, doi: 10.1088/1758-5082/4/2/025005.
[109] D. Pahovnik, J. Majer, E. Agar, and S. Kovai, "Synthesis of hydrogel polyHIPEs from functionalized glycidyl methacrylate," *Polym. Chem.,* vol. 7, no. 32, pp. 5132-5138, 2016, doi: 10.1039/c6py01122e.
[110] V. Karageorgiou and D. Kaplan, "Porosity of 3D biomaterial scaffolds and osteogenesis," *Biomaterials,* vol. 26, no. 27, pp. 5474-5491, 2005, doi: 10.1016/j.biomaterials.2005.02.002.
[111] C. M. Murphy and F. J. O'Brien, "Understanding the effect of mean pore size on cell activity in collagen-glycosaminoglycan scaffolds," *Cell Adhesion & Migration,* vol. 4, no. 3, pp. 377-381, 2010, doi: 10.4161/cam.4.3.11747.
[112] A. Sadiasa, T. H. Nguyen, and B.-T. Lee, "In vitro and in vivo evaluation of porous PCL-PLLA 3D polymer scaffolds fabricated via salt leaching method for bone tissue engineering applications," *Journal of Biomaterials Science, Polymer Edition,* vol. 25, no. 2, pp. 150-167, 2014, doi: 10.1080/09205063.2013.846633.
[113] M. Cavo and S. Scaglione, "Scaffold microstructure effects on functional and mechanical performance: Integration of theoretical and experimental approaches for bone tissue engineering applications," *Materials Science & Engineering C,* vol. 68, pp. 872-879, 2016, doi: 10.1016/j.msec.2016.07.041.
[114] A. G. Mikos, A. J. Thorsen, L. A. Czerwonka, Y. Bao, R. Langer, D. N. Winslow, and J. P. Vacanti, "Preparation and characterization of poly(l-lactic acid) foams," *Polymer,* vol. 35, no. 5, pp. 1068-1077, 1994, doi: 10.1016/0032-3861(94)90953-9.
[115] R. Shtrichman *et al.*, "The Generation of Hybrid Electrospun Nanofiber Layer with Extracellular Matrix Derived from Human Pluripotent Stem Cells, for Regenerative Medicine Applications," *Tissue Engineering Part A,* vol. 20, no. 19-20, pp. 2756-2767, 2014, doi: 10.1089/ten.tea.2013.0705.
[116] L. T. Saldin, M. C. Cramer, S. S. Velankar, L. J. White, and S. F. Badylak, "Extracellular matrix hydrogels from decellularized tissues: Structure and function," *Acta Biomater,* vol. 49, pp. 1-15, Feb 2017, doi: 10.1016/j.actbio.2016.11.068.
[117] X. J. Sun *et al.*, "Heparin-chitosan-coated acellular bone matrix enhances perfusion of blood and vascularization in bone tissue engineering scaffolds," *Tissue Eng Part A,* vol. 17, no. 19-20, pp. 2369-78, Oct 2011, doi: 10.1089/ten.TEA.2011.0027.

[118] T. J. Keane, I. T. Swinehart, and S. F. Badylak, "Methods of tissue decellularization used for preparation of biologic scaffolds and in vivo relevance," *Methods,* vol. 84, pp. 25-34, Aug 2015, doi: 10.1016/j.ymeth.2015.03.005.

[119] A. Gilpin and Y. Yang, "Decellularization Strategies for Regenerative Medicine: From Processing Techniques to Applications," *BioMed research international,* vol. 2017, pp. 9831534-9831534, 2017, doi: 10.1155/2017/9831534.

[120] N. Datta, H. L. Holtorf, V. I. Sikavitsas, J. A. Jansen, and A. G. Mikos, "Effect of bone extracellular matrix synthesized in vitro on the osteoblastic differentiation of marrow stromal cells," *Biomaterials,* vol. 26, no. 9, pp. 971-977, 2005, doi: 10.1016/j.biomaterials.2004.04.001.

[121] R. Thibault, L. Scott Baggett, A. Mikos, and F. Kasper, "Osteogenic Differentiation of Mesenchymal Stem Cells on Pregenerated Extracellular Matrix Scaffolds in the Absence of Osteogenic Cell Culture Supplements," *Tissue Engineering Part A,* vol. 16, no. 2, pp. 431-40, 2010, doi: 10.1089/ten.tea.2009.0583.

[122] G. Tour, M. Wendel, and I. Tcacencu, "Cell- Derived Matrix Enhances Osteogenic Properties of Hydroxyapatite," *Tissue Engineering Part A,* vol. 17, no. 1-2, pp. 127-137, 2011, doi: 10.1089/ten.tea.2010.0175.

[123] X. Dong *et al.*, "RGD-modified acellular bovine pericardium as a bioprosthetic scaffold for tissue engineering," *Journal of Materials Science: Materials in Medicine,* vol. 20, no. 11, pp. 2327-2336, 2009-11-01 2009, doi: 10.1007/s10856-009-3791-4.

[124] T. W. Gilbert, S. Wognum, E. M. Joyce, D. O. Freytes, M. S. Sacks, and S. F. Badylak, "Collagen fiber alignment and biaxial mechanical behavior of porcine urinary bladder derived extracellular matrix," *Biomaterials,* vol. 29, no. 36, pp. 4775-4782, 2008-12-01 2008, doi: 10.1016/j.biomaterials.2008.08.022.

[125] J. Hodde, A. Janis, D. Ernst, D. Zopf, D. Sherman, and C. Johnson, "Effects of sterilization on an extracellular matrix scaffold: Part I. Composition and matrix architecture," *Journal of Materials Science: Materials in Medicine,* vol. 18, no. 4, pp. 537-543, 2007-04-01 2007, doi: 10.1007/s10856-007-2300-x.

[126] J. Hodde and M. Hiles, "Virus safety of a porcine-derived medical device: Evaluation of a viral inactivation method," *Biotechnology and Bioengineering,* vol. 79, no. 2, pp. 211-216, 2002, doi: https://doi.org/10.1002/bit.10281.

[127] M. Grünert, C. Dombrowski, M. Sadasivam, K. Manton, S. Cool, and V. Nurcombe, "Isolation of a native osteoblast matrix with a specific affinity for BMP2," *Journal of Molecular Histology,* vol. 38, no. 5, pp. 393-404, 2007, doi: 10.1007/s10735-007-9119-0.

[128] D. Vllasaliu, F. H. Falcone, S. Stolnik, and M. Garnett, "Basement membrane influences intestinal epithelial cell growth and presents a barrier to the movement of macromolecules," *Experimental Cell Research,* vol. 323, no. 1, pp. 218-231, 2014, doi: 10.1016/j.yexcr.2014.02.022.

[129] T. Hoshiba and J. Gong, "Fabrication of cell- derived decellularized matrices on three-dimensional (3D)-printed biodegradable polymer scaffolds," *Micro- and Nanosystems Information Storage and Processing Systems,* vol. 24, no. 1, pp. 613-617, 2018, doi: 10.1007/s00542-017-3470-1.

[130] T. Hoshiba, N. Kawazoe, and G. Chen, "The balance of osteogenic and adipogenic differentiation in human mesenchymal stem cells by matrices that mimic stepwise tissue development," *Biomaterials,* vol. 33, no. 7, p. 2025, 2012, doi: 10.1016/j.biomaterials.2011.11.061.

[131] P. M. Baptista, M. M. Siddiqui, G. Lozier, S. R. Rodriguez, A. Atala, and S. Soker, "The use of whole organ decellularization for the generation of a vascularized liver organoid," *Hepatology,* vol. 53, no. 2, pp. 604-617, 2011-02-01 2011, doi: 10.1002/hep.24067.

[132] A.-M. Kajbafzadeh, N. Javan-Farazmand, M. Monajemzadeh, and A. Baghayee, "Determining the Optimal Decellularization and Sterilization Protocol for Preparing a Tissue Scaffold of a

Human-sized Liver Tissue," *Tissue Eng Part C Methods,* vol. 19, no. ja, pp. 642-651, 2012, doi: 10.1089/ten.TEC.2012.0334.
[133] R. Owen, "Tissue Engineering an In Vitro Model of Owusteoporosis," Doctor of Philosophy, Materials science and engineering, University of Sheffield, United Kingdom, 2017.
[134] O. Syed, N. J. Walters, R. M. Day, H.-W. Kim, and J. C. Knowles, "Evaluation of decellularization protocols for production of tubular small intestine submucosa scaffolds for use in oesophageal tissue engineering," *Acta Biomaterialia,* vol. 10, no. 12, pp. 5043-5054, 2014/12/01/ 2014, doi: https://doi.org/10.1016/j.actbio.2014.08.024.
[135] M. Tello *et al.*, "Generating and characterizing the mechanical properties of cell- derived matrices using atomic force microscopy," *Methods,* vol. 94, no. C, pp. 85-100, 2016, doi: 10.1016/j.ymeth.2015.09.012.
[136] T. Hoshiba *et al.*, "Decellularized Extracellular Matrix as an In Vitro Model to Study the Comprehensive Roles of the ECM in Stem Cell Differentiation," in *Stem Cells Int.* vol. 2016, ed, 2016.
[137] J. S. Cartmell and M. G. Dunn, "Development of cell-seeded patellar tendon allografts for anterior cruciate ligament reconstruction," *Tissue Eng,* vol. 10, no. 7-8, pp. 1065-1075, 2004, doi: 10.1089/ten.2004.10.1065.
[138] T. Hoshiba, T. Yamada, H. Lu, N. Kawazoe, and G. Chen, "Maintenance of cartilaginous gene expression on extracellular matrix derived from serially passaged chondrocytes during in vitro chondrocyte expansion," *Journal of Biomedical Materials Research - Part A,* vol. 100, no. 3, pp. 694-702, 2012, doi: 10.1002/jbm.a.34003.
[139] S. R. Meyer, B. Chiu, T. A. Churchill, L. Zhu, J. R. T. Lakey, and D. B. Ross, "Comparison of aortic valve allograft decellularization techniques in the rat," *Journal of Biomedical Materials Research Part A,* vol. 79, no. 2, pp. 254-262, 2006, doi: 10.1002/jbm.a.30777.
[140] I. Prasertsung, S. Kanokpanont, T. Bunaprasert, V. Thanakit, and S. Damrongsakkul, "Development of acellular dermis from porcine skin using periodic pressurized technique," *Journal of Biomedical Materials Research Part B: Applied Biomaterials,* vol. 85, no. 1, pp. 210-219, 2008, doi: 10.1002/jbm.b.30938.
[141] I. Marcos-Campos, D. Marolt, P. Petridis, S. Bhumiratana, D. Schmidt, and G. Vunjak-Novakovic, "Bone scaffold architecture modulates the development of mineralized bone matrix by human embryonic stem cells," *Biomaterials,* vol. 33, no. 33, pp. 8329-8342, 2012, doi: 10.1016/j.biomaterials.2012.08.013.
[142] Y. Hashimoto, S. Funamoto, T. Kimura, K. Nam, T. Fujisato, and A. Kishida, "The effect of decellularized bone/ bone marrow produced by high- hydrostatic pressurization on the osteogenic differentiation of mesenchymal stem cells," *Biomaterials,* vol. 32, no. 29, 2011, doi: 10.1016/j.biomaterials.2011.06.008.
[143] D. K. Chang, M. R. Louis, A. Gimenez, and E. M. Reece, "The Basics of Integra Dermal Regeneration Template and its Expanding Clinical Applications," (in eng), *Semin Plast Surg,* vol. 33, no. 3, pp. 185-189, Aug 2019, doi: 10.1055/s-0039-1693401.
[144] S. E. Navone *et al.*, "Decellularized silk fibroin scaffold primed with adipose mesenchymal stromal cells improves wound healing in diabetic mice," *Stem cell research & therapy,* vol. 5, no. 1, pp. 7-7, 2014, doi: 10.1186/scrt396.
[145] X. D. Chen, V. Dusevich, J. Q. Feng, S. C. Manolagas, and R. L. Jilka, "Extracellular Matrix Made by Bone Marrow Cells Facilitates Expansion of Marrow- Derived Mesenchymal Progenitor Cells and Prevents Their Differentiation Into Osteoblasts," *Journal of Bone and Mineral Research,* vol. 22, no. 12, pp. 1943-1956, 2007, doi: 10.1359/jbmr.070725.
[146] H. Lee, S. Yang, M. Kim, and G. Kim, "A scaffold with a bio-mimetically designed micro/ nano-fibrous structure using decellularized extracellular matrix," *RSC Adv.,* vol. 6, no. 35, pp. 29697-29706, 2016, doi: 10.1039/c5ra27845g.

[147] H. Lu, T. Hoshiba, N. Kawazoe, I. Koda, M. Song, and G. Chen, "Cultured cell- derived extracellular matrix scaffolds for tissue engineering," *Biomaterials,* vol. 32, no. 36, pp. 9658-9666, 2011, doi: 10.1016/j.biomaterials.2011.08.091.
[148] T. Hoshiba, "Cultured cell- derived decellularized matrices: a review towards the next decade," *J. Mater. Chem. B,* vol. 5, no. 23, pp. 4322-4331, 2017, doi: 10.1039/c7tb00074j.
[149] T. W. Gilbert, T. L. Sellaro, and S. F. Badylak, "Decellularization of tissues and organs," *Biomaterials,* vol. 27, no. 19, pp. 3675-3683, 2006, doi: 10.1016/j.biomaterials.2006.02.014.
[150] Y. Anasiz, R. Ozgul, and D. Uckan-Cetinkaya, "A New Chapter for Mesenchymal Stem Cells: Decellularized Extracellular Matrices," *Stem Cell Reviews and Reports,* vol. 13, no. 5, pp. 587-597, 2017, doi: 10.1007/s12015-017-9757-x.
[151] J. M. Maria, M. Alysson, G. Fred, and V. Ajit, "Human embryonic stem cells express an immunogenic nonhuman sialic acid," *Nature Medicine,* vol. 11, no. 2, p. 228, 2005, doi: 10.1038/nm1181.
[152] C. Tekkatte, G. P. Gunasingh, K. Cherian, and K. Sankaranarayanan, "" Humanized" Stem Cell Culture Techniques: The Animal Serum Controversy," *Stem Cells Int.,* vol. 2011, 2011, doi: 10.4061/2011/504723.
[153] Y. Liu, A. Kalén, O. Risto, and O. Wahlström, "Fibroblast proliferation due to exposure to a platelet concentrate in vitro is pH dependent," *Wound Repair and Regeneration,* vol. 10, no. 5, pp. 336-340, 2002, doi: 10.1046/j.1524-475X.2002.10510.x.
[154] I. S. Blande *et al.*, "TRANSPLANTATION AND CELLULAR ENGINEERING: Adipose tissue mesenchymal stem cell expansion in animal serum- free medium supplemented with autologous human platelet lysate," *Transfusion,* vol. 49, no. 12, pp. 2680-2685, 2009, doi: 10.1111/j.1537-2995.2009.02346.x.
[155] C. Rauch, E. Feifel, E.-M. Amann, H. P. Spötl, H. Schennach, W. Pfaller, and G. Gstraunthaler, "Alternatives to the use of fetal bovine serum: human platelet lysates as a serum substitute in cell culture media," *ALTEX,* vol. 28, no. 4, pp. 305-316, 2011, doi: 10.14573/altex.2011.4.305.
[156] K. Witzeneder, A. Lindenmair, C. Gabriel, K. Höller, D. Theiß, H. Redl, and S. Hennerbichler, "Human-derived alternatives to fetal bovine serum in cell culture," *Transfusion medicine and hemotherapy : offizielles Organ der Deutschen Gesellschaft fur Transfusionsmedizin und Immunhamatologie,* vol. 40, no. 6, pp. 417-423, 2013, doi: 10.1159/000356236.
[157] L. M. M. Vianna, L. Kallay, T. Toyono, R. Belfort, J. D. Holiman, and A. S. Jun, "Use of human serum for human corneal endothelial cell culture," *British Journal of Ophthalmology,* vol. 99, no. 2, p. 267, 2015, doi: 10.1136/bjophthalmol-2014-306034.
[158] D. A. Qassim, "BONE TISSUE ENGINEERING FOR CORRECTING OF CLEFT PALATE DURING ORAL AND MAXILLOFACIAL SURGERY," 2021.
[159] Y. Zhou, M. Park, E. Cheung, L. Wang, and X. L. Lu, "The effect of chemically defined medium on spontaneous calcium signaling of in situ chondrocytes during long-term culture," *Journal of Biomechanics,* vol. 48, no. 6, pp. 990-996, 2015, doi: 10.1016/j.jbiomech.2015.02.005.
[160] D. Salzig, J. Leber, K. Merkewitz, M. C. Lange, N. Köster, and P. Czermak, "Attachment, Growth, and Detachment of Human Mesenchymal Stem Cells in a Chemically Defined Medium," *Stem cells international,* vol. 2016, pp. 5246584-5246584, 2016, doi: 10.1155/2016/5246584.
[161] L. Myung-Suk *et al.*, "Enhanced Cell Growth of Adipocyte-Derived Mesenchymal Stem Cells Using Chemically- Defined Serum-Free Media," *International Journal of Molecular Sciences,* vol. 18, no. 8, p. 1779, 2017, doi: 10.3390/ijms18081779.
[162] Y. Nakashima *et al.*, "A Liquid Chromatography with Tandem Mass Spectrometry-Based Proteomic Analysis of Cells Cultured in DMEM 10% FBS and Chemically Defined Medium Using Human Adipose-Derived Mesenchymal Stem Cells," *International journal of molecular sciences,* vol. 19, no. 7, 2018, doi: 10.3390/ijms19072042.
[163] Y. Masato *et al.*, "Dexamethasone enhances osteogenic differentiation of bone marrow- and muscle-derived stromal cells and augments ectopic bone formation induced by bone

morphogenetic protein-2," *PLoS ONE,* vol. 10, no. 2, p. e0116462, 2015, doi: 10.1371/journal.pone.0116462.
[164] J. E. Ireton, J. G. Unger, and R. J. Rohrich, "The role of wound healing and its everyday application in plastic surgery: a practical perspective and systematic review," (in eng), *Plast Reconstr Surg Glob Open,* vol. 1, no. 1, Apr 2013, doi: 10.1097/GOX.0b013e31828ff9f4.
[165] H. E. desJardins-Park, S. Mascharak, M. S. Chinta, D. C. Wan, and M. T. Longaker, "The Spectrum of Scarring in Craniofacial Wound Repair," (in eng), *Front Physiol,* vol. 10, p. 322, 2019, doi: 10.3389/fphys.2019.00322.
[166] L. Chen, Z. H. Arbieva, S. Guo, P. T. Marucha, T. A. Mustoe, and L. A. DiPietro, "Positional differences in the wound transcriptome of skin and oral mucosa," (in eng), *BMC Genomics,* vol. 11, p. 471, Aug 12 2010, doi: 10.1186/1471-2164-11-471.
[167] R. Iglesias-Bartolome *et al.*, "Transcriptional signature primes human oral mucosa for rapid wound healing," (in eng), *Sci Transl Med,* vol. 10, no. 451, Jul 25 2018, doi: 10.1126/scitranslmed.aap8798.
[168] J. E. Glim, M. van Egmond, F. B. Niessen, V. Everts, and R. H. J. Beelen, "Detrimental dermal wound healing: What can we learn from the oral mucosa?," *Wound Repair and Regeneration,* vol. 21, no. 5, pp. 648-660, 2013, doi: https://doi.org/10.1111/wrr.12072.
[169] S. Guo and L. A. Dipietro, "Factors affecting wound healing," (in eng), *J Dent Res,* vol. 89, no. 3, pp. 219-29, Mar 2010, doi: 10.1177/0022034509359125.
[170] C. Politis, J. Schoenaers, R. Jacobs, and J. O. Agbaje, "Wound Healing Problems in the Mouth," (in eng), *Front Physiol,* vol. 7, p. 507, 2016, doi: 10.3389/fphys.2016.00507.
[171] A. M. Soltani *et al.*, "Hypertrophic scarring in cleft lip repair: a comparison of incidence among ethnic groups," (in eng), *Clin Epidemiol,* vol. 4, pp. 187-91, 2012, doi: 10.2147/clep.S31119.
[172] T. J. Sitzman *et al.*, "The Americleft Project: Burden of Care from Secondary Surgery," (in eng), *Plast Reconstr Surg Glob Open,* vol. 3, no. 7, p. e442, Jul 2015, doi: 10.1097/gox.0000000000000415.
[173] D. Pilger, C. Von Sonnleithner, and E. Bertelmann, "Assessing full thickness oral mucosal grafting: complications and postoperative outcomes in a broad collective of patients," *BMJ Open Ophthalmology,* vol. 5, no. 1, p. e000337, 2020-02-01 2020, doi: 10.1136/bmjophth-2019-000337.
[174] C. Fuchs, L. Pham, J. Henderson, K. J. Stalnaker, R. R. Anderson, and J. Tam, "Multi-faceted enhancement of full-thickness skin wound healing by treatment with autologous micro skin tissue columns," *Sci Rep,* vol. 11, no. 1, pp. 1688-1688, 2021, doi: 10.1038/s41598-021-81179-7.
[175] A. Przekora, "A Concise Review on Tissue Engineered Artificial Skin Grafts for Chronic Wound Treatment: Can We Reconstruct Functional Skin Tissue In Vitro?," *Cells,* vol. 9, no. 7, p. 1622, 2020-07-06 2020, doi: 10.3390/cells9071622.
[176] A. K. Lundgren, L. Sennerby, D. Lundgren, A. Taylor, J. Gottlow, and S. Nyman, "Bone augmentation at titanium implants using autologous bone grafts and a bioresorbable barrier. An experimental study in the rabbit tibia," *Clinical Oral Implants Research,* vol. 8, no. 2, pp. 82-89, 1997, doi: https://doi.org/10.1034/j.1600-0501.1997.080202.x.
[177] I. Elgali, O. Omar, C. Dahlin, and P. Thomsen, "Guided bone regeneration: materials and biological mechanisms revisited," (in eng), *Eur J Oral Sci,* vol. 125, no. 5, pp. 315-337, Oct 2017, doi: 10.1111/eos.12364.
[178] J. Liu and D. G. Kerns, "Mechanisms of Guided Bone Regeneration: A Review," *The Open Dentistry Journal,* vol. 8, no. 1, pp. 56-65, 2014-05-16 2014, doi: 10.2174/1874210601408010056.
[179] K. Alain and J. Querellou, "Cultivating the uncultured: limits, advances and future challenges," *Extremophiles,* vol. 13, no. 4, pp. 583-594, 2009-07-01 2009, doi: 10.1007/s00792-009-0261-3.

[180] L. Goers, P. Freemont, and K. M. Polizzi, "Co-culture systems and technologies: taking synthetic biology to the next level," *Journal of The Royal Society Interface,* vol. 11, no. 96, p. 20140065, 2014-07-06 2014, doi: 10.1098/rsif.2014.0065.

[181] S. Bertrand, N. Bohni, S. Schnee, O. Schumpp, K. Gindro, and J.-L. Wolfender, "Metabolite induction via microorganism co-culture: A potential way to enhance chemical diversity for drug discovery," *Biotechnology Advances,* vol. 32, no. 6, pp. 1180-1204, 2014/11/01/ 2014, doi: https://doi.org/10.1016/j.biotechadv.2014.03.001.

[182] X. Chen, Z. Peng, and Z. Yang, "Metabolomics studies of cell–cell interactions using single cell mass spectrometry combined with fluorescence microscopy," *Chemical Science,* vol. 13, no. 22, pp. 6687-6695, 2022, doi: 10.1039/d2sc02298b.

[183] E. Alias *et al.*, "Doxorubicin-induced cardiomyocyte toxicity – protective effects of endothelial cells in a tri-culture model system," *Journal of interdisciplinary nanomedicine,* vol. 3, no. 3, pp. 122-132, 2018, doi: 10.1002/jin2.42.

[184] A. Aguirre, J. A. Planell, and E. Engel, "Dynamics of bone marrow-derived endothelial progenitor cell/mesenchymal stem cell interaction in co-culture and its implications in angiogenesis," *Biochemical and Biophysical Research Communications,* vol. 400, no. 2, pp. 284-291, 2010/09/17/ 2010, doi: https://doi.org/10.1016/j.bbrc.2010.08.073.

[185] E. Y. Plotnikov *et al.*, "Cell-to-cell cross-talk between mesenchymal stem cells and cardiomyocytes in co-culture," *Journal of Cellular and Molecular Medicine,* vol. 12, no. 5a, pp. 1622-1631, 2008-09-01 2008, doi: 10.1111/j.1582-4934.2007.00205.x.

[186] S. M. Richardson, R. V. Walker, S. Parker, N. P. Rhodes, J. A. Hunt, A. J. Freemont, and J. A. Hoyland, "Intervertebral Disc Cell–Mediated Mesenchymal Stem Cell Differentiation," *Stem Cells,* vol. 24, no. 3, pp. 707-716, 2006-03-01 2006, doi: 10.1634/stemcells.2005-0205.

[187] C. Csaki, U. Matis, A. Mobasheri, and M. Shakibaei, "Co-culture of canine mesenchymal stem cells with primary bone-derived osteoblasts promotes osteogenic differentiation," *Histochemistry and Cell Biology,* vol. 131, no. 2, pp. 251-266, 2009-02-01 2009, doi: 10.1007/s00418-008-0524-6.

[188] K. L. Moffat, I.-N. E. Wang, S. A. Rodeo, and H. H. Lu, "Orthopedic Interface Tissue Engineering for the Biological Fixation of Soft Tissue Grafts," *Clinics in Sports Medicine,* vol. 28, no. 1, pp. 157-176, 2009-01-01 2009, doi: 10.1016/j.csm.2008.08.006.

[189] I. C. Lee, J.-H. Wang, Y.-T. Lee, and T.-H. Young, "The differentiation of mesenchymal stem cells by mechanical stress or/and co-culture system," *Biochemical and Biophysical Research Communications,* vol. 352, no. 1, pp. 147-152, 2007/01/05/ 2007, doi: https://doi.org/10.1016/j.bbrc.2006.10.170.

[190] L. Zhang, N. Tran, H.-Q. Chen, C. J.-F. Kahn, S. Marchal, F. Groubatch, and X. Wang, "Time-related changes in expression of collagen types I and III and of tenascin-C in rat bone mesenchymal stem cells under co-culture with ligament fibroblasts or uniaxial stretching," *Cell and Tissue Research,* vol. 332, no. 1, pp. 101-109, 2008-04-01 2008, doi: 10.1007/s00441-007-0564-6.

[191] M. A. Burkhardt *et al.*, "Synergistic interactions of blood-borne immune cells, fibroblasts and extracellular matrix drive repair in an in vitro peri-implant wound healing model," *Sci Rep,* vol. 6, no. 1, pp. 21071-21071, 2016, doi: 10.1038/srep21071.

[192] F. Wein and A. Bruinink, "Human triple cell co-culture for evaluation of bone implant materials," *Integrative Biology,* vol. 5, no. 4, pp. 703-711, 2013-04-25 2013, doi: 10.1039/c3ib20250j.

[193] E. Dohle *et al.*, "Co-culture model for cutaneous wound healing to assess a porous fiber-based drug delivery system," *Tissue Eng Part C Methods,* vol. 26, no. ja, pp. 475-484, 2020, doi: 10.1089/ten.TEC.2020.0145.

[194] G. Borciani, G. Montalbano, N. Baldini, C. Vitale-Brovarone, and G. Ciapetti, "Protocol of Co-Culture of Human Osteoblasts and Osteoclasts to Test Biomaterials for Bone Tissue

Engineering," *Methods and Protocols,* vol. 5, no. 1, p. 8, 2022-01-14 2022, doi: 10.3390/mps5010008.
[195] S. Puwanun, "Developing tissue engineering strategy for cleft palate repair," 2014, 2014.
[196] R. L. Dahlin, L. A. Kinard, J. Lam, C. J. Needham, S. Lu, F. K. Kasper, and A. G. Mikos, "Articular chondrocytes and mesenchymal stem cells seeded on biodegradable scaffolds for the repair of cartilage in a rat osteochondral defect model," *Biomaterials,* vol. 35, no. 26, pp. 7460-7469, 2014-08-01 2014, doi: 10.1016/j.biomaterials.2014.05.055.
[197] N. S. Hwang *et al.*, "Chondrogenic Priming Adipose-Mesenchymal Stem Cells for Cartilage Tissue Regeneration," *Pharmaceutical Research,* vol. 28, no. 6, pp. 1395-1405, 2011-06-01 2011, doi: 10.1007/s11095-011-0445-2.
[198] J. Zhou, H. Lin, T. Fang, X. Li, W. Dai, T. Uemura, and J. Dong, "The repair of large segmental bone defects in the rabbit with vascularized tissue engineered bone," *Biomaterials,* vol. 31, no. 6, pp. 1171-1179, 2010/02/01/ 2010, doi: https://doi.org/10.1016/j.biomaterials.2009.10.043.
[199] S. J. Bidarra, C. C. Barrias, M. A. Barbosa, R. Soares, J. Amédée, and P. L. Granja, "Phenotypic and proliferative modulation of human mesenchymal stem cells via crosstalk with endothelial cells," *Stem Cell Research,* vol. 7, no. 3, pp. 186-197, 2011/11/01/ 2011, doi: https://doi.org/10.1016/j.scr.2011.05.006.
[200] J. Guerrero *et al.*, "Cell interactions between human progenitor-derived endothelial cells and human mesenchymal stem cells in a three-dimensional macroporous polysaccharide-based scaffold promote osteogenesis," *Acta Biomaterialia,* vol. 9, no. 9, pp. 8200-8213, 2013/09/01/ 2013, doi: https://doi.org/10.1016/j.actbio.2013.05.025.
[201] Y. Liu, S.-H. Teoh, M. S. K. Chong, C.-H. Yeow, R. D. Kamm, M. Choolani, and J. K. Y. Chan, "Contrasting Effects of Vasculogenic Induction Upon Biaxial Bioreactor Stimulation of Mesenchymal Stem Cells and Endothelial Progenitor Cells Cocultures in Three-Dimensional Scaffolds Under In Vitro and In Vivo Paradigms for Vascularized Bone," *Tissue Engineering Part A,* vol. 19, no. 7-8, pp. 893-904, 2013, doi: 10.1089/ten.tea.2012.0187.
[202] Skottke, Gelinsky, and Bernhardt, "In Vitro Co-culture Model of Primary Human Osteoblasts and Osteocytes in Collagen Gels," *International Journal of Molecular Sciences,* vol. 20, no. 8, p. 1998, 2019-04-23 2019, doi: 10.3390/ijms20081998.
[203] A. I. Pangesty and M. Todo, "Improvement of Mechanical Strength of Tissue Engineering Scaffold Due to the Temperature Control of Polymer Blend Solution," *Journal of Functional Biomaterials,* vol. 12, no. 3, p. 47, 2021-08-14 2021, doi: 10.3390/jfb12030047.
[204] R. Pace and K. Burg, "Toxic effects of resazurin on cell cultures," *Incorporating Methods in Cell Science International Journal of Cell Culture and Biotechnology,* vol. 67, no. 1, pp. 13-17, 2015, doi: 10.1007/s10616-013-9664-1.
[205] C. Bueno, M. L. Villegas, S. G. Bertolotti, C. M. Previtali, M. G. Neumann, and M. V. Encinas, "The Excited- State Interaction of Resazurin and Resorufin with Aminesin Aqueous Solutions. Photophysics and Photochemical Reaction ¶," *Photochemistry and Photobiology,* vol. 76, no. 4, pp. 385-390, 2002, doi: 10.1562/0031-8655(2002)0760385TESIOR2.0.CO2.
[206] L. Antonini, V. Kothe, G. Reilly, R. Owen, J. Marcuzzo, and C. Malfatti, "Effect of Ti6Al4V surface morphology on the osteogenic differentiation of human embryonic stem cells," *Journal of Materials Research,* vol. 32, no. 20, pp. 3811-3821, 2017, doi: 10.1557/jmr.2017.392.
[207] E. Birmingham, G. Niebur, P. McHugh, G. Shaw, F. Barry, and L. McNamara, "OSTEOGENIC DIFFERENTIATION OF MESENCHYMAL STEM CELLS IS REGULATED BY OSTEOCYTE AND OSTEOBLAST CELLS IN A SIMPLIFIED BONE NICHE," *Eur. Cells Mater.,* vol. 23, pp. 13-27, 2012.
[208] H. Tullberg-Reinert and G. Jundt, "In situ measurement of collagen synthesis by human bone cells with a Sirius Red- based colorimetric microassay: effects of transforming growth factor β2 and ascorbic acid 2- phosphate," *Histochemistry and Cell Biology,* vol. 112, no. 4, pp. 271-276, 1999, doi: 10.1007/s004180050447.

[209] G. Radha, B. Venkatesan, P. Rajashree, E. Vellaichamy, and S. Balakumar, "Insights into the apatite mineralization potential of thermally processed nanocrystalline Ca 10 x Fe x (PO 4) 6 (OH) 2," *New J. Chem.,* vol. 43, no. 3, pp. 1358-1371, 2019, doi: 10.1039/c8nj03579b.

[210] Y. H. Wang, Y. Liu, P. Maye, and D. W. Rowe, "Examination of Mineralized Nodule Formation in Living Osteoblastic Cultures Using Fluorescent Dyes," *Biotechnology Progress,* vol. 22, no. 6, pp. 1697-1701, 2006, doi: 10.1021/bp060274b.

[211] A. Kiziltay, A. Marcos-Fernandez, J. San Roman, R. A. Sousa, R. L. Reis, V. Hasirci, and N. Hasirci, "Poly(ester-urethane) scaffolds: effect of structure on properties and osteogenic activity of stem cells," *Journal of Tissue Engineering and Regenerative Medicine,* vol. 9, no. 8, pp. 930-942, 2015, doi: 10.1002/term.1848.

[212] S. Taherkhani and F. Moztarzadeh, "Fabrication of a poly(ε-caprolactone)/starch nanocomposite scaffold with a solvent-casting/salt-leaching technique for bone tissue engineering applications," *Journal of Applied Polymer Science,* vol. 133, no. 23, pp. n/a-n/a, 2016, doi: 10.1002/app.43523.

[213] C. I. Boissard, P. E. Bourban, A. E. Tami, M. Alini, and D. Eglin, "Nanohydroxyapatite/poly(ester urethane) scaffold for bone tissue engineering," *Acta Biomater,* vol. 5, no. 9, pp. 3316-27, Nov 2009, doi: 10.1016/j.actbio.2009.05.001.

[214] A. Bignon *et al.*, "Effect of micro- and macroporosity of bone substitutes on their mechanical properties and cellular response," *Journal of Materials Science: Materials in Medicine,* vol. 14, no. 12, pp. 1089-1097, 2003-12-01 2003, doi: 10.1023/b:jmsm.0000004006.90399.b4.

[215] Y. Zhu *et al.*, "In vitro cell proliferation evaluation of porous nano-zirconia scaffolds with different porosity for bone tissue engineering," *Biomed Mater,* vol. 10, no. 5, p. 055009, Sep 21 2015, doi: 10.1088/1748-6041/10/5/055009.

[216] A. Samourides, L. Browning, V. Hearnden, and B. Chen, "The effect of porous structure on the cell proliferation, tissue ingrowth and angiogenic properties of poly(glycerol sebacate urethane) scaffolds," *Mater Sci Eng C Mater Biol Appl,* vol. 108, p. 110384, Mar 2020, doi: 10.1016/j.msec.2019.110384.

[217] M. M. Nava, L. Draghi, C. Giordano, and R. Pietrabissa, "The Effect of Scaffold Pore Size in Cartilage Tissue Engineering," *Journal of Applied Biomaterials & Functional Materials,* vol. 14, no. 3, pp. e223-e229, 2016, doi: 10.5301/jabfm.5000302.

[218] A. J. Engler, S. Sen, H. L. Sweeney, and D. E. Discher, "Matrix Elasticity Directs Stem Cell Lineage Specification," *Cell,* vol. 126, no. 4, pp. 677-689, 2006-08-01 2006, doi: 10.1016/j.cell.2006.06.044.

[219] B. Aldemir Dikici, G. C. Reilly, and F. Claeyssens, "Boosting the Osteogenic and Angiogenic Performance of Multiscale Porous Polycaprolactone Scaffolds by In Vitro Generated Extracellular Matrix Decoration," *ACS Appl Mater Interfaces,* vol. 12, no. 11, pp. 12510-12524, Mar 18 2020, doi: 10.1021/acsami.9b23100.

[220] H. Wu, G. Yin, X. Pu, J. Wang, X. Liao, and Z. Huang, "Preliminary Study on the Antigen-Removal from Extracellular Matrix via Different Decellularization," *Tissue Eng Part C Methods,* vol. 28, no. 6, pp. 250-263, Jun 2022, doi: 10.1089/ten.TEC.2022.0025.

[221] A. Azhim, T. Ono, Y. Fukui, Y. Morimoto, K. Furukawa, and T. Ushida, "Preparation of decellularized meniscal scaffolds using sonication treatment for tissue engineering," *EMBC,* pp. 6953-6956, 2013, doi: 10.1109/EMBC.2013.6611157.

[222] F. Starnecker, F. Konig, C. Hagl, and N. Thierfelder, "Tissue-engineering acellular scaffolds-The significant influence of physical and procedural decellularization factors," *J Biomed Mater Res B Appl Biomater,* vol. 106, no. 1, pp. 153-162, Jan 2018, doi: 10.1002/jbm.b.33816.

[223] I. Perea-Gil *et al.*, "In vitro comparative study of two decellularization protocols in search of an optimal myocardial scaffold for recellularization," *Am J Transl Res,* vol. 7, no. 3, pp. 558-73, 2015.

[224] T. Hoshiba, H. Lu, T. Yamada, N. Kawazoe, T. Tateishi, and G. Chen, "Effects of extracellular matrices derived from different cell sources on chondrocyte functions," *Biotechnol Progress,* vol. 27, no. 3, pp. 788-795, 2011, doi: 10.1002/btpr.592.

[225] B. D. Elder, S. V. Eleswarapu, and K. A. Athanasiou, "Extraction techniques for the decellularization of tissue engineered articular cartilage constructs," *Biomaterials,* vol. 30, no. 22, pp. 3749-3756, 2009, doi: 10.1016/j.biomaterials.2009.03.050.

[226] P. Vavken, S. Joshi, and M. M. Murray, "TRITON-X is most effective among three decellularization agents for ACL tissue engineering," *Journal of Orthopaedic Research,* vol. 27, no. 12, pp. 1612-1618, 2009, doi: 10.1002/jor.20932.

[227] A. Farag, C. Vaquette, C. Theodoropoulos, S. M. Hamlet, D. W. Hutmacher, and S. Ivanovski, "Decellularized Periodontal Ligament Cell Sheets with Recellularization Potential," *Journal of Dental Research,* vol. 93, no. 12, pp. 1313-1319, 2014, doi: 10.1177/0022034514547762.

[228] K. Tamama, H. Kawasaki, and A. Wells, "Epidermal growth factor (EGF) treatment on multipotential stromal cells (MSCs). Possible enhancement of therapeutic potential of MSC," *J Biomed Biotechnol,* vol. 2010, p. 795385, 2010, doi: 10.1155/2010/795385.

[229] M. Krampera *et al.*, "HB-EGF/HER-1 signaling in bone marrow mesenchymal stem cells: inducing cell expansion and reversibly preventing multilineage differentiation," *Blood,* vol. 106, no. 1, pp. 59-66, 2005/07/01/ 2005, doi: https://doi.org/10.1182/blood-2004-09-3645.

[230] M. Shahbazi *et al.*, "The role of insulin as a key regulator of seeding, proliferation, and mRNA transcription of human pluripotent stem cells," *Stem Cell Res Ther,* vol. 10, no. 1, pp. 228-11, 2019, doi: 10.1186/s13287-019-1319-5.

[231] M. P. Chong, G. J. Barritt, and M. F. Crouch, "Insulin potentiates EGFR activation and signaling in fibroblasts," *Biochem Biophys Res Commun,* vol. 322, no. 2, pp. 535-41, Sep 17 2004, doi: 10.1016/j.bbrc.2004.07.150.

[232] M. F. Crouch, D. A. Davy, F. S. Willard, and L. A. Berven, "Insulin induces epidermal growth factor (EGF) receptor clustering and potentiates EGF-stimulated DNA synthesis in Swiss 3T3 cells: A mechanism for costimulation in mitogenic synergy," *Immunol Cell Biol,* vol. 78, no. 4, pp. 408-414, 2000, doi: 10.1046/j.1440-1711.2000.00929.x.

[233] I. Kratchmarova, B. Blagoev, M. Haack-Sorensen, M. Kassem, and M. Mann, "Cell Signalling: Mechanism of divergent growth factor effects in mesenchymal stem cell differentiation," *Science (American Association for the Advancement of Science),* vol. 308, no. 5727, pp. 1472-1477, 2005, doi: 10.1126/science.1107627.

[234] S. Puwanun, F. J. Bye, M. M. Ireland, S. MacNeil, G. C. Reilly, and N. H. Green, "Production and characterization of a novel, electrospun, tri-layer polycaprolactone membrane for the segregated co-culture of bone and soft tissue," *Polymers (Basel),* vol. 8, no. 6, pp. 221-221, 2016, doi: 10.3390/polym8060221.

[235] B. A. Dikici, S. Dikici, G. C. Reilly, S. MacNeil, and F. Claeyssens, "A novel bilayer polycaprolactone membrane for guided bone regeneration: Combining electrospinning and emulsion templating," *Materials (Basel),* vol. 12, no. 16, p. 2643, 2019, doi: 10.3390/ma12162643.